The Ionic Bonding Energy and Effective Atomic Charge of Several Silicate Minerals(Dissertation_全文)

AUTHOR(S):

Tamada, Osamu

学位申請論文

玉田 攻

The Ionic Bonding Energy and Effective Atomic Charge of Several Silicate Minerals.

by

Osamu TAMADA

The Ionic Bonding Energy and Effective Atomic Charge of Several Silicate Minerals.

by

Osamu TAMADA

May, 1980

Kyoto, Japan.

Contents

Abstract

The Born's energetic model for the bonding energy of ionic crystals was applied on the three classical problems in mineralogy as the first approximation for the energetic study of silicate minerals; the order-disorder of Al and Si ions in alkali feldspars, the stability relations of olivine, modified spinel and spinel, and the intra-crystalline cation distributions in olivines and orthopyroxenes, in order to rationalize the above problems and to reveal the energetics of these crystals. The electrostatic energies were actually calculated by the method of Bertaut, and the repulsive energies or qualitatively the size effects were always taken into considerations.

The order-disorder phenomenon in alkali feldspars is explained from the energetic viewpoint as was at first expected. The positive feedback effect of the cation distributions was observed in the electrostatic potentials in the tetrahedral sites, which is the important mechanism in the order-disorder of Al and Si ions.

The characteristic features of the olivine, modified spinel and spinel structures were discussed from the viewpoint of the electrostatic energies of them and of their constituent ions for the better understanding of the structures. The above energetic treatments failed to explain the stability relations of olivine, modified spinel and spinel at atomospheric pressure. This is because the electrostatic energies

of modified spinel and spinel are far lower than that of olivine in contrast to the thermodynamic stability relations and because the difference of the electrostatic energies are too large to be compensated by the repulsive energies. Then the problem remains in the future. The effect of the ionic size of M ions on the electrostatic energies of olivine and spinel, and their constituent ions are also discussed by plotting these electrostatic energies against the ratio of ionic sizes of r_M/r_{Si}.

The olivine structure has the anomalous feature that the potential of the smaller M1 site is far higher than that of the larger M2 site in contrast to the opposite relation in the potentials of orthopyroxene. The anomalous cation distributions in olivines can be explained on the above anomalous feature of the olivine structure if only one assumption was assumed that the Mg ion is more ionic and then has the larger atomic charge than the transition metal ions in the crystals.

The electrostatic stability also demands that the atomic charge of the M2 site of olivine is larger than that of the M1 site in their endmembers of the chemical composition, in contrast to the inverse relation in the atomic charges of orthopyroxene. The above one assumption and the demand are examined by the X-ray charge refinements carried out by Fujino et al., Tamada et al., and Sasaki et al. and then the relative relations in the atomic charges demanded by the electrostatic stability are consistent with those determined by the X-ray method in olivines and orthopyroxenes.

This has the important meaning that the silicate minerals cannot be always assumed to be the fully ionic crystals and that the Born's energetic models should be amended to take the concept "net atomic charges" into account when it is applied on the silicate minerals.

The concept of the electrostatic stability seems to have the predictional ability about the relative values of the net atomic charges. It is, therefore, important to take the concept into consideration in the X-ray charge refinements.

The accurate structure determinations of the Co and Ni-olivines were carried out in order to see the atomic charges and the electron density distributions around the cation sites. The asphericities of the electron density distributions are observed around the transition metal ions. This encourages us to study the electron distributions of d-electrons in the octahedral sites by the X-ray method.

Capter I Introduction

One of the main purposes in mineralogy has been to determine the crystal structures of minerals. Before the development of the X-ray method, the observation of the minerals by the optical microscope was the major method to do it. Since the X-ray diffraction by crystals was discovered by Laue in 1912, it has become the most powerful method to determine the crystal structure of minerals. In the early days of the development of this method, it was not an easy work to collect the intensity data of reflections and to calculate the atomic positions of crystal, but now the intensity data can be easily and accurately collected by the automatic diffractometer controled by the computer system, and the calculations to determine the atomic positions of crystal and the electron density distributions can be easily and rapidly carried out by the electronic computer. Even the bonding electron distributions including those of d-electrons and the atomic net charges in crystals have been studied by the X-ray method in recent years. Furthermore the development of the electron microscope has made possible the direct observation of the fine textures of minerals.

Compared with the rapid increase of the structural information of minerals, the development of theoretical or crystal chemical studies has been very slow in mineralogy. In the crystal chemical studies of the stability relations of crystals, there exist two principle methods. One method is the

predictional one depending on the so-called Pauling's rules for ionic crystals, which is rather qualitative but has wide applications to minerals. The other is strict calculation of internal energies based on some crystallographic methods, which gives the exact internal energies of crystals, but few applications have been reported on minerals. The stability of silicate minerals has been discussed mainly by the first method, as the second method requires precise crystallographic data and is difficult in setting the energetic model and in the calculation of the energy. The Pauling's rules for the ionic crystals have been main basis of the crystal chemical discussion for the stability of silicate minerals.

Now the basis of the crystal chemical discussions of silicate minerals must be translated from the qualitative Pauling's rules for ionic crystals to the quantitative value of "energy". For the calculation of quantitative internal energy, the Born's model for ionic crystals has been adopted as a first approximation.

The Born's energetic model for ionic crystals is a classical and simple model of bonding energy between two ions, which is derived from the quantum mechanics. The explicit expression is

$$U_{ij} = \frac{q_i q_j}{r_{ij}} + \lambda_{ij} \exp(-\frac{r_{ij}}{\rho_{ij}})$$

where U_{ij} is the bonding energy between i and j ions, q_i is the electric charge of i ion, r_{ij} is the interatomic distance between i and j ions and λ and ρ are the repulsive constants.

The first term corresponds to the electrostatic energy and the second the repulsive energy. The repulsive energy is sometimes represented by the repulsive constants A_i and B_i proper to each ions as $C(B_i + B_j) \exp\left(\frac{A_i + A_j - r_{ij}}{B_i + B_j}\right)$.

The repulsive term describes that filled electronic shells act as if they are fairly hard and each ion resists overlapping with the electron distributions of neighbouring ions, following the Pauli exclusion principle as mentioned by Kittel (1967). The difficulty in the estimation of the repulsive energy is due to that there are almost no reliable repulsive constants. Then the effect of the repulsive energy can be replaced qualitatively by the size effect if filled electronic shells are assumed to act as if they are rigid balls.

In the following discussions crystals are assumed to be, in principle, ionic and the Born's model is settled on the basis of the discussions. The electrostatic energy is actually calculated and the repulsive energy or qualitatively the size effect is always taken into account.

Then the relative crystallographic stability of some silicate minerals is discussed on the following problems in terms of energy by applying the Born's model; the order-disorder phenomenon of Al and Si ions in feldspars, the stability relations of olivine, modified spinel and spinel under atmospheric and high pressures, and the intra-crystalline cation distributions of olivines and orthopyroxenes. The purpose of this study is to reveal the energetics of these

problems in the silicate minerals.

In the course of this study the accurate structures of olivines together with the charges of the constituent ions were necessary for the calculations of the electrostatic energy and for the discussion about the net atomic charges. Then these structure determinations have been precisely carried out.

Chapter II The programs to calculate the electrostatic energy.

A computer program to calculate the electrostatic energy of crystal and the constituent ions by the method of Bertaut was written by the author. The program is shown in Appendix 1. It consists of a main program and a subprogram SYMM which must be prepared for each space group in order to give the symmetry operations to each ion. The output data of low albite are shown together as an example in Appendix 1. The required input data are lattice parameters, the radius R of assumed charge distribution of ions, the number NZ of the chemical formula unit in the unit cell, the radius range β of $\alpha=2\pi hR$ in the summation of Fourier series where h is the distance from the origin in the reciprocal space, the correction factor G of self-energy, the correction factor Q for the termination error, the number NP of unequivalent ions, the number NS of general positions of ion and atomic coordinates and charges. The correction factor Q for radius range β is taken from Templeton (1955) and Templeton and Jones (1956). The output results are obtained in units, erg, eV and kcal/mol.

The computer program to calculate the electrostatic energy together with the standard error derived from the errors of structural data, was also written by the author. The program is shown in Appendix 2. It consists of a main program and two subprograms SYMM and MAD where the subprogram SYMM is the same used in the above program. The output data of high

albite are shown together as an example in Appendix 2. In this case the input data of the errors of the structural data must be added to the above input data.

The above two programs were written separately for the convenience because the first took less CPU time in contrast to the large CPU time of the latter.

Chapter III The applications of Born's bonding model on the polymorphic phenomena.

III-1 The application of Born's model on the order-disorder phenomenon of Al and Si ions in K-feldspars and albites.

III-1-A Introduction

It is widely known that both K-feldspars and albites have polymorphs of the high and low temperature types. K-feldspars have, in general, monoclinic symmetry, space group C2/m and two tetrahedral sites T1 and T2 (8j in Wykoff notation) which Al and Si ions occupy, but the low temperature type of K-feldspar, microcline, and the high and low albites have triclinic symmetry, space group $C\bar{1}$ and four tetrahedral sites T1(0), T1(m), T2(0) and T2(m) (2i in Wykoff notation) which Al and Si ions occupy.

Chao et al. (1940) first reported the structural basis of these polymorphisms. They found the large difference between the sizes of two tetrahedral sites (T sites) in orthoclase and concluded that the larger Al ion in ionic radius occupied the larger T site while the smaller Si ion occupied the smaller T site in the feldspar. After Chao et al. experimental studies of relations between the ionic size of Al and Si ions and the size of the occupied crystal site have been reported by many workers (Cole et al., 1949; Ferguson et al., 1958; Ribbe et al., 1969). Smith (1954)first reported the average Al-O and Si-O distances of various compounds which contained $AlO_4$and SiO_4 tetrahedra, in order to estimate the Al and Si distributions in the T sites of feldspars. Recently Prewitt et al. (1976) studied the synthetic sample of the high albite from 24°C to 1105°C by the X-ray method and reported the temperature dependence of the structure.

In the X-ray method the occupancy of Al and Si ions in T sites of feldspars was determined by comparing the T-O distance with the pure Al-O and Si-O distances which are obtained from other various crystals. Therefore the determined occupancy largely depends on the pure distances. Recently the neutron diffraction method has been used to determine directly the occupancies of Al and Si ions in the T sites (Prince et al., 1972; Brown et al., 1973; Harlow et al., 1973) and the results were, in principle, consistent with those of the X-ray method.

There have been a number of experimental studies about the order-disorder in feldspars as some studies are given above, but only few theoretical or non-experimental studies. Gait et al. (1970) applied the Pauling's second rule, the electrostatic valence balance rule for ionic crystals, on the low albite. The coordination number of Na ion, the pure Al-O and Si-O distances and the Al and Si distributions in the T sites, are derived by minimizing the value of "charge unbalance", where the value does not have the energy dimension, but it is one of the devices derived from the Pauling's rule. They concluded that the low albite have an ordered state of 82% Al ions in one T site. Tamada et al. (1976, 1977) roughly calculated the electrostatic energies of the high and low K-feldspars and albites, and electrostatic potentials of their T sites. They concluded that it was reasonable for Al and Si ions to be distributed randomly in T sites in the high temperature types and to be ordered in T sites in the low temperature types.

During the preparation of this paper a paper by Brown and Fenn (1979) was published, where structure energies of the alkali feldspars were calculated in the relation of the phenomenon of the large anisotropy of alkali ions and they also reported that the Al ion favored the T1(0) site in the high albite on the basis of electrostatic energy of the whole crystal.

The estimation of the ordering by the X-ray method is based on the difference of ionic radius between Al and Si ions. The estimation by the neutron method is based on the difference of the atomic scattering factors between them. The results by these two methods is consistent with each other as a whole. Now the difference between the electric charges of Al and Si ions must be given an attention to, because it is expected that the electrostatic energy plays an important role in the site preferences of Al and Si ions between the T sites of feldspars.

In this paper we will, therefore, try to estimate the Al and Si distributions in terms of the energy of the electrostatic energy and the Born's repulsive energy roughly estimated, to rationalize the above experimental results on the assumption that the crystals are ionic. If only the effects of the neighbouring four oxygens around the T site were taken into account, the larger Al ion would prefer the larger T site in terms of the size effect and the electrostatic potential of the larger T site would be higher, which is also favourable for the Al ions in terms of the electrostatic stability. The size effect would correspond to the estimation from the Born's repulsive energy. Then it is expected that it is reasonable

for the Al ion to occupy the larger T site in terms of the energetics. The Si ion is in the same situation for the smaller T site. Then it will be natural that the present approach based on the energetic model is consistent with the experimental results. One of the purposes of the present study is to assure this natural result from the actual energetic estimations as the first step of application of the Born's model.

III-1-B Computation and results

Electrostatic energies and potentials were calculated by the method of Bertaut (1952), using the program explained in Chapter II. Linear atomic shape was used as the optimum atomic shape after Jones and Templeton (1956). The standard errors caused by the errors of the structural data determined by the X-ray method were estimated only for the last calculation of each feldspar. The termination errors were corrected using the correction factor reported by Templeton (1955) and Jones and Templeton (1956). The summation of the infinite series in the reciprocal space was terminated at $h=3/2R$ and hence, the termination error was smaller than 0.3×10^{-3}, where h is the distance from the origin to a reciprocal lattice point and R is an assumed radius of charge distribution of ions.

Electrostatic energies of K-feldspars and potentials of their T sites, and those of albites and potentials of their T sites are listed in Table 1 and Table 2, respectively, for the assumed various distributions of Al and Si ions in the T sites, together with the standard errors. Sources of the structural data, T-O distances and Al contents are also listed in the footnotes of Tables. The above structural data are based on the refinement for anisotropic temperature factors of atoms, but in Table 3 electrostatic energies of the high albite and the potentials of their T sites calculated based on the structural data of isotropic quarter-atom model of Na ion, are

Table 1. The electrostatic energies (kcal/mol) of K-feldspars and the electrostatic potentials (kcal/mol.e) of T sites for the various Al distributions.

	Al distributions				
	T1(0)	T1	T1(m)	T2(0) T2	T2(m)	disordered
(1) Heated Sanidine(Eifel)					
E.S.Energy of Crystal	-13389			-13383		-13369(8)
E.S.Potential of T1	-1001.3*			-1068.5		-1034.9(1.6)
T2	-1074.8			-1005.7*		-1040.3(2.3)
(2) Low Sanidine(7002,Eifel)					
E.S.Energy of Crystal	-13381			-13370		-13359(7)
E.S.Potential of T1	- 997.0*			-1064.4		-1030.7(1.5)
T2	-1076.2			-1006.9*		-1041.6(2.1)
(3) Orthoclase(Spencer C)					
E.S.Energy of Crystal	-13404			-13379		-13374(14)
E.S.Potential of T1	- 991.8*			-1059.4		-1025.6(3.5)
T2	-1084.8			-1015.5*		-1050.2(4.8)
(4) Adularia(7007, Gotthard)					
E.S.Energy of Crystal	-13400			-13361		-13364(7)
E.S.Potential of T1	- 983.4*			-1051.0		-1017.2(1.5)
T2	-1090.4			-1021.3*		-1055.9(2.2)

(5) Intermediate Microcline(Spencer U)

E.S.Energy of Crystal		-13464	-13422	-13397	-13395	-13371(10)
E.S.Potential of	T1(0)	- 892.5*	-1026.8	-1017.7	-1037.1	- 993.8(3.3)
	T1(m)	-1069.4	- 934.9*	-1081.5	-1060.2	-1036.7(6.0)
	T2(0)	-1083.7	-1104.9	- 961.2*	-1087 7	-1059.6(3.8)
	T2(m)	-1104.8	-1085.2	-1089.3	- 962.8*	-1060.7(4.9)

(6) Maximum Microcline(Pellotsalo)

E.S.Energy of Crystal		-13503	-13403	-13392	-13393	-13374(12)
E.S.Potential of	T1(0)	- 859.4*	- 992.8	- 983.6	-1001.5	- 959.3(3.3)
	T1(m)	-1092.5	- 958.4*	-1105.9	-1083.1	-1060.0(6.5)
	T2(0)	-1092.7	-1115.2	- 970.1*	-1096.9	-1068.9(4.0)
	T2(m)	-1108.5	-1090.3	-1094.7	- 968.0*	-1065.6(5.4)

Structural data were taken from

(1) Weitz(1972)

(2) Phillips and Ribbe(1973)

(3) Colville and Ribbe(1968)

(4) Phillips and Ribbe(1973)

(5) Bailey(1969)

and (6) Brown and Bailey(1964).

Errors of energy and potentials of each feldspar, caused from the errors of structural data were calculated only in the disordered distribution. They are shown in the parentheses. In the case (5) the errors were calculated only based on the errors of atomic positions and not based on the errors of cell parameters because they cannot be found in the source paper.

The mean T-O distances and the Al distributions listed in Smith(1974) are as follows:

	T-O distance(Å)				Al content			
	T1(0)	T1(m)	T2(0)	T2(m)	T1(0)	T1(m)	T2(0)	T2(m)
(1) Heated Sanidine		1.645		1.641		0.26		0.225
(2) Low Sanidine		1.649		1.637		0.29		0.195
(3) Orthoclase		1.656		1.628		0.345		0.125
(4) Adularia		1.665		1.621		0.395		0.07
(5) Int.Microcline	1.694	1.642	1.618	1.616	0.63	0.235	0.045	0.03
(6) Max.Microcline	1.741	1.614	1.611	1.612	0.97	0.015-0.01		0.00

Table 2. The electrostatic energies (kcal/mol) of high and low albites and the electrostatic potentials (kcal/mol.e) of T sites for the various Al distributions.

	Al distributions				
	T1(0)	T1(m)	T2(0)	T2(m)	disordered
(1) High Albite(Amelia)					
E.S.Energy of Crystal	-13438	-13420	-13416	-13427	-13376(13)
E.S.Potential of T1(0)	- 922.2*	-1059.8	-1048.9	-1069.7	-1025.4(4.1)
T1(m)	-1076.6	- 940.4*	-1083.5	-1067.4	-1042.2(6.5)
T2(0)	-1070.0	-1087.7	- 944.9*	-1077.4	-1045.2(4.2)
T2(m)	-1079.1	-1059.9	-1065.7	- 934.4*	-1035.0(5.6)
(2) High Albite(Synthetic)					
E.S.Energy of Crystal	-13444	-13425	-13426	-13434	-13383(7)
E.S.Potential of T1(0)	- 923.7*	-1061.2	-1050.2	-1071.3	-1026.8(2.3)
T1(m)	-1079.9	- 943.7*	-1086.8	-1070.6	-1045.5(3.7)
T2(0)	-1067.5	-1085.5	- 942.7*	-1075.3	-1042.9(2.3)
T2(m)	-1079.9	-1060.5	-1066.5	- 935.0*	-1035.7(3.2)
(3) Low Albite(Ramona)					
E.S.Energy of Crystal	-13510	-13387	-13387	-13397	-13371(10)
E.S.Potential of T1(0)	- 845.8*	- 982.2	- 971.8	- 990.7	- 947.8(3.1)
T1(m)	-1104.6	-968.4*	-1114.4	-1095.5	-1070.9(5.9)
T2(0)	-1094.1	-1114.3	- 969.0*	-1102.3	-1070.1(3.4)
T2(m)	-1102.4	-1084.8	-1091.7	- 960.1*	-1059.9(5.0)

(4) Low Albite(Tiburon)

E.S.Energy of Crystal		-13519	-13400	-13399	-13412	-13383
E.S.Potential of	T1(0)	- 849.9*	- 986.3	- 976.0	- 994.8	- 952.0
	T1(m)	-1105.4	- 969.2*	-1115.2	-1096.4	-1071.8
	T2(0)	-1096.0	-1116.1	- 970.8*	-1104.2	-1072.0
	T2(m)	-1100.2	-1082.7	-1089.6	- 957.9*	-1057.8

Structural data were taken from

(1) Ribbe et al.(1969)

(2) Prewitt et al.(1976). (Data obtained at 24°C)

(3) Ribbe et al.(1969)

(4) Wainwright(1968, as reported in Smith,1974).

Errors of energy and potentials of each feldspar,caused from the errors of structural data were calculated only in the disordered distribution. They are shown in the parentheses. In the case (4) there was no error calculation because the structural error cannot be found in the source paper.

The mean T-O distances and indicated Al distributions listed in Smith(1974) are as follews:

	T-O distance (Å)				Al content			
	T1(0)	T1(m)	T2(0)	T2(m)	T1(0)	T1(m)	T2(0)	T2(m)
(1) High Albite	1.648	1.644	1.639	1.643	0.28	0.25	0.21	0.24
(2) High Albite	1.646	1.641	1.641	1.642				
(3) Low Albite	1.746	1.610	1.615	1.612	1.005	-0.015	0.025	0.00
(4) Low Albite	1.740	1.609	1.614	1.615	0.965	-0.025	0.015	0.025

Table 3. The electrostatic energies (kcal/mol) of high albite and the electrostatic potentials (kcal/mol.e) of T sites for the various Al distributions, which were calculated using the structural data for the isotropic quarter atom model of Na ion.

	Al distributions				
	T1(0)	T1(m)	T2(0)	T2(m)	disordered
(1) High Albite(Synthetic)					
E.S.Energy of Crystal	-13268	-13251	-13251	-13259	-13208
E.S.Potential of T1(0)	- 924.3*	-1061.8	-1050.8	-1071.9	-1027 4
T1(m)	-1078.2	- 942.1*	-1085.2	-1068.9	-1043.8
T2(0)	-1067.0	-1085.0	- 942.1*	-1074.7	-1042.4
T2(m)	-1079.3	-1059.9	-1065.9	- 934.4*	-1035.1

Structural data were taken from
(1) Prewitt et al.(1976) (data obtained at 24°C).

shown to know the effect of the large anisotropy of alkali ions in the feldspars.

The calculations were carried out for three or five cases in each feldspar, when all the Al ions occupied each T site (ordered cases) and when Al and Si ions were distributed randomly in the T sites (disordered case). In the ordered cases of the monoclinic feldspars the average charges 3.5e and 4e (e; electron unit) were assigned to the T sites occupied by Al ions and not occupied by them, respectively, because the monoclinic feldspars have only two T sites while the content of Al ion is one forth of the Al and Si ions. In the ordered cases of the triclinic feldspars the average charges 3e and 4e were assigned to the T site occupied by Al ions and other three sites occupied by Si ions, respectively. In the disordered case the average charge 3.75e was assigned to all the T sites.

Typical CPU times were about 50 seconds for the monoclinic feldspars and 70 seconds for the triclinic feldspars by the calculations of the FACOM M-190 computer of Kyoto University, and about 380 seconds when the standard errors were calculated together, although the summation of the infinite series was terminated at h=1/R for the monoclinic feldspars and h=3/4R for the triclinic feldspars for the saving of CPU time.

III-1-C Discussion

(1) The distributions of Al and Si ions in the T sites.

At first the entropy S and the volume V for the ordered distributions of Al and Si ions in the T sites of each feldspar must be taken into account in order to compare the Gibbs' free energies G between these distributions. It is easy to suppose that the entropies of the configurations are the same each other for the completely ordered distributions which are assumed in the calculations, and then entropy differences are far small. The volume differences are equal to zero because the original cell parameters are used for all the calculations of ordered cases in each feldspar. The difference of the free energies G is, therefore, equal to that of internal energies E which are here represented by the sum of the electrostatic and Born's repulsive energies.

In the high temperature types of K-feldspars and albites the differences of electrostatic energies of the whole crystal for the various ordered distributions of Al and Si ions are small, about 5 kcal/mol for the heated sanidine and smaller than 25 kcal/mol for the high albites as shown in Table 1 and 2. These differences are included in the range of standard errors. The energy differences increase from the high to low temperature types as observed in the K-feldspars. In the low temperature types the differences are very large. The crystals are remarkably stabilized both in the maximum microcline and the

low albite when Al ions occupy the T1(0) site and Si ions the other three T sites. The energy differences between the Al distribution in T1(0) site and the other three ordered distributions amount to more than 100 kcal/mol. Of course these differences are large enough and meaningful compared with the standard errors. The present result is consistent with the result of the high albite by Brown and Fenn (1979).

The same results are also observed in the potentials of T sites at the disordered distribution and in the potentials of T site occupied by Al ions of each ordered distribution (the potentials of *mark), if it is kept in mind that the electrostatic stability forces the Al^{3+} ion to occupy the site with the high electrostatic potential and the Si^{4+} ion to occupy the site with the low electrostatic potential. In the disordered distributions the potentials of T sites are almost equal to each other in the high temperature types. The differences of them become large from the high to low temperature types and the potential of the T1(0) site is remarkably high in the low temperature types. The potentials of T sites occupied by Al ions of each ordered distribution (the potential of *mark) are in the same situation as the potentials of disordered distributions already mentioned.

It is concluded based on the electrostatic energy that Al and Si ions are distributed randomly between T sites of the high temperature types, while they are ordered in low temperature types. The T1(0) site is occupied by Al ions and the other three sites occupied by Si ions.

In the intermediate and maximum microclines it is already known that a large part of Al ions occupy the T1(0) site, but the problem is still left how the residual Al ions should be distributed in the other three T sites except the T1(0) site. Electrostatic energies of the whole crystal are stable for the distribution of Al ions first in the T1(m) site, and second in the T2(0) and T2(m) sites within the standard errors. It is, therefore, expected that the residual Al ions prefer the T sites in this order. The potentials of T sites at the disordered distribution and those of the T site occupied by Al ions of each ordered distribution (the potentials of *mark) lead to the same result.

In the high and low albites Al ions, of course, prefer the T1(0) site, too. The electrostatic stability indicates that the residual Al ions occupy first the T2(m) site, and second the T1(m) and T2(0) sites. This result is inconsistent with the result determined by Ribbe et al. (1969) in the high and low albites as shown in the footnote, but it is consistent with the results by Wainwright and Starkey (unpublished, as reported in Smith, in 1974) and by Prewitt et al. (1976) in the high albite, and by Wainwright and Starkey (1968) and by Harlow et al. (1973) in the low albite (see the textbook by Smith, 1974, p71). The Al ions, therefore, appear to concentrate first in T1(0) site, secondary in T2(m) site and in the last T1(m) and T2(0) sites. The order of concentration of Al ions is different between the K-feldspars and the albites.

The repulsive energies of the T site when the Al and Si ions occupy the T site and the total repulsive energy of two or four T sites for the assumed ordered cases of the Al and Si ions are listed in Table 4. Only the interactions between the Al or Si ion in the T site and the neighbouring four oxygens are taken into account in the above repulsive energies because the repulsive energy becomes rapidly negligible with increase of the distance between the two ions. The repulsive constants are taken from Miyamoto et al. (1979 and private comm.) which were reported just before this writing. The reliability of these constants are, therefore, unknown, but it is almost unlikely that the results change into the opposite sense from those on this present repulsive energies because it is also unlikely for the results based on the repulsive energies to break the size effect.

In Table 4 only the repulsive energies of the each high and low two temperature types of K-feldspars and albites are estimated. The total repulsive energies ($R.E.T_{\cdot}$) for the various assumed distributions of Al and Si ions are almost same for the high temperature types and remarkably small for the low temperature types when the Al ion occupy the T1(0) site. The order of the stability in terms of the repulsive energy for the various assumed distributions are quite as same as that obtained in terms of the electrostatic energy. It is, therefore, concluded that the electrostatic and repulsive energies affect the distributions of the Al and Si ions in the same sense and the distributions estimated from this energetics

Table 4. The rough estimations of the Born's repulsive energy of the T site (R.E.Al) when the Al ion occupy the T site, that of the T site (R.E.Si) when the Si ion occupy the T site and the total repulsive energy (R.E.T) of two or four T sites when the Al ion occupies the each T site (ordered cases). (In kcal/mol)

	T1		T2	
	T1(0)	T1(m)	T2(0)	T2(m)
(1) Heated Sanidine (Eifel)				
R.E.Al	417.0		433.7	
R.E.Si	195.6		202.8	
R.E.T	1018.2		1027.7	
(6) Maximum Microcline (Pellostsalo)				
R.E.Al	177.2	553.8	577.9	570.9
R.E.Si	89.3	253.5	263.3	260.5
R.E.T	954.5	1166.9	1181.2	1177.0
(2) High Albite (Synthetic)				
R.E.Al	412.0	432.7	431.5	428.5
R.E.Si	193.5	202.3	201.8	200.5
R.E.T	1016.6	1028.5	1027.8	1026.1
(4) Low Albite (Tiburon)				
R.E.Al	178.4	576.4	554.0	551.6
R.E.Si	89.9	263.0	253.6	252.5
R.E.T	947.5	1172.4	1159.4	1158.1

Repulsive energies between Al or Si ions and neighbouring four oxygens are only taken into account. Structural data were refered to the footnotes in Tables 1 and 2.

Repulsive constants are taken from Miyamoto et al.(1979 and private comm.)as

	A_i (Å)	B_i (Å)
Al^{3+}	0.641	0.0069
Si^{4+}	0.608	0.0172
O^{2-}	1.770	0.1052

in the expression of $U_{ij} = C(B_i + B_j) \exp \frac{A_i + A_j - r_{ij}}{B_i + B_j}$
where C = 1.0 kcal/mol.

is quite consistent with the experimental results determined by the X-ray or neutron method as was expected above. In other words the structures seem to be modified in order to gain the larger energetic stability. This consistency assures the usefulness for the Born's model for ionic crystals to be applied on the order-disorder of Al and Si ions in other feldspars and also encourages us to apply it on the Al and Si distributions in other silicate minerals, for example, to those in the T(A) and T(B) sites of orthopyroxenes.

(2) The positive feedback effect on the Al and Si ordering.

It is observed in Tables 1 and 2 that the potential of a certain T site of each feldspar becomes high when Al ions are distributed in the T site, low when Al ions are not distributed in the T site and in the middle when Al and Si ions are distributed randomly. For example, the potential of the T1 site of the heated sanidine is -1001.3 kcal/mol.e when Al ions are distributed in the T1 site, -1068.5 kcal/mol.e when Al ions in the T2 site and -1034.9 kcal/mol.e when the Al and Si ions are distributed randomly, as shown in Table 1. The potential of a T site is heightened with increase of Al ions in the T site and lowered with increase of Si ions in the T site. As mentioned above, Al ion prefers the site with higher potential and Si ion prefers the site with lower potential in order to gain the larger electrostatic stability. Therefore the above result leads to the positive feedback in the Al and Si ordering in the T sites as follows: If some of Al ions concentrated in a T site for some structural reason, the potential of the site would be heightened and the more Al ions would concentrate in the site. It is also same for Si ions if it is kept in mind that Si ions are in the inverse situation for the electrostatic potential. This positive feedback effect is disturbed by the entropy term in the high temperature types, but affects strongly on the Al and Si ordering in the low temperature types. The almost complete ordering of Al and Si ions in the low temperature types as in the maximum microcline and the low albite is

considered to be ascribed to this positive feedback effect and the structural modification.

Alkali atoms in feldspars have the large anisotropy of displacements. This is observed in their temperature factor and in the difference Fourier maps around them. In order to know the effect of the anisotropy of alkali atoms on the electrostatic energies and potentials they were calculated based on the structural data of the high albite, refined for the isotropic quarter atom model of Na atoms. The results which are shown in Table 3, are consistent with those based on the anisotropic single atom model of Na atoms, both for the Al and Si order-disorder phenomenon and the positive feedback effect. Thus it is concluded that the effect of the anisotropy of alkali atoms is not essential for the present discussions.

III-2 The energetic study of polymorphs of M_2SiO_4 stoichiometry (M=Ni, Mg, Co, Fe and Mn).

III-2-A Introduction

$(Mg, Fe)_2SiO_4$ polymorphs, olivine (α phase), modified spinel (β phase) and spinel (γ phase), are important silicate minerals in earth sciences because they are considered to be the main constituent minerals in the upper mantle and the seismic velocity changes at the depth of 400-600km in the mantle are thought to be due to the phase transitions among these polymorphs.

Stability relations of these polymorphs have been extensively studied (see, for example, Akimoto et al., 1976), but comparatively few theoretical or crystal chemical studies have been made on the relevant transitions. Kamb (1968) first discussed the stability relation of olivine and spinel on the basis of the Pauling's rules for ionic crystals. Baur (1972) simulated nine different polymorphs of Mg_2SiO_4 stoichiometry using the distance least squares (DLS) method. He supported Kamb's explanation for the stability relation from the viewpoint of the geometrical adjustment of structures. Sung and Burns (1978) compared the structural features of olivine, modified spinel and spinel, and discussed the mechanism for the olivine to spinel transition. The above crystal chemical discussions were based on the Pauling's rules for ionic crystals, which are, in principle, based on the electrostatic energy. It is, therefore, important to see the electrostatic energies of these polymorphs in order to reveal their energetics.

The applications of the electrostatic energy to the

tability relations of the silicate minerals are not so many. Raymond (1971) estimated the Madelung constants for several silicates. Whittaker (1971) discussed the site preferences in amphiboles in terms of electrostatic energy. Ohashi and Burnham (1972) estimated electrostatic and repulsive energies of cation sites in ortho- and clino-pyroxenes, and discussed the site preference. Tamada et al. (1976, 1977) reported the consistency between the results on the Al and Si distributions in alkali feldspars, obtained by the X-ray or neutron method and by electrostatic energies. Tokonami et al. (1972) discussed the stability relations of olivine, modified spinel and spinel, on the basis of electrostatic and repulsive energies, and concluded mainly based on the result of electrostatic energy that modified spinel was not so unstable compared with the other two phases.

The purpose of the present study is, first, to reveal the structural features and the stability relations of these polymorphs, second, to demonstrate the effect of ionic size on the electrostatic stability. In all the following discussions the polymorphs are assumed to be ionic and the electrostatic and Born's repulsive energies are taken into account for the bonding energy between ions.

II-2-B Computation and results

Electrostatic energies of M_2SiO_4 polymorphs are calculated by the method of Bertaut (1952), under the assumption that crystals are ionic and the constituent ions M, Si and O have the electric charges of 2e, 4e and -2e, respectively, corresponding to the oxidation numbers. Linear atomic shape was used as optimum atomic shape after Jones and Templeton (1956), where the value 0.75-0.80Å was used for the assumed radius R of charge distribution of ions, in order to avoid the overlap of the charge distributions. The standard deviations caused by the propagation of errors are estimated from those of cell parameters and atomic positions. The summation of infinite series in the reciprocal space was terminated at h=1/R where h is the distance from the origin to a reciprocal lattice point. The calculation error caused by the termination effect is less than 10^{-3} (Templeton, 1955; Jones and Templeton, 1956), which is comparable with the estimated standard errors.

Electrostatic energies of M_2SiO_4 polymorphs and their constituent ions are shown in Table 1 together with standard errors, sources of atomic positions used and R-factors. Typical CPU times were about 100 seconds for olivine and spinel, and 450 seconds for modified spinel for the computation by FACOM M-190 computer, using the program written by the author.

Electrostatic energies of the M ions, the Si ions, the O ions and the whole crystals are plotted against the ionic radius ratio r_M/r_{Si} in Figs. 1, 2, 3 and 4.

Table 1. Electrostatic energies of M_2SiO_4 polymorphs and their constituent ions with standard errors estimated from the errors of cell parameters and atomic positions. (In kcal/mol)

Olivines		Modified spinel		Spinels	
		Ni_2SiO_4 [a]			
Crystal	-5773.8(1.5)			Crystal	-5821.6(1.3)
Ni1	-1086.6(0.8)			Ni	-1162.4(0.7)
Ni2	-1179.6(0.6)			Si	-4407.7(2.9)
Si	-4300.5(2.1)			O	-1227.6(0.2)
O1	-1283.6(0.7)				
O2	-1265.8(0.9)				
O3	-1215.8(0.7)				
		Mg_2SiO_4 [b]			
Crystal	-5766.1(0.8)				
Mg1	-1082.1(0.3)				
Mg2	-1159.2(0.3)				
Si	-4318.0(1.0)				
O1	-1276.0(0.4)				
O2	-1268.4(0.4)				
O3	-1214.3(0.3)				
		Co_2SiO_4 [c]			
Crystal	-5744.4(1.3)	Crystal	-5790.8(5.8)	Crystal	-5786.3(1.1)
Co1	-1063.4(0.6)	Co1	-1131.4(10.6)	Co	-1129.8(0.5)
Co2	-1155.9(0.5)	Co2	-1140.3(6.5)	Si	-4435.2(2.3)
Si	-4317.7(1.8)	Co3	-1163.8(5.1)	O	-1219.5(0.2)
O1	-1272.2(0.6)	Si	-4365.1(11.6)		
O2	-1262.0(0.8)	O1	- 976.5(6.1)		
O3	-1208.8(0.6)	O2	-1416.8(9.1)		
		O3	-1239.2(9.6)		
		O4	-1240.5(3.1)		
		Fe_2SiO_4 [d]			
Crystal	-5722.6(1.2)			Crystal	-5749.9(0.9)
Fe1	-1041.0(0.6)			Fe	-1101.1(0.5)
Fe2	-1135.7(0.5)			Si	-4454.4(2.0)
Si	-4346.6(1.8)			O	-1210.8(0.2)
O1	-1261.5(0.7)				
O2	-1253.3(0.8)				
O3	-1203.5(0.5)				

Mn_2SiO_4 e)

Crystal	-5670.4(1.5)
Mn1	-1014.7(0.7)
Mn2	-1101.6(0.5)
Si	-4348.0(2.2)
O1	-1247.5(0.8)
O2	-1245.2(0.9)
O3	-1191.9(0.6)

Sources of Atomic Coordinates and R factors:

a) Olivine: Tamada et al.(in preparation) R=0.029.
Spinel : Marumo et al.(1974). R=0.017.

b) Olivine: Fujino et al. (in preparation). R=0.0209.

c) Olivine: Tamada et al.(in preparation) R=0.028.
Modified spinel: Morimoto et al.(1974). R=0.053.
Spinel : Marumo et al.(1977) R=0.0154.

d) Olivine: Fujino et al.(in preparation). R=0.0255.
Spinel : Marumo et al.(1977) R=0.0138.

e) Olivine: Fujino et al.(in preparation). R=0.0310.

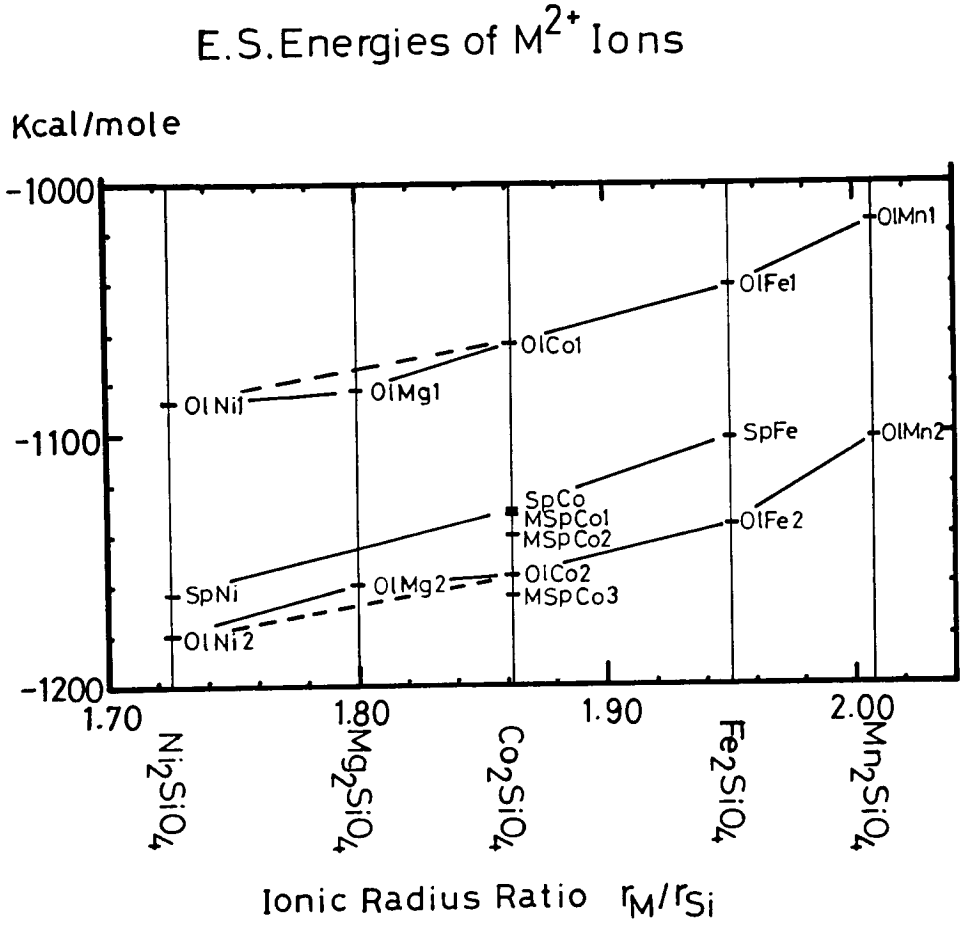

Fig. 1. Electrostatic energies of M ions of M_2SiO_4 polymorphs versus ionic radius ratio r_M/r_{Si}. Olivine, modified spinel and spinel are abbreviated as Ol, MSp, Sp in the figure.

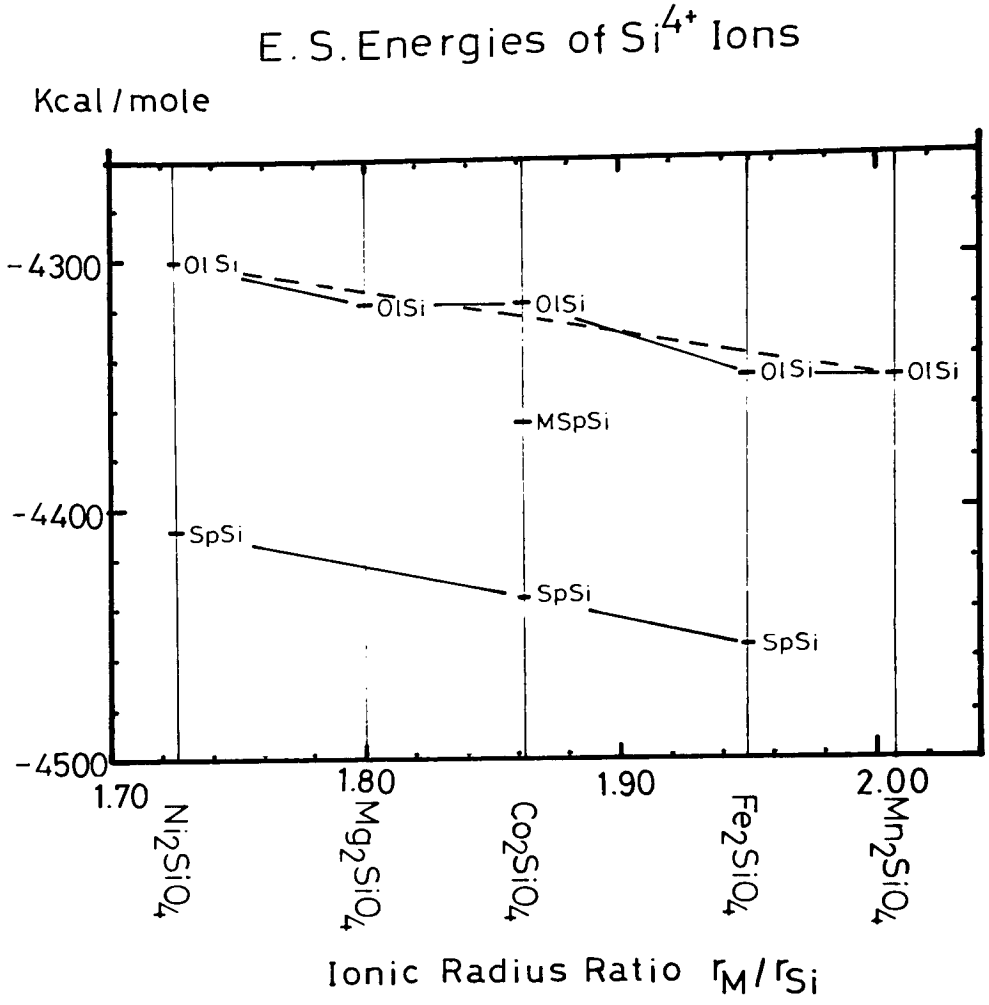

Fig. 2. Electrostatic energies of Si ions of M_2SiO_4 polymorphs versus ionic radius ratio r_M/r_{Si}. Olivine, modified spinel and spinel are abbreviated as Ol, MSp and Sp in the figure.

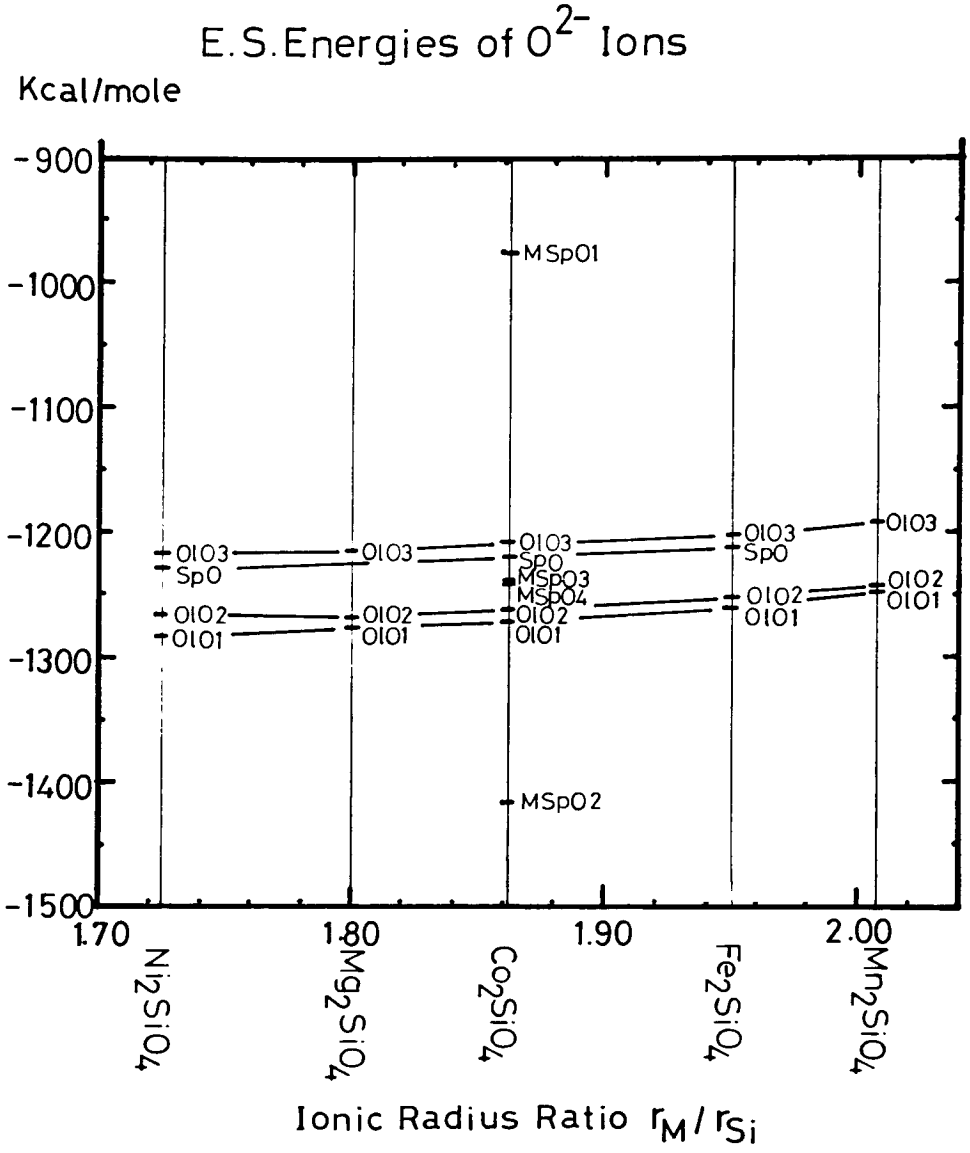

Fig. 3. Electrostatic energies of O ions of M_2SiO_4 polymorphs versus ionic radius ratio r_M/r_{Si}. Olivine, modified spinel and spinel are abbreviated as Ol, MSp and Sp in the figure.

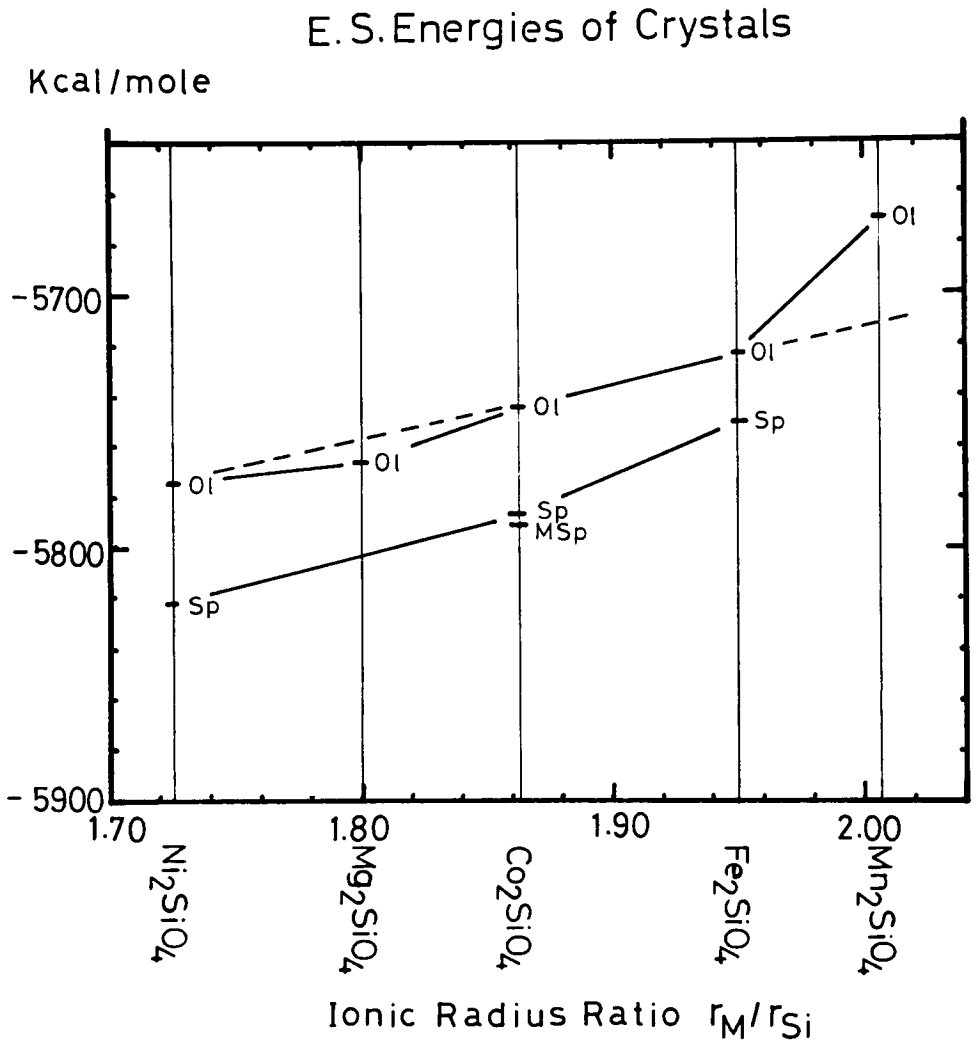

Fig. 4. Electrostatic energies of crystals of M_2SiO_4 polymorphs versus ionic radius ratio r_M/r_{Si}. Olivine, modified spinel and spinel are abbreviated as Ol, MSp and Sp in the figure.

III-2-C Discussion

(1) Characteristics of each polymorph

Olivine

A characteristic feature of the olivine structure is the large difference in electrostatic energy between the M1 and M2 sites; the former is about 90 kcal/mol higher than the latter. The electrostatic energy of the M2 site of olivine is the lowest among those of the M sites of the three polymorphs except that of the M3 site of modified spinel. The electrostatic energy of the M1 site is, on the other hand, the highest among those of the M sites of the polymorphs as shown in Table 1 and Fig.1. The highest electrostatic energy of the M1 site does not result from the contribution of the nearest neighbouring oxygens because the M-O distance of the M2 site is longer than that of the M1 site (Table 2). The M1 octahedron shares four edges with the adjacent M octahedra and two edges with the adjacent Si tetrahedra, while the M2 octahedron shares two edges with the adjacent M octahedra and one edge with the Si tetrahedron (Kamb, 1968). It is, therefore, reasonable in the light of Pauling's rule for edge sharing that the electrostatic energy of the M1 site is higher than that of the M2 site.

Another feature of olivine structure is the highest electrostatic energy of the Si site among those of the Si sites of three polymorphs. This is consistent with the Pauling's rule for edge sharing. The Si tetrahedron of olivine shares three edges with the adjacent M octahedra while the Si tetrahedra of

Table 2. Interatomic distances of polyhedra of Co_2SiO_4 polymorphs/(Morimoto et al.,1974).

Bonds	Mean distances (Å)
	α - Co_2SiO_4
Col - O	2.125
Co2 - O	2.143
Si - O	1.627
	β - Co_2SiO_4
Col - O	2.107
Co2 - O	2.115
Co3 - O	2.121
Si - O	1.642
	γ - Co_2SiO_4
Co - O	2.104
Si - O	1.646

modified spinel and spinel share no edge with the adjacent M octahedra (Kamb, 1968; Morimoto et al., 1974).

The electrostatic energy of olivine is about 25-50 kcal/mol higher than those of modified spinel and spinel. The instability of olivine is mainly due to the high electrostatic energies of the M1 and Si sites.

Modified spinel

The electrostatic energies of M sites of the modified spinel are rather low compared with those of M sites of other polymorphs, especially that of the M3 site is the lowest. The lowest electrostatic energy of the M3 site among three M sites of modified spinels, as well as that of the M2 site of olivine does not result from the contribution of the nearest neighbouring oxygens because the M3-O distance is the largest (Table 2). The M1 and M2 octahedra of the modified spinel share six edges with the adjacent M octahedra, while the M3 octahedron shares seven edges with the adjacent M octahedra. It would be essential for these low energies of the M sites that each M octahedron shares no edge with the adjacent Si tetrahedron.

The Si tetrahedron does not share edges with M octahedra and therefore the relative stability of Si site of modified spinel to that of olivine is reasonable in the light of the Pauling's rule for edge sharing. But it cannot be explained by the Pauling's rule that the electrostatic energy of Si site is higher than that of spinel.

The main feature of the modified spinel is the extremity in electrostatic energies of two oxygens. The electrostatic energy of the O1 ion is remarkably high, and that of the O2 ion is remarkably low compared with any O ion of the three polymorphs. The energy difference between the O1 or O2 ion and the other O ions of the polymorphs amounts to a few hundreds kcal/mol. Morimoto et al. (1969, 1970) and Moore and Smith (1969, 1970) reported that the O1 and O2 ions break the Pauling's electrostatic valence rule. The results in electrostatic energies are consistent with this fact.

The electrostatic energy of modified spinel is as low as that of spinel and remarkably lower than that of olivine. This stability largely depends on the low electrostatic energies of M sites.

Spinel

The electrostatic energy of the M site of spinel is not so low compared with those of the M sites of the other polymorphs except that of the M1 site of olivine. The M octahedron shares six edges with the adjacent M octahedra and does not share edge with Si tetrahedra. A part of the instability of M site of spinel may be caused by the fact that the shared edges are longer than the unshared edges in spinel (Kamb, 1968).

The feature of spinel structure is that the electrostatic energy of Si site is remarkably low compared with those of Si sites of the other polymorphs. This feature is not ascribed to the contributions of the nearest neighbouring oxygens

because the Si tetrahedron of spinel has the largest mean Si-O distance (Table 2). The Si tetrahedron does not share edge with the M octahedron. This is consistent with the remarkable stability of Si site of spinel.

The electrostatic energy of spinel is as low as modified spinel and much lower than that of olivine. The high stability of spinel depends largely on the low electrostatic energy of Si site.

(2) The stability relations of olivine, modified spinel and spinel.

Tokonami et al. (1972) calculated electrostatic energies of three polymorphs of Co_2SiO_4 and obtained the result that olivine should be electrostatically the most stable while modified spinel the least stable. Electrostatic energies of olivine, modified spinel and spinel were reported as -5808.8, -5789.2 and -5796.8 kcal/mol, respectively. In the present systematic calculations as shown in Table 1, modified spinel and spinel are electrostatically more stable than olivine, even if the standard errors are taken into account. Accurate structure determinations of different M_2SiO_4 modified spinels are required for further consideration to settle the problem.

The explanation for much greater stability of the olivine structure at atomospheric pressure was proposed by Kamb (1968) on the basis of the Pauling's rule for edge sharing for ionic crystals. According to Kamb the olivine structure is unfavorable relative to spinel as far as shared edges are concerned, but it is counterbalanced by shortening of the shared edges. The shared edges in the spinel structure are much longer than unshared edges, whereas the olivine structure allows the shared edges to shorten in a natural way. He suggested that this basic difference is the primary cause of the large difference in stability between the olivine and spinel forms. This explanation has been widely accepted (Baur, 1972; Morimoto et al., 1974; Sung and Burns, 1978). But the present study shows that spinel is electrostatically

more stable than olivine. The Kamb's explanation is not supported by the comparison of electrostatic energies. An extension and amendment of the Pauling's rule regarding shared edges was proposed by Baur (1972) on the basis of the simulations of nine different polymorphs of Mg_2SiO_4 by the method of the distance least squares (DLS). It is as follows: Ionic structure with shared polyhedral edges and faces can only be stable if their geometry allows the shortening of the shared polyhedral edges. The geometry of the olivine structure allows the shortening of the shared polyhedral edges, but that of spinel does not allow it on the basis of simulations by the DLS method. He suggested that the instability of spinel at atomospheric pressure was ascribed to this unfavourable geometrical adjustment.

Since the stress of geometrical adjustment is the short range interaction between ions which has the relation with the size effect, the Born's repulsive energy must be taken into consideration.

In order to study the stability relations of these polymorphs at atmospheric pressure and room temperature from the energetic viewpoint, it is necessary to compare their Gibbs' free energy $G=U+PV-TS$. The energy differences $P\Delta V$ and $T\Delta S$ between them are far smaller than 1 kcal/mol and quite negligible at the above conditions. Then the difference of the Gibbs' free energy ΔG is almost equal to that of the internal energy ΔU, which is now assumed to depend on the electrostatic energy and the repulsive energy as proposed by Born for ionic

crystals. The Born's repulsive energies of α, β and γ-Co_2SiO_4 were estimated as 716.8, 708.1 and 714.0 kcal/mol respectively by Tokonami et al. (1972), applying the values of the bulk modulus of CoO and the basic radii of O, Si and Co ions estimated by them on the equation by Huggins and Sakamoto (1957).

Miyamoto et al. (1979) reported the repulsive constants of Mg^{2+}, and Si^{4+} and O^{2-} ions by applying the least squares method on the forsterite structure to determine the constants in order that each ion in the structure has the energy minimum at the actual positions. They also estimated the repulsive energies of α and γ-Mg_2SiO_4 as 435.8 and 433.4 kcal/mol using the above constants.

The differences of the repulsive energy between olivine and spinel estimated by Tokonami et al. and Miyamoto et al. are too small to compensate the difference of the electrostatic energy about 40 kcal/mol. The thermodynamic fact that the olivine form is stable at the atomospheric pressure and room temperature can not now be explained by the above energetics based on the electrostatic energy and the Born's repulsive energy for ionic crystals. The large difference of the electrostatic energy, about 40 kcal/mol can be modified by no means as far as the crystals are assumed to be ionic, and only slightly reduced to one forth of it, about 10 kcal/mol even if the net atomic charges of half of the formal charges were introduced for the constituent ions. Thus the discrepancy between the above energetics and the thermodynamical fact must be attributed to the assumption that either the energetic

model above used can be applied to these polymorphs, or to the estimated repulsive energies. The assumption is the basis of the present discussion and the problem becomes too complex to be studied if the assumption was changed. The assumption is kept without changing in order to develop the discussion in the present study. The repulsive constants were determined by the complex and delicate procedures and the repulsive energies are not generally accepted in the present stage. It is therefore, reasonable to consider that the estimated repulsive energy is responsible for the discrepancy. If the discrepancy is attributed to the repulsive energies, they can be estimated qualitatively as follows and the stability relations of these polymorphs under high pressures can be discussed on the basis of following two criteria.

The repulsive energy is the basis of resistance to the compression because it forces the ions to act as if they are fairly hard and to resist overlapping, then it is essential for the stability of minerals under high pressures. This suggests that the structure with high repulsive energy can survive under high pressures. Hereafter, this will be referred to as the first criterion. Electrostatic energies of modified spinel and spinel are almost the same each other and much lower than that of olivine as mentioned above. Olivine is thermodynamically stable at the atmospheric pressure and room temperature. The repulsive energy of olivine, therefore, has to be much smaller than those of modified spinel and spinel as far as the Born's model is applied on these polymorphs, as shown schematically in Fig. 5.

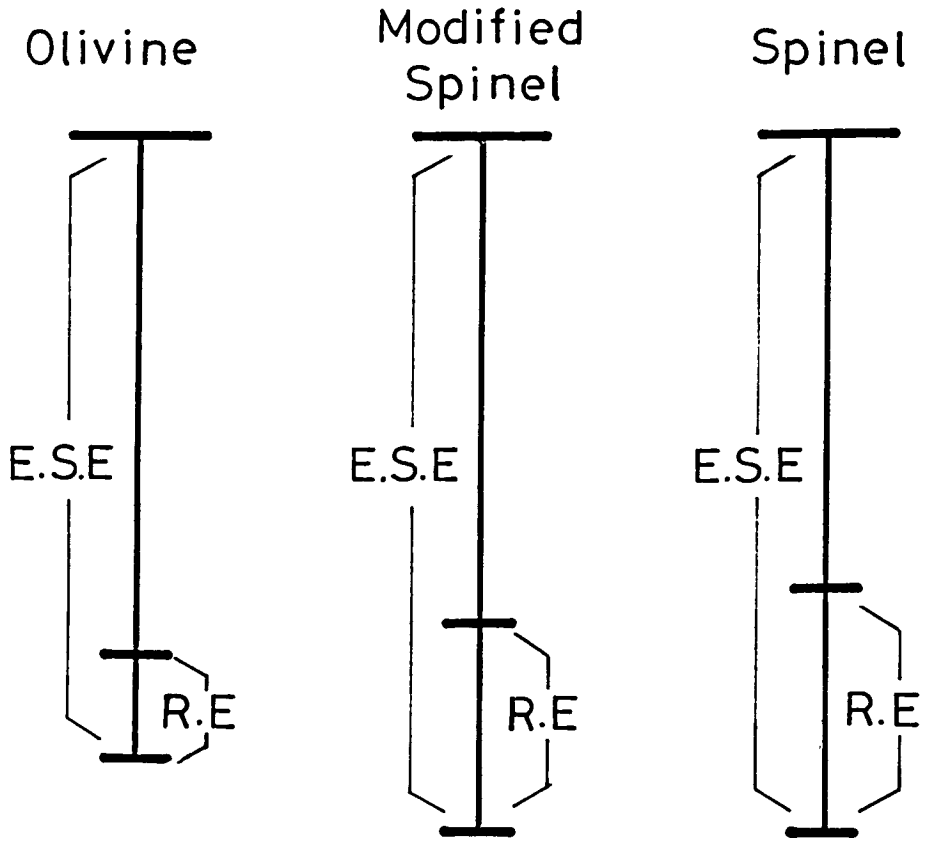

Fig. 5. Schematic figure of electrostatic energies and repulsive energies of olivine, modified spinel and spinel. Electrostatic energy and repulsive energy are abbreviated as E.S.E. and R.E. in the figure.

In order that a compound can survive under high pressures, the constituent ions must equally resist the compressive force and the force must never be concentrated on a certain ion. This leads to another criterion of being stable under high pressures. Now, let the structure be called "energetically simple", if the electrostatic energy of each atomic site is nearly equal to each other. Then it can be said that the "energetically simple" structure tends to survive under high pressures.

On the basis of the above two criteria, the stabilities of these polymorphs are interpreted as follows: The olivine structure is unstable under high pressures because it has lower repulsive energy and is energetically not simple as discussed above in terms of electrostatic energies in individual sites. The modified spinel structure has high repulsive energy, but it lacks the energetic simplicity, especially for the O ions. It cannot, therefore, survive under very high pressures. The spinel structure, on the other hand, satisfies these two criteria. It can, therefore, survive under high pressures.

These two criteria await further applications for other examples to assure their validity and usefulness.

(3) The effect of ionic size on electrostatic energy.

Electrostatic energies of the M ions, Si ions O ions and the whole crystal are plotted against ionic radius ratio r_M/r_{Si} in Figs. 1, 2, 3 and 4. The ionic radii by Shannon and Prewitt (1969) were used for the ionic radius ratio in the figures. Electrostatic energies of the M1 and M2 ions of olivine and the M ion of spinel become higher with increase of the ionic radius ratio. This increase is natural because the surroundings of these M ions are expanded with increase of this ratio. A characteristic feature of Fig. 1 is the slight deviation of electrostatic energies of the M1 and M2 ions in Mg_2SiO_4 olivine from the plotted line of those of transition metal olivines. A rapid increase of electrostatic instability of the M1 and M2 ions from Fe_2SiO_4 olivine are also noted. The main feature in electrostatic energies of Si sites is that those of Si sites of olivine and spinel become lower with increase of the ionic radius ratio. It is due to the compression around Si site with increase of the size of M ion. A part of decrease of electrostatic stability of olivine and spinel with increase of the ratio is compensated by the lowering of electrostatic energy of Si ion. Electrostatic energy of Si ion of Mg_2SiO_4 olivine appears to be slightly lower and that of Mn_2SiO_4 olivine appears to be slightly higher than the trend of other Si ions. Electrostatic energies of O sites of olivine and spinel show an only slight increase with increase of the ionic radius ratio. Fig. 3 shows that electrostatic energies of O sites of the polymorphs fall in

a small range of energy except the O1 and O2 sites of modified spinel.

As the summation of electrostatic energies of M, Si and O sites, those of the whole crystals become higher with increase of ionic radius ratio. In other words, the increase of ionic size of M ion results in the decrease of electrostatic stability of olivine and spinel. This means that the crystals become unstable in the larger side of ionic size of M ion. Electrostatic energy of Mg_2SiO_4 olivine as well as those of M and Si ions, is slightly out of the line of those of transition metal olivines. This is because of the slight difference of atomic positions of Mg_2SiO_4 olivine from those of transition metal olivines, since these electrostatic energies only depend on the structural data.

In olivine the electrostatic energy culminates at Mn_2SiO_4. A similar feature is observed in electrostatic energies of M and Si ions. Then let's examine the stability of Ca_2SiO_4 olivine in which Ca ion has the same valence and slightly larger ionic size than Mn ion. Transition metal and Mg silicates of M_2SiO_4 have the olivine structure under the whole temperature range and atmospheric pressure, whereas Ca_2SiO_4 silicate shows four different kind of crystal structures, one of which is olivine, under the same external conditions (Smith et al., 1965). Therefore it may be deduced that the olivine structure of Ca_2SiO_4 silicate is not far more stable than the other crystal structures. This is anticipated from the rapid increase of electrostatic energy with increase of ionic size.

A gradual increase in electrostatic energy is observed at Fe_2SiO_4 in spinel. Mn_2SiO_4 spinel has never been synthesized. Instead, Mn_2SiO_4 olivine decomposes into MnO (rock salt structure) plus $MnSiO_3$ (tetragonal garnet structure) at 140 kbar and 1000°C without phase transition to the spinel structure (Ito et al., 1974). Electrostatic energies of spinels and their constituent ions have all the same trend as those of olivines and their constituent ions. It is then expected that there is also a rapid increase in electrostatic energy at Mn_2SiO_4 spinel. From these results we can derive the following views: There is an change in energetic stability between Fe_2SiO_4 and Mn_2SiO_4 of olivine and spinel. The olivine structure is more tolerant than the spinel structure in the larger side of ionic size of M ions as suggested by Kamb (1968).

Chapter IV Accurate structure refinements of synthetic Co and Ni-olivines and a theoretical explanation of the atomic charges of olivines and orthopyroxenes.

IV-1 Accurate structure refinements of synthetic Co_2SiO_4 and Ni_2SiO_4 olivines.

IV-1-A Introduction

Mg and transition metal olivines are considered to compose the main constituent of the lower crust and the upper mantle. It is, therefore, valuable both in crystal chemistry, and earth sciences to determine accurate structures of Mg and transition metal olivines, including the charges of ion and the electron density distributions.

Only few refinements of the crystal structures of Co_2SiO_4 and Ni_2SiO_4 olivines have been reported. Brown (1970) refined a series of olivine structures including Co_2SiO_4 and Ni_2SiO_4 olivines, in which the observed intensity data were corrected for Lorentz and polarization factors, but not for absorption and extinction factors. The final R and weighted R factors were 0.056 and 0.052 for 474 reflections of Co_2SiO_4 and 0.062 and 0.059 for 1076 reflections of Ni_2SiO_4, respectively.

Morimoto et al. (1974) discussed the structural relations between α, β and γ phases of Co_2SiO_4. Intensity data were corrected for Lorentz and polarization factors, but not for absorption and extinction factors. The final R and weighted R factors of α phase were 0.046 and 0.035 for 501 reflections.

The olivine structure shows the anomalous intra-crystalline cation distribution (Finger, 1970, Ghose and Wan, 1975, Rajamani et al, 1975). Tamada (1976, 1977) proposed an explanation on this phenomenon on the basis of the electrostatic stability. Only one assumption was included in this explanation that Mg ion was more ionic and had a larger atomic charge

than transition metal ions in the olivine structure. He also proposed on the same criterion that the atomic charge in the M2 site is larger than that in the M1 site of the endmembers of olivine in which the same two ions occupy simultaneously both the M1 and M2 sites. It is interesting to know the atomic charges of Co and Ni-olivines in connection with the above two relations of them.

Regarding the atomic charges in crystals, some methods to determine the net atomic charge by the X-ray method have been already proposed. These methods are in general classified into two major methods. One is the method to determine the charge by the integration of the electron density around the atoms and the second is the method to determine the occupancies of the valence shell by the least squares method. As one of the second methods the L-shell projection method was proposed by Stewart (1970) in which the occupancies of the valence-shell was determined by the least squares after the positional and thermal parameters have been obtained from a conventional least squares refinement. Coppens et al. (1971) porposed the extended L-shell projection method in which all the structural and thermal parameters together with the valence-shell occupancies are simultaneously refined. Recently Coppens et al. (1979) introduced a new fitting parameter k into the L-shell or extended L-shell projection method which incorporates expansion and contraction of the atomic valence shell together with a variation of its occupancy. Now Sasaki et al. (1977, 1978, 1979 and in preparation) have prepared the computer

program EARTH to estimate the net atomic charges in crystals by the X-ray method, following to and modifying the above major two methods. Iwata et al. (1973) determined the accurate structure of $[Co(NH_3)_6][Co(CN)_6]$ and reported the electron density distributions around Co ions. They first suggested that the asphericities of electron distributions around Co ion were ascribed to 3d electrons of the transition metal in the octahedral sites. Marumo et al. (1974, 1977) reported the accurate structures of γ-Ni_2SiO_4, Fe_2SiO_4 and Co_2SiO_4, and also suggested that the asphericities of the electron distributions around the transition metal ions in these crystals were ascribed to 3d electrons of such transition metals in the octahedral site.

In the present study the accurate crystal structures of two olivines, together with the charges of ions and the electron distributions around cations have been determined in connection with the proposed relations of the atomic charges in the olivine structure and the discussions of the electron density distributions of 3d electrons around the transition metal ions.

IV-1-B Experimental

Single crystals of Co_2SiO_4 olivine were synthesized by melting the mixture of SiO_2 and CoO powder at 1500°C. Gem-quality crystals were obtained in a platinum crucible after slow cooling. Single crystals of Ni_2SiO_4 olivine were synthesized by Dr. M. Ojima of ISSP, University of Tokyo, by the flux method. Spherical crystals of diameters 0.21 mm for Co_2SiO_4 and 0.20 mm for Ni_2SiO_4 were prepared for collecting the intensity data, by air polishing on a sand paper. Polarized microscope observation and Weisenberg photographs proved the crystals to be free from inclusion or cracks.

The intensity data were collected by the ω-2θ scanning technique on an automated four-circle diffractometer Phillips PW1100 using $MoK\alpha$ radiation monocromated by a graphite plate. In total, 2113 and 1936 independent reflections were collected for Co_2SiO_4 and Ni_2SiO_4 olivines in the 2θ range of 6° to 134°. The scanning speed was 4°/min and scanning was repeated up to three times when the intensity data were weak. The scanning width was $(1.70 + 0.30 \tan\theta)°$ for Co_2SiO_4 and $(1.50 + 0.30 \tan\theta)°$ for Ni_2SiO_4. Experimental conditions are summarized in Table 1.

The computer calculations were carried out with HITAC 8800/8700 computer using the full matrix least squares program LINUS (Coppens and Hamilton, 1970), after the correction procedure for Lorentz, polarization and absorption factors with the program PTPHI prepared for the PW1100 diffractometer.

Table 1. Experimental conditions.

	Co-olivine	Ni-olivine
Diameters of spherical crystals	0.21 mm	0.20 mm
Monochrometer	Graphite	Graphite
Radiation of X-ray	MoKα	MoKα
Collimeter	0.8 mmϕ	0.8 mmϕ
2θ range	6°<2θ<134°	6°<2θ<134°
Scanning speed	4°/min	4°/min
Max. repetition of scanning	3	3
Scanning width	(1.70+0.30tanθ)°	(1.50+0.30tanθ)°
Collected reflections	2113	1936
Used reflections	2010	1819
Apparatus	PW1100 (Phillips)	PW1100 (Phillips)

The isotropic secondary extinction effect (Zachariasen, 1967) was corrected in the process of the least squares refinements. 2010 reflections for Co_2SiO_4 and 1819 reflections for Ni_2SiO_4, with the condition $Fo>3\sigma(Fo)$ where σ is the standard error of the counting statistics, were used for the refinements, setting the unit weight to each reflection. The scattering factors for the various ionic states of Ni, Co, Si and O atoms, which are necessary for the charge refinement, were referred to International Tables for X-Ray Crystallography Vol. III and IV (1968, 1974), Fukamachi (1971) and Tokonami (1965). Real and imaginary dispersion correction factors $\Delta f'$ and $\Delta f''$ for atomic scattering factors were also referred to International Tables for Crystallography Vol. IV (1974).

The charge refinement was carried out by two methods, one of which are to fit the atomic scattering factors of ions to the intensity data by the least squares method and the second one is to sum the electron density distribution from the center of the cation to the valley of the distribution, although it is a problem to determine the radius of the spherical summation. The former consists of two calculation methods. One of them is to determine the parameter x in the atomic scattering factor $f(s)=fc(s)+fv(s)+xfv(s)'$. Another one is to determine the parameters x and κ in the atomic scattering factor $f(s)=fc(s)+fv(s/\kappa)+xfv(s/\kappa)'$. In the above expressions fc is the atomic scattering factor of electrons, fv that of valence electrons, fv' the difference between scattering factors of two ionic states and $s=\sin\theta/\lambda$. The parameter κ was intro-

duced by Coppens et al. (1979) as the correction of the expansion or the contraction of the electron distribution in the crystalline state against that in the free ionic state as mentioned above. For each of the former two calculation methods the following two calculations were actually carried out. The condition of the neutrality for the summation of charges in a crystal is constrained at first and ommited at the second time. In the second method of the direct spherical summation of the electron density around the centered atom the correction for the termination effect of the Fourier series was carried out and the effective distribution radius ER proposed by Sasaki et al. (in preparation) was used for the spherical summation. These methods by the first fitting procedure and the second spherical summation are following to Sasaki et al. (1977, 1978, 1979) and the details of those are described in Sasaki et al. (in preparation).

After the extended L-shell refinement of 46 variables (1 scale factor, 11 positional parameters, 28 anisotropic temperature coefficients, 5 charge refinement parameters and 1 isotropic secondary extinction coefficient) the final R and weighted R factors are 0.0277 and 0.0280 for Co_2SiO_4 and 0.0289 and 0.0310 for Ni_2SiO_4, respectively. The isotropic secondary extinction coefficient g is 0.4285×10^{-4} for Co_2SiO_4 and 0.3099×10^{-4} for Ni_2SiO_4. The final observed and calculated structure factors for Co_2SiO_4 and Ni_2SiO_4 are listed in Appendixes 3 and 4.

IV-1-C Results and discussion

The crystal data are listed in Table 2, and the final atomic coordinates, anisotropic and equivalent isotropic temperature factors for atoms in Co_2SiO_4 and Ni_2SiO_4 are given in Table 3. Interatomic distances and angles of olivines are listed in Tables 4 and 5, which are calculated using the program ORFFE (Busing, Martin & Levy, 1964). The net atomic charges obtained by the above methods are shown in Table 6.

No significant differences are observed between the obtained results and those obtained by Brown (1970) and Morimoto et al. (1974) in cell parameters and atomic coordinates, although the values of isotropic temperature factors obtained by Brown are relatively small and the present results are intermediate between the values by Brown and Morimoto et al.

In Table 6 the charges (L1) are obtained by the first fitting method to determine the value x under the constraint of the neutrality of crystal, while the charges (L2) are free from the constraint of the neutrality. The charges (R1) are obtained by the method to determine the values x and κ under the constraint of the neutrality of crystal, while the charges (R2) are free from the constraint of the neutrality.

The atomic charges (EN) of cations are determined by the spherical summation of the electron distribution around the atom. The atomic charges (EN) of O atoms were determined by the fitting procedure (R1), in which the atomic charges of cations were constrained to be those of (EN).

Table 2. Crystal data of Co_2SiO_4 and Ni_2SiO_4 Olivines.

Cell parameters	Co_2SiO_4	Ni_2SiO_4
a(Å)	4.7797(8)	4.7277(5)
b(Å)	10.2976(6)	10.1173(5)
c(Å)	5.9986(3)	5.9125(4)
V($Å^3$)	295.23	282.89
Space group	Pbnm	Pbnm
Z	4	4
ρcalc. (gcm^{-3})	4.723	4.919
μ(MoKα) (cm^{-1})	118.56	134.70

Table 3. Final atomic coordinates, anisotropic temperature factors and equivalent isotropic temperature factors for atoms in Co_2SiO_4 and Ni_2SiO_4 olivines.

Atom	x	y	z	B11	B22	B33	B12	B31	B23	B_{iso}
				Co_2SiO_4						
Co1	0.0	0.0	0.0	0.0043	0.0013	0.0029	0.0000	-0.0004	-0.0003	0.46
Co2	0.99123(5)	0.27639(2)	0.25	54	10	32	00	00	00	0.45
Si	0.42824(10)	0.09483(5)	0.25	33	09	27	00	00	00	0.36
O1	0.76733(22)	0.09232(12)	0.25	34	13	35	02	00	00	0.46
O2	0.21584(24)	0.44864(11)	0.25	55	09	38	-0.0002	00	00	0.49
O3	0.28153(17)	0.16398(8)	0.03347(14)	54	14	32	0.0001	-0.0003	0.0005	0.53
				Ni_2SiO_4						
Ni1	0.0	0.0	0.0	0.0037	0.0010	0.0025	0.0000	-0.0004	-0.0002	0.37
Ni2	0.99242(6)	0.27374(2)	0.25	45	08	28	01	0.0000	0.0000	0.37
Si	0.42717(12)	0.09430(6)	0.25	30	07	22	-0.0001	00	00	0.29
O1	0.76939(27)	0.09332(15)	0.25	29	11	33	0.0000	00	00	0.40
O2	0.21721(29)	0.44516(13)	0.25	44	08	33	01	00	00	0.39
O3	0.27435(20)	0.16312(10)	0.03011(16)	48	12	27	01	-0.0003	03	0.43

Table 4. Interatomic distances and angles in Co_2SiO_4 olivine.

		SiO_4 tetrahedron		
				angles at Si
Si-O1 (x1)	1.621(1) Å	O1-O2 (x1)	2.743(2) Å	113.67(6)°
Si-O2 (x1)	1.655(1) Å	O1-O3‴(x2)	2.761(1) Å	115.77(4)°
Si-O3‴(x2)	1.639(1) Å	O2-O3‴(x2)	2.570(1) Å	102.54(4)°
		O3‴O3'(x1)	2.598(2) Å	104.85(6)°
mean	1.639 Å	mean	2.667 Å	109.19°
		CoO_6 octahedron		
M1 octahedron				angles at Co1
Co1-O1(x2)	2.095(1) Å	O1-O2 (x2)	2.879(2) Å	86.92(3)°
Co1-O2(x2)	2.091(1) Å	O1-O2'(x2)	3.039(1) Å	93.08(3)°
Co1-O3(x2)	2.168(1) Å	O1-O3 (x2)	2.876(1) Å	84.83(4)°
		O1-O3'(x2)	3.148(1) Å	95.17(4)°
		O2-O3 (x2)	2.570(1) Å	74.19(4)°
		O2-O3'(x2)	3.398(1) Å	105.81(4)°
mean	2.118 Å	mean	2.985 Å	90.0°
M2 octahedron				angles at Co2
Co2-O1 (x1)	2.177(1) Å	O1-O3 (x2)	2.876(1) Å	81.58(3)°
Co2-O2 (x1)	2.073(1) Å	O1-O3'(x2)	3.032(1) Å	91.16(3)°
Co2-O3 (x2)	2.225(1) Å	O2-O3 (x2)	3.221(2) Å	97.01(4)°
Co2-O3'(x2)	2.067(1) Å	O2-O3'(x2)	2.923(1) Å	89.83(3)°
		O3-O3"(x1)	2.598(2) Å	71.42(4)°
		O3"O3'(x1)	3.401(2) Å	110.69(5)°
		O3-O3'(x2)	3.002(1) Å	88.67(2)°
mean	2.139 Å	mean	3.009 Å	89.88°

Table 5. Interatomic distances and angles in Ni_2SiO_4 olivine.

SiO_4 tetrahedron

				angle at Si
Si-O1 (x1)	1.618(2)Å	O1-O2 (x1)	2.746(2)Å	113.98(8)°
Si-O2 (x1)	1.656(1)Å	O1-O3‴(x2)	2.769(2)Å	116.25(5)°
Si-O3‴(x2)	1.642(1)Å	O2-O3‴(x2)	2.560(2)Å	101.83(5)°
		O3‴O3'(x1)	2.601(2)Å	104.70(7)°
mean	1.640 Å	mean	2.668 Å	109.14 °

CoO_6 octahedron

M1 octahedron

				angle at Ni1
Ni1-O1(x2)	2.065(1)Å	O1-O2 (x2)	2.853(2)Å	87.27(4)°
Ni1-O2(x2)	2.069(1)Å	O1-O2'(x2)	2.992(1)Å	92.73(4)°
Ni1-O3(x2)	2.107(1)Å	O1-O3 (x2)	2.809(2)Å	84.63(5)°
		O1-O3'(x2)	3.085(2)Å	95.37(5)°
		O2-O3 (x2)	2.560(2)Å	75.63(5)°
		O2-O3'(x2)	3.299(2)Å	104.37(5)°
mean	2.080 Å	mean	2.933 Å	90.0°

M2 octahedron

				angle at Ni2
Ni2-O1 (x1)	2.108(2)Å	O1-O3 (x2)	2.809(2)Å	82.00(4)°
Ni2-O2 (x1)	2.034(2)Å	O1-O3'(x2)	2.969(2)Å	91.04(4)°
Ni2-O3 (x2)	2.173(1)Å	O2-O3 (x2)	3.147(2)Å	96.81(4)°
Ni2-O3'(x2)	2.053(1)Å	O2-O3'(x2)	2.886(2)Å	89.83(3)°
		O3-O3"(x1)	2.601(2)Å	73.52(5)°
		O3‴O3'(x1)	3.313(2)Å	107.57(6)°
		O3-O3'(x2)	2.967(1)Å	89.17(2)°
mean	2.099 Å	mean	2.956 Å	89.90°

Table 6. The atomic charges determined by the X-ray charge refinement.

	M(1)	M(2)	Si	O(1)	O(2)	O(3)	R factor	Excess charge
Co-olivine								
(L1)	1.6(1)	2.1(1)	2.4(2)	-1.4(1)	-1.4(1)	-1.6(1)	0.0277	
(L2)	1.0(2)	1.4(2)	2.0(2)	-1.7(1)	-1.7(1)	-1.9(1)	0.0276	-2.8
(R1)	1.6(2)	2.1(2)	2.3(2)	-1.5(1)	-1.4(1)	-1.6(1)	0.0276	
(R2)	1.1(2)	1.5(3)	2.0(3)	-1.7(2)	-1.6(2)	-1.8(1)	0.0276	-2.2
(EN)	1.60(11)	1.45(12)	2.21(10)	-1.24	-1.24	-1.39		
Ni-olivine								
(L1)	1.7(2)	1.8(2)	2.2(2)	-1.4(1)	-1.5(1)	-1.4(1)	0.0289	
(L2)	1.3(2)	1.4(3)	2.0(3)	-1.6(2)	-1.6(2)	-1.6(1)	0.0288	-1.8
(R1)	1.7(2)	1.8(2)	2.3(3)	-1.4(2)	-1.5(2)	-1.4(2)	0.0286	
(R2)	1.6(3)	1.6(3)	2.1(3)	-1.5(2)	-1.6(2)	-1.5(3)	0.0286	-0.8
(EN)	1.78(12)	1.71(12)	2.39(11)	-1.46	-1.49	-1.46		

The charge (L1) of each ions is almost as same as the charge (R1). The introduction of the fitting variable κ does not have a significant effect on the charges refined for both olivines. The constraint of the neutrality of crystal has a significant effect on the charges and the release of the constraint produces the considerable excess charges. The effect is smaller for Ni_2SiO_4 than for Co_2SiO_4. The charges of Si and O ions in the charges (L1) and (R1) appear to be almost constant, 2.3e and 1.5e, respectively, whereas the charges of Co and Ni are different between those in the M1 and M2 sites and the charges of the M2 site are larger than those of the M1 site, especially in Co_2SiO_4. The ratio of the atomic charge and the formal charge 4e of Si ion seems to be small compared with those of Co, Ni and O ions, which suggests the covalency of Si ion. The atomic charges (EN) show almost the same tendency as those (L1) and (R1), but those (EN) of the M1 site are larger than those of the M2 site in both olivines, although the differences are almost within the errors. The charge of Mg ion (Fujino et al., in preparation) is clearly larger than those of the Co and Ni ions in the olivine structure.

The difference Fourier syntheses were carried out using the same intensity data as used in the refinements, 2010 reflections for Co_2SiO_4 and 1819 reflections for Ni_2SiO_4 and using the parameters determined by the charge refinement (L1). The site symmetries of the M1 and M2 sites of olivine are $\bar{1}$ and m, which are distorted from the octahedral symmetry. In

the high symmetry site as the perfect octahedral site, eight electron density peaks would be automatically produced around the centered Co^{2+} and Ni^{2+} ions by the symmetry operations if one peak was observed around the ions. In the low symmetry site as the M1 and M2 sites of olivine there are little effects of symmetry operations on the electron density distributions and then each peak has the larger meaning for its existence.

In the M1 site of Co-olivine as shown in Fig. 1 the intense four peaks are observed around the Co ion, although the weak two peaks, 0.52Å from the Co ion and the peak height $0.8 e\text{Å}^{-3}$, are observed upper-leftwards and lower-rightwards on the figure at x=0.50. The two of them, 0.52Å from the centered Co ion and the peak height $1.5 e\text{Å}^{-3}$, are located at the right and left-hands of the Co ion at x=0.49 and 0.51. The other two of them, 0.43Å from the Co ion are above and under the Co ion at x=0.59 and 0.41 and the peak height is $1.4 e\text{Å}^{-3}$. The negative peaks, 0.46Å and 0.54Å from the Co ion and the peak height $-1.0 e\text{Å}^{-3}$ and $-1.1 e\text{Å}^{-3}$ respectively, are also observed up and down-wards from the Co ion on the figure plane at x=0.55 and 0.45.

In the M2 site of Co-olivine as shown in Fig. 2 the peaks are weak in general compared with those in the M1 site. The two intense peaks, 0.57Å from the Co ion and the peak height $1.1 e\text{Å}^{-3}$ are observed at the right and left hands of the Co ion at x=-0.01. The weak peak, 0.53Å from the Co ion and the peak height $0.7 e\text{Å}^{-3}$ is located above the Co ion at x=0.10 and the two weak peaks, 0.50Å from the Co ion and the peak height

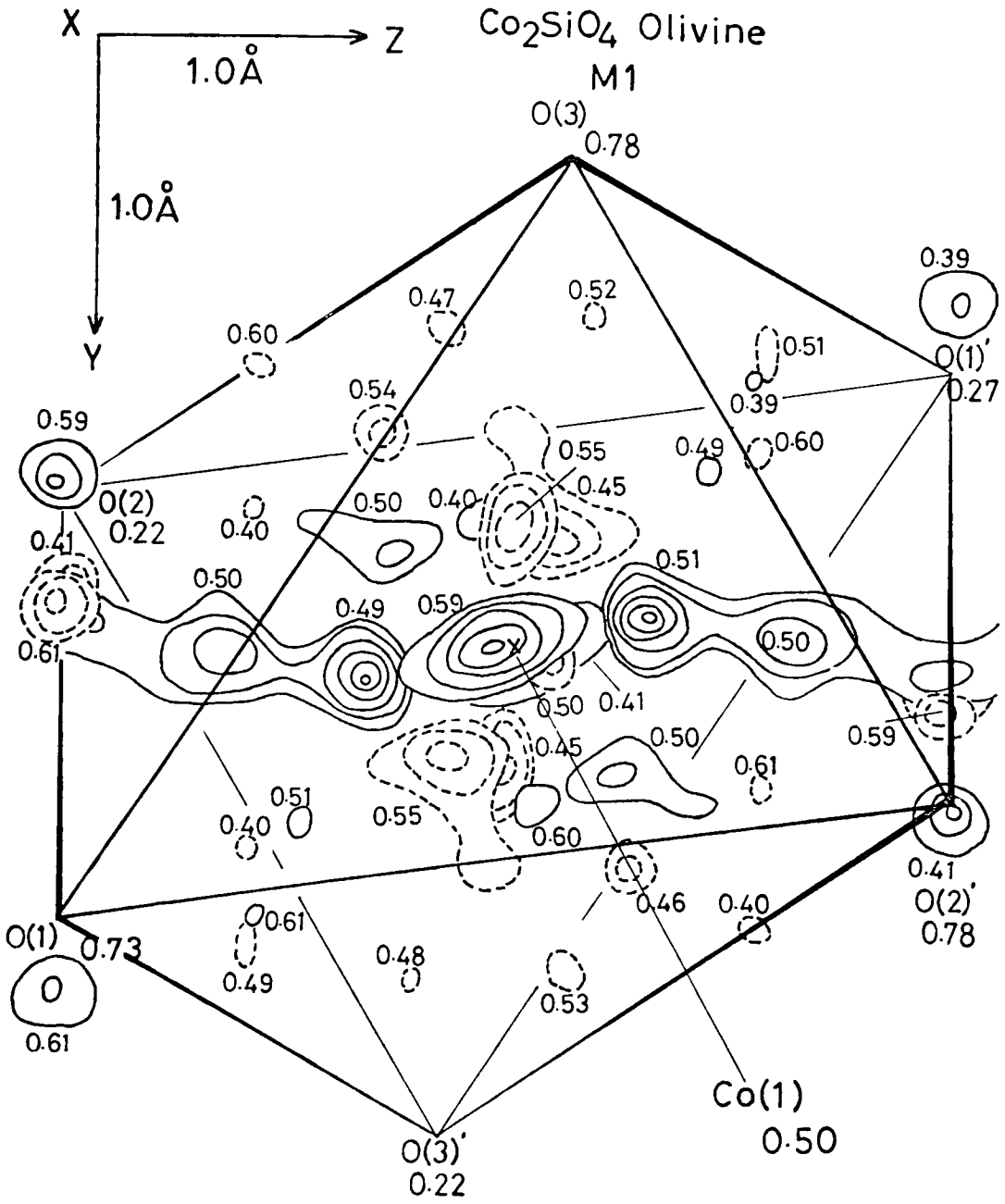

Fig. 1 The (100) sections of the difference Fourier map around the M1 site of Co_2SiO_4 olivine. The upper and lower sections of the central atom are projected together on the figure. Positive and negative contours are represented by the solid and dotted lines, respectively. Contours are at the intervals of $0.2e\mathring{A}^{-3}$ and start from $0.6e\mathring{A}^{-3}$ for the positive and $-0.6e\mathring{A}^{-3}$ for the negative peaks. Figure beside each peak gives the value of x coordinate.

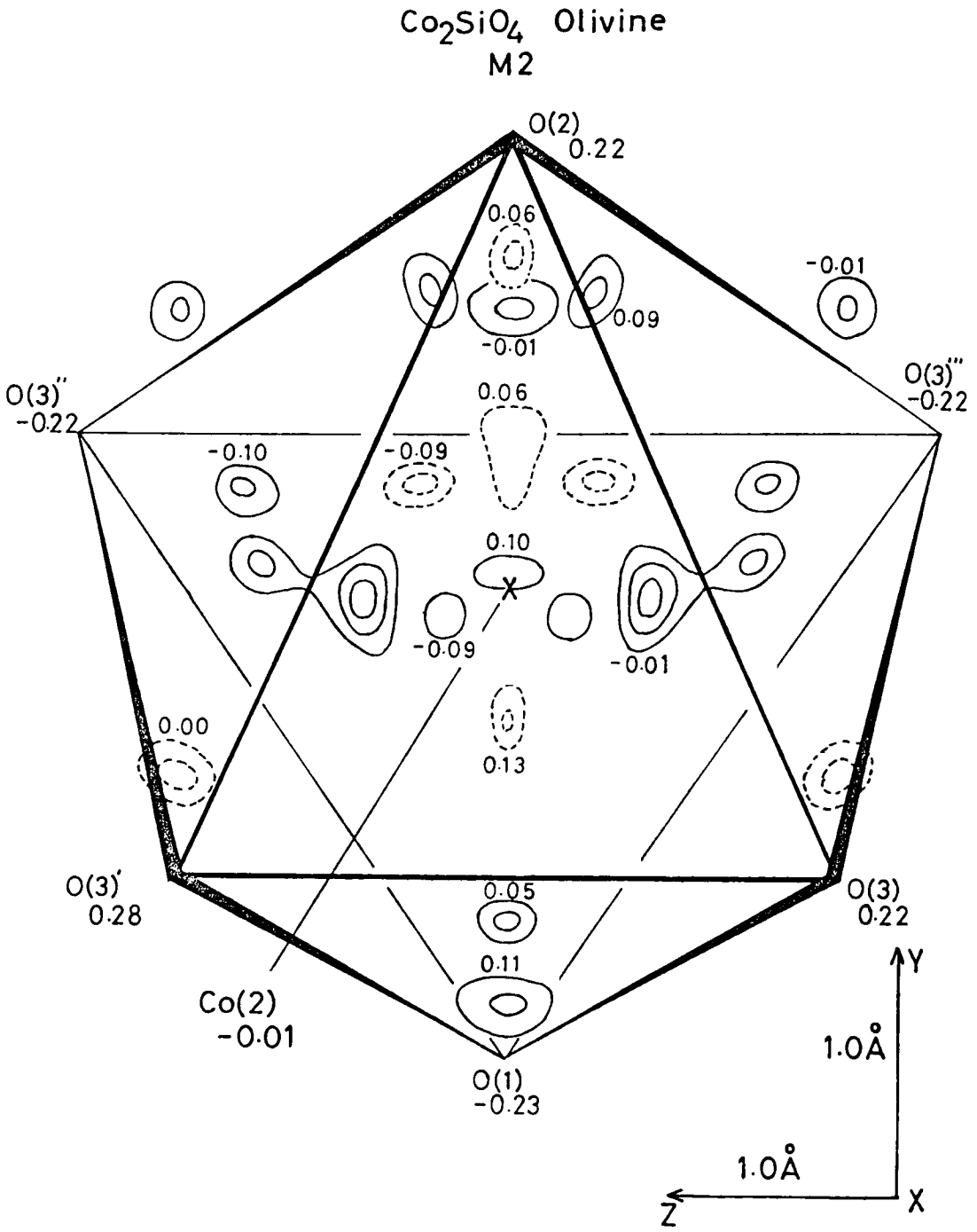

Fig. 2 The (100) sections of the difference F ourier map around the M2 site of Co_2SiO_4 olivine. The upper and lower sections of the central atom are projected together on the figure. Positive and negative contours are represented by the solid and dotted lines, respectively. Contours are at the intervals of $0.2e\mathring{A}^{-3}$ and start from $0.6\mathring{A}^{-3}$ for the positve and-$0.6e\mathring{A}^{-3}$ for the negative peaks. Figure beside each peak gives the value of x coordinate.

$0.7e\mathring{A}^{-3}$ are also located under the Co ion at x=-0.09. The negative peaks, $0.83\mathring{A}$, $0.65\mathring{A}$ and $0.66\mathring{A}$ and the peak heights $-0.8e\mathring{A}^{-3}$, $-0.7e\mathring{A}^{-3}$ and $-0.8e\mathring{A}^{-3}$ also observed up and downwards on the figure plane at x=0.13, 0.06 and -0.09, respectively. In general the peak heights are weaker and the distances of the peaks from the centered ion are longer in the M2 site of Co-olivine, but the configurations of the peaks resemble each other in the M1 and M2 sites as there are two intense peaks at the right and left hands of the Co ion and the peaks are observed above and under the Co ion both in the M1 and M2 sites. As a whole the peaks appear to be located along the four directions of body diagonal of the Co-O bonds and to be lacked in the residual four directions.

In the M1 site of Ni-olivine as shown in Fig. 3 the eight electron density peaks are observed around the Ni ion, although the two peaks, $1.0\mathring{A}$ from the Ni ion and the peak height $0.8e\mathring{A}^{-3}$, which are located right-upwards and left-downwards on the figure plane at x=0.44 and 0.56 respectively, are somewhat distant from the Ni ion. The intense two peaks of them, $0.49\mathring{A}$ from the Ni ion and the peak height $1.2e\mathring{A}^{-3}$, are located right-downwards and left-upwards on the figure plane at x=0.47 and 0.53, respectively. The next two of them, $0.63\mathring{A}$ from the Ni ion and the peak height $0.9e\mathring{A}^{-3}$, are located up- and downwards of the Ni ion at x=0.47 and 0.53, respectively. The other two peaks, $0.54\mathring{A}$ from the Ni ion and the peak height $0.7e\mathring{A}^{-3}$ are located above and under the Ni ion at x=0.59 and 0.41. All the above eight peaks are located approximately

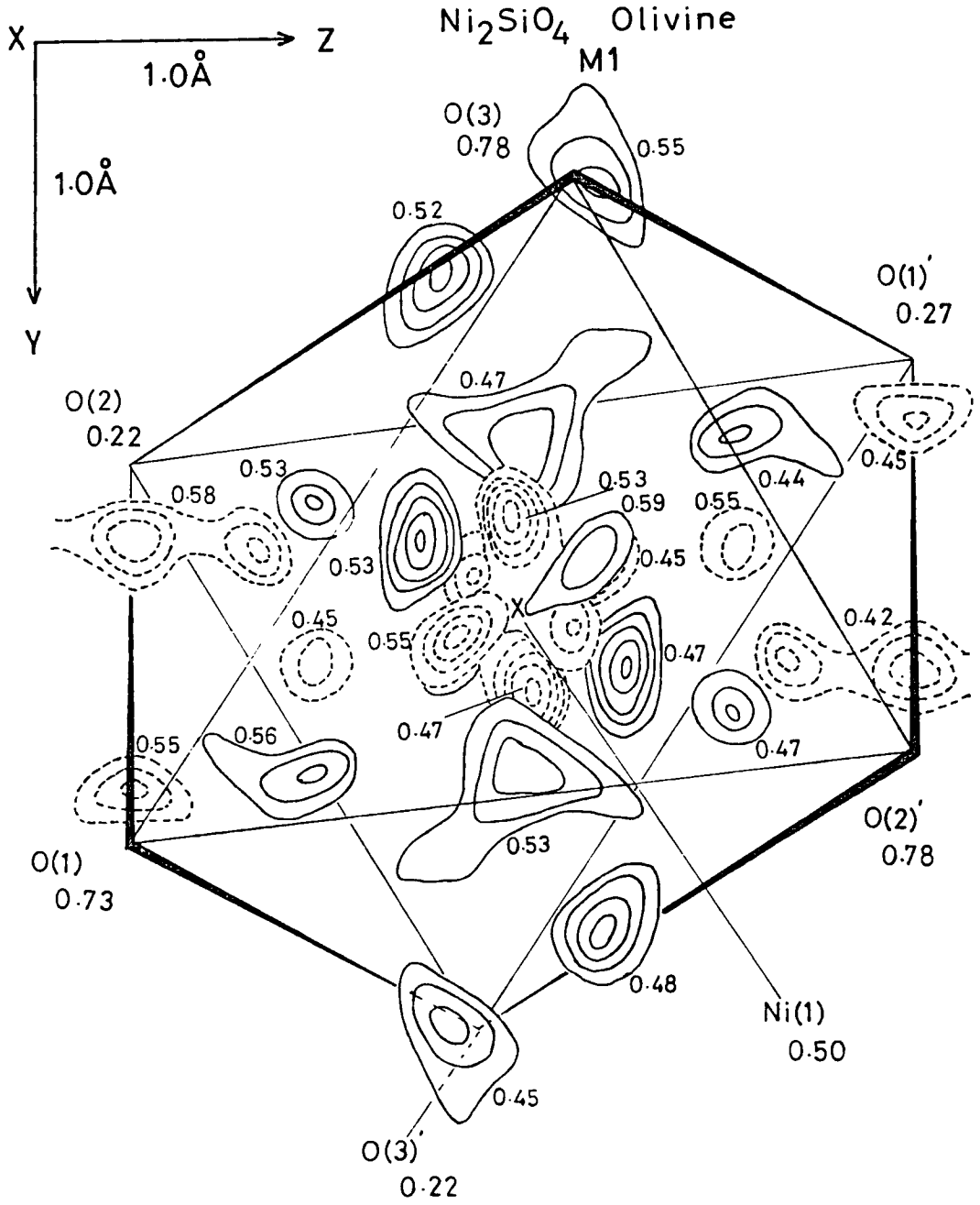

Fig. 3 The (100) sections of the difference Fourier map around the M1 site of Ni_2SiO_4 olivine. The upper and lower sections of the central atom are projected together on the figure. Positive and negative contours are represented by the solid and dotted lines, respectively. Contours are at the intervals of $0.2e\mathring{A}^{-3}$ and start from $0.4e\mathring{A}^{-3}$ for positive and $-0.4e\mathring{A}^{-3}$ for the negative peaks. Figure beside each peak gives the value of x coordinate.

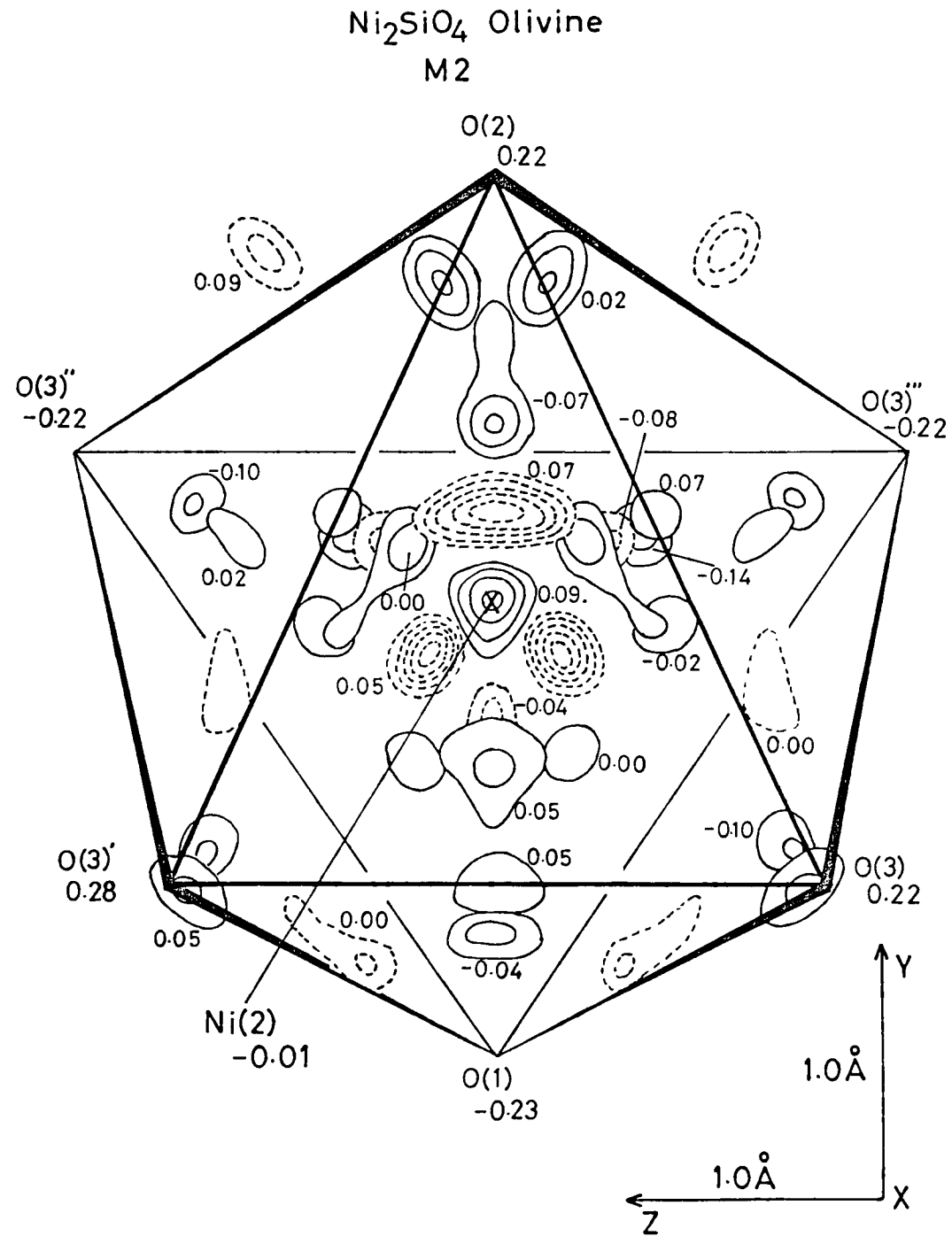

Fig. 4 The (100) sections of difference Fourier map around the M1 site of Co_2SiO_4 olivine. The upper and lower sections of the central atom are projected together on the figure. Positive and negative contours are represented by the solid and dotted lines, respectively. Contours are at the intervals of $0.2e\mathring{A}^{-3}$ and start from $0.6e\mathring{A}^{-3}$ for the positive and $-0.6e\mathring{A}^{-3}$ for the negative peaks. Figure beside each peak gives the value of x coordinate.

along the body diagonals of the Ni-O bonds. The negative peaks are also surrounding the Ni ion. The intense two of them 0.28Å from the Ni ion and the peak height -1.0eÅ^{-3} are located left-downwards and right-upwards on the figure plane at x=0.55 and 0.45 respectively. The other two intense negative peaks, 0.39Å from the Ni ion and the peak height -1.2eÅ^{-3} are located up- and downwards on the figure plane at x=0.53 and 0.47.

In the M2 site of Ni-olivine as shown in Fig. 4 the intense peak, 0.47Å from the Ni ion and the peak height 1.2eÅ^{-3}, is observed just above the Ni ion at x=0.09. The two peaks, 0.43Å from the Ni ion and the peak height 0.9eÅ^{-3}, are located right and left-upwards at x=0.00. The peaks, 0.77Å and 0.72Å from the Ni ion and the peak height 1.0eÅ^{-3} and 0.9eÅ^{-3}, are observed up and downwards on the figure plane at x=-0.07 and x=0.05. Above five peaks are intense or moderately intense and located approximately along the body diagonals of the Ni-O bonds, but the intense peaks cannot be observed along the residual three directions of the body diagonal, although the weak two peaks, 0.70Å from the Ni ion and the peak height 0.7eÅ^{-3} are located right- and left-downwards on the figure plane at x=-0.02 and the weak peak, 0.35Å from the Ni ion and the peak height 0.7eÅ^{-3}, are stretching from the right to the left hand under the Ni ion at x=-0.08, which cannot be shown in the figure because the figure becomes complicated by this writing. The intense three negative peaks, 0.54Å and 0.46Å from the Ni ion and the peak height -1.5Å^{-3} are located upwards and right- and left-downwards at x=0.07 and 0.05. As a whole

the intense negative peaks are located around the Ni ion, and the positive peaks appear to be located approximately along the all directions of body diagonal of the Ni-O bonds in both the M1 and M2 sites of Ni olivine, although the two peaks are somewhat distant from the Ni ion in the M1 site and the three peaks are weak in the M2 site.

The main difference of the electron density maps between the Co and Ni-olivines is that the peaks around the M1 and M2 sites of Co-olivine are less in number and are explicitly lacked along some directions of the body diagonal of the Co-O bonds while there are many peaks around the M1 and M2 sites of Ni-olivine and they appear to be located along almost all the directions of the body diagonal although some of them are not explicitly located. The Co^{2+} ion has seven 3d-electrons, which occupy five t_{2g} orbitals and two e_g orbitals in the octahedral field in the high spin state (The Co ion is known to be in the high spin state in the olivine structure). The energetic degeneracy of the t_{2g} and e_g orbitals is expected to be broken in the distorted site as the M1 and M2 sites of olivine and then the five electrons occupy each of the five 3d orbitals and the remaining two the energetically lower two t_{2g} orbitals. The t_{2g} orbitals are theoretically stretching along the body-diagonal direction of bonds in the octahedral field. Therefore it seems to be reasonable that the peaks are located approximately along the body-diagonal directions of the Co-O bonds and are lacked along some directions. On the other hand the Ni^{2+} ion has eight 3d-electrons and then five 3d-electrons occupy

each of the five 3d orbitals and the remaining three occupy all the three t_{2g} orbitals. Therefore it seems to be reasonable that the peaks are located approximately along all the body-diagonal directions although some peaks are expected to be weak.

Marumo et al. (1974, 1977) reported the electron density maps of γ-Fe_2SiO_4, Co_2SiO_4 and Ni_2SiO_4 by synthesizing difference Fourier maps. The eight peaks are observed around the Co^{2+} and Ni^{2+} ions of γ-Co_2SiO_4 and Ni_2SiO_4. The peak height on the threefold rotation axis around the Ni ion is $0.9e\mathring{A}^{-3}$ and the other, $1.0e\mathring{A}^{-3}$. On the other hand, the difference of the peak heights is somewhat larger in γ-Co_2SiO_4. The height of the two peaks on the threefold rotation axis around the Co ion is $1.0e\mathring{A}^{-3}$ and the other, $0.8e\mathring{A}^{-3}$. In contrast to γ-Co_2SiO_4 and Ni_2SiO_4, only two peaks, the peak height $1.2e\mathring{A}^{-3}$ exist around the Fe ion. The distances of the peaks from the centered cations are all $0.46\mathring{A}$ in all the above crystals. The tendency in the spinel structure that some of eight peaks around the Ni ion become weak or diminish around the Co or Fe ions, looks to be consistent with that in the olivine structure although the distances from the centered cations to the peaks spread in wide range in the olivine structure in contrast to the fixed value $0.46\mathring{A}$ in the spinel structure.

Fujino et al. (in preparation) examined the electron density distributions around the M1 and M2 sites of Fe, Mn and Mg-olivines. The four peaks are observed around the Fe ion of Fe-olivine. The main feature of the electron density maps of

Mn-olivine is the existence of two intense peaks, 0.48-0.50Å from the Mn ion and the peak height 1.3eÅ^{-3}. The Mn^{2+} ion has five 3d-electrons which occupy two e_g and three t_{2g} orbitals in the octahedral field. Therefore the existence of two intense peaks means that even the Mn^{2+} ion with half-filled 3d-orbitals shows the asphericity in the electron density distributions around the M1 and M2 site of olivine. This result makes the problem complicated. Now it is difficult to give the consistent interpretation about the electron density distributions around the cations of olivines. No peak with the peak height greater than 0.3eÅ^{-3} was observed around the Mg ion of forsterite which has no 3d-electron and then the large aspherisities observed in the figures seems to have relation to 3d-electrons, as was already pointed out by Iwata and Saito (1973) in the crystal $\left[Co(NH_3)_6\right]\left[Co(CN)_6\right]$ and Marumo et al. (1974, 1977) in the spinel structure.

IV-2 A theoretical explanation of the atomic charges of olivines and orthopyroxenes based on the electrostatic stability.

IV-2-A Introduction

Many workers have studied the intra-crystalline distributions of cations in the olivine structure in connection with the applications as geothermometer and geobarometer. They have found a characteristic anomaly in the cation distributions (Finger, 1970, Ghose and Wan, 1975). Rajamani et al. (1975) summarized the experimental results of the intra-crystalline distributions between Mg and transition metal ions of olivines and orthopyroxenes. Transition metal ions have the strong tendency to occupy the smaller M1 site of olivines, while they are distributed in a natural way in orthopyroxenes in terms of the size effect that the larger ion occupies the larger site and the smaller ion the smaller site. Therefore, the anomalous site preference that, for example, the larger Co and Fe ions occupy the smaller M1 site and the smaller Ni ion shows the quite high preference for the M1 site, is observed in the intra-crystalline distributions between Mg and transition metal ions in the olivine structure.

Tamada (1976, 1977) proposed an explanation on this characteristic phenomenon of the olivine structure based on the electrostatic stability. Only one assumption was included in this explanation that Mg ion was more ionic and had a larger atomic charge than transition metal ions in the olivine structure. Fujino et al. (1976) reported the atomic charges of tephroite (Mn-olivine) and forsterite (Mg-olivine) determined by the X-ray charge refinement. The charge of Mg ion

was larger than that of Mn ion and the charge of the ion in the M2 site was larger than that in the M1 site in these two olivines. Tamada also pointed out that the electrostatic stability required a ion of the M2 site having a larger atomic charge than that of the M1 site in the endmembers of olivine. This is because these effect can be explained by the concept of the electrostatic stability based on the large difference of electrostatic potentials between the M1 and M2 sites.

This paper gives the theoretical basis to the atomic charges determined by the X-ray method, by confirming the consistency between the atomic charges and the expected values for them derived from the concept of the electrostatic stability.

IV-2-B The electrostatic potentials of the M1 and M2 sites of the olivine and orthopyroxene structures.

The electrostatic potentials of the M1 and M2 sites of the olivine and orthopyroxene structures were calculated for the various assumed charges assigned to ions to see the relative relations of them. The charge of Si ion was fixed to be 2e (e; electron charge unit) in the calculations (only in the first calculation the formal charges were assigned to all the ions). This assumption is reasonable for the purpose of the calculations only to compare the relative values of potentials of two sites. The same charge was assigned to the same kind of ions even if they occupy the different sites. This is because of avoiding the complexity in calculations and also avoiding the effect of self-interaction of the charge to the potential. The neutrality of whole crystal is also assumed.

According to the above three conditions for the assigned charges the electrostatic potentials were calculated by the method of Bertaut (1952) together with the standard errors derived from those of the atomic positions. The termination errors were corrected to be less than 3×10^{-4} after Templeton (1955) and Jones and Templeton (1956).

The electrostatic potentials of the M1 and M2 sites of the olivine and orthopyroxene structures are listed in Tables 1 and 2, respectively. For all the cases of calculation for the various sets of charges the potential of the larger M2 site of the olivine structure is always lower than that of

Table 1 The comparison of electrostatic potentials of the M1 and M2 sites of Fe-olivine for the various assumed charges assigned to ions.

	atoms	charges(e) assigned	potentials(kcal/mol.e)
(1)	Fe1	2.0	-520.7(0.3)
	Fe2	2.0	-568.0(0.2)
	Si	4.0	
	O	-2.0	
(2)	Fe1	0.5	-149.3
	Fe2	0.5	-167.8
	Si	2.0	
	O	-0.75	
(3)	Fe1	1.0	-260.4
	Fe2	1.0	-284.1
	Si	2.0	
	O	-1.0	
(4)	Fe1	1.5	-371.4
	Fe2	1.5	-400.2
	Si	2.0	
	O	-1.25	
(5)	Fe1	2.0	-482.4
	Fe2	2.0	-516.4
	Si	2.0	
	O	-1.5	

The structural data were taken from Fujino et al. (in preparation). The calculation errors caused from the termination effect are less than 3×10^{-4}. The errors caused from the structural data are listed in the parentheses of the first calculation only.

Table 2 The comparison of electrostatic potentials of the M1 and M2 sites of Fe-orthopyroxene for the various assumed charges assigned to ions.

atoms	charges(e) assigned	potentials(kcal/mol.e)
(1) Fe1	2.0	-598.1(1.4)
Fe2	2.0	-548.3(1.0)
Si	4.0	
O	-2.0	
(2) Fe1	0.5	-216.0
Fe2	0.5	-175.6
Si	2.0	
O	-0.83333...	
(3) Fe1	1.0	-299.1
Fe2	1.0	-274.2
Si	2.0	
O	-1.0	
(4) Fe1	1.5	-382.2
Fe2	1.5	-372.8
Si	2.0	
O	-1.16666...	
(5) Fe1	2.0	-465.3
Fe2	2.0	-471.3
Si	2.0	
O	-1.33333...	

The structural data were taken from Sueno et al.(1976). The calculation errors caused from the termination effect are less than 3×10^{-4}. The errors caused from the structural data are listed in the parentheses of the first calculation only.

the smaller M1 site, while that of the smaller M1 site of the orthopyroxene structure is always lower than that of the larger M2 site except the unprobable case when the charge 2e is assigned to Fe ion, as same as that of Si ion in the least calculation. Moreover the difference of the potentials between the M1 and M2 sites of orthopyroxene is only small in the above exceptional case.

In general the potential of the smaller cation site is lower than that of the larger cation site because the neighbouring anions largely contribute to the smaller cation site and this is true in the majority of the cases. It will be, therefore, concluded that the above relation of the potentials of the M1 and M2 sites of the olivine structure is anomalous and it is the characteristic feature of the olivine structure. On the other hand the relation of those of the orthopyroxene structure is usual as in other crystals. The anomalous and characteristic relation of the potentials of the olivine structure suggests the anomalous cation distributions.

The above relations of the potentials are common also for the other kind of olivines and orthopyroxenes as shown schematically in Fig. 1.

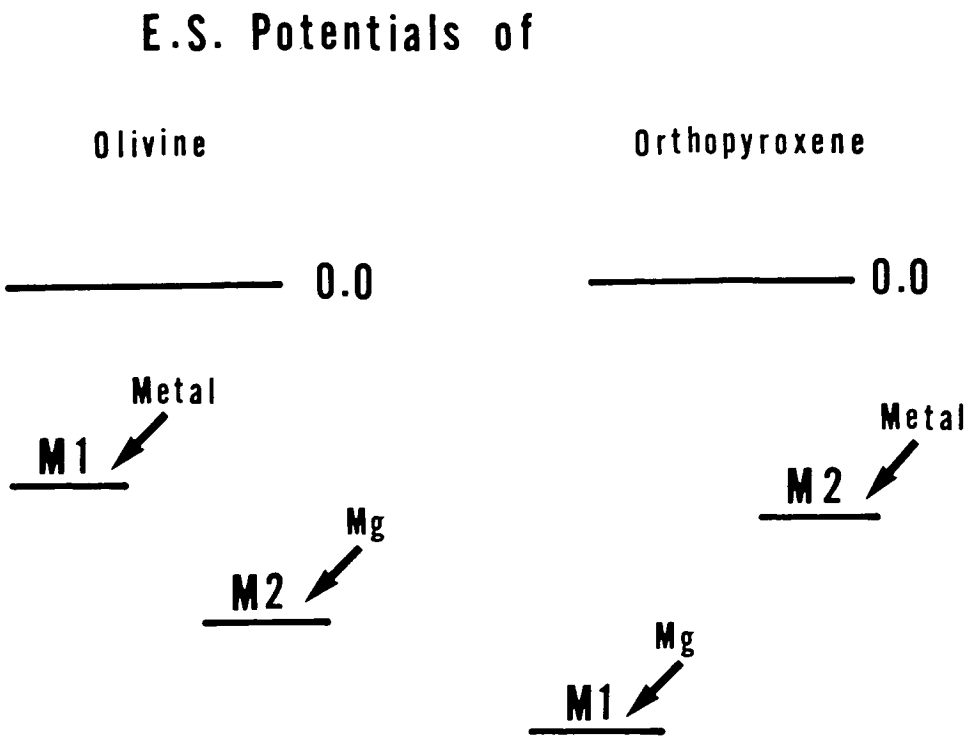

Fig. 1. The schematic relations of the electrostatic potentials of the M1 and M2 sites of the olivine and orthopyroxene structures.

IV-2-C Discussion

Rajamani et al. (1975) summarized the observed site preferences of the transition metal ions in the olivine structure and in the orthopyroxene structure, which are shown in Fig. 2. Small cation as Ni ion prefers the M1 site and transition metal ions gradually become to prefer the M2 site with increase of the ionic radius in the both structures. This is explained by the size effect of cation and site. This effect can be quantitatively explained by the repulsive energy of Born's model for ionic crystals if the two constants which are involved in the repulsive term, were taken in our hand. But now we cannot have the reliable values and the concept of the size effect is sufficient for the present purpose of the qualitative discussion.

Ni ion is remarkably enriched in the M1 site of the olivine structure while it is only slightly enriched in the M1 site of the orthopyroxene structure. The larger Co ion shows a strong preference for the smaller M1 site in olivine in contrast to its strong preference for the M2 site in orthopyroxene. The larger Fe ion is only slightly enriched in the smaller M1 site in olivine while it shows the high preference for the M2 site in orthopyroxene. Mn ion prefers the M2 site both in olivine and orthopyroxene, but the degree of ordering is far higher in orthopyroxene. As a whole the line of the site preference of transition metal ions in the olivine structure which is shown by the broken line in Fig. 2,

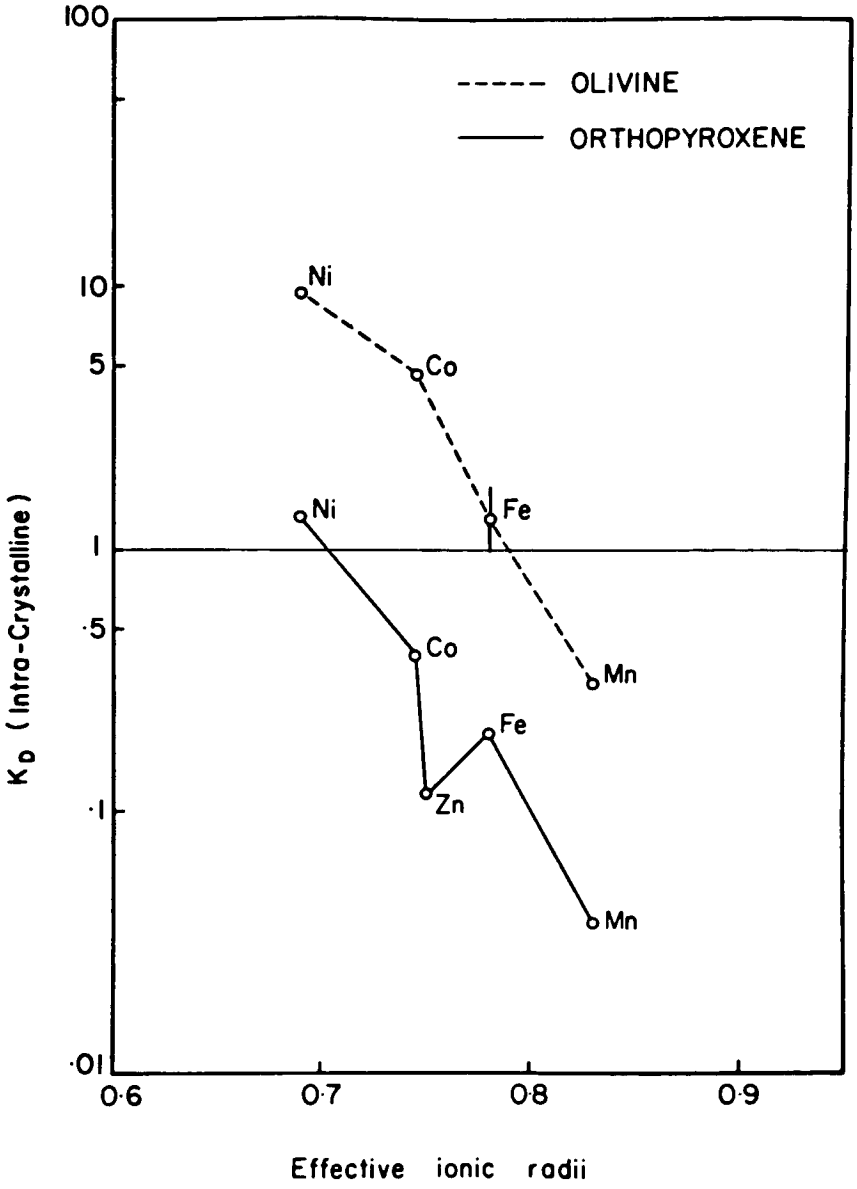

Fig. 2. Log-linear plot of intra-crystalline distribution coefficient between Mg and transition metal ions (M) ($K_D=(M/Mg)_{M1}/(M/Mg)_{M2}$) versus effective ionic radii for a number of transition metal olivines and orthopyroxenes. (from Rajamani et al., 1975)

is shifted toward the preference for the M1 site in contrast to the shift toward the preference for the M2 site in the orthopyroxene structure.

The difference of the site preferences between the olivine and orthopyroxene structures cannot be explained by the size effect and the crystal field stabilization energy (CFSE) only (Ghose and Wan, 1974, Rajamani et al., 1975). Wood (1974) reported the CFSE of the Ni-olivine to be 27.3 and 25.7 kcal/gram for the M1 and M2 sites, respectively from the optical absorption spectrum, which is consistent with the experimental result by Tamada (1973), obtained by the same optical absorption method. Ni ion gains the maximum CFSE among transition metal ions because of its electron configuration ($3d^8$). Transition metal ions must gain the larger excess CFSE in the M1 site of orthopyroxene than in that of olivine because of the larger difference of the site sizes in orthopyroxene in contrast to the smaller difference in olivine. This result of the CFSE leads to the opposite trend from the experimental results of the site preference in olivines and orthopyroxenes. It is, therefore, supposed that other factors are acting against the site preference of cations in olivine and orthopyroxene. Ghose and Wan (1974) and Rajamani et al. (1975) attributed the factors to "covalency" and "ionicity", respectively. Their explanations were not consistent with each other.

The difference of the site preference between the olivine and orthopyroxene structures can be given the explanation by

the electrostatic stability based on the one assumption that Mg ion is more ionic and has the larger atomic charge in the olivine and orthopyroxene structures than the transition metal ions. The electrostatic potentials of the M2 site of olivine and the M1 site of orthopyroxene are always lower than the other site as mentioned above. The electrostatic energy of crystal is lowered when the ion with larger net atomic charge occupies the site of lower potential. Mg ion, therefore, prefers the M2 site of olivine and the M1 site of orthopyroxene and then transition metal ions are forced to occupy the M1 site of olivine and the M2 site of orthopyroxene as shown in Fig. 1. The shift of the line of the site preference of the transition metal ions toward the M1 site in the olivine structure is explained by this electrostatic effect.

The electrostatic stability also forces the atomic charges to be larger in the M2 site of the olivine structure and in the M1 site of the orthopyroxene structure by the same reason when the both M1 and M2 sites are simultaneously occupied by the same kind of ions as it is realized in the endmembers of the crystals.

The atomic charges of olivines and orthopyroxenes determined by the X-ray method are shown in Table 3. The atomic charges (L1), (L2), (R1) and (R2) are all determined by the fitting procedure of the atomic scattering factors f(s) of various ionic states fitted to the intensity data by the least squares method. In the atomic charges (R1) and (R2) a new fitting parameter κ in the atomic scattering factor

Table 3. The atomic charges (electron unit ; e) of olivines and orhtopyroxenes determined by the X-ray method.

Olivines

	M1	M2	Si	O1	O2	O3	R-value	Excess charges
(1) Mg-olivine								
(L1)	2.1(1)	3.1(1)	1.8(1)	-1.9(1)	-1.6(1)	-1.7(1)	0.0209	
(L2)	0.6(3)	1.3(3)	1.3(1)	-2.0(1)	-1.7(1)	-1.8(1)	0.0221	-3.7
(R1)	1.9(1)	2.9(1)	1.8(1)	-1.8(1)	-1.6(1)	-1.7(1)	0.0208	
(R2)	0.7(3)	1.4(3)	1.3(2)	-1.9(1)	-1.7(1)	-1.8(1)	0.0209	-3.7
(EN)	1.76(3)	1.74(3)	2.11(3)	-1.52	-1.29	-1.40		
(2) Mn-olivine								
(L1)	1.3(1)	2.2(2)	2.6(2)	-1.5(1)	-1.4(1)	-1.6(1)	0.0310	
(L2)	-0.2(2)	0.5(2)	1.6(2)	-2.1(1)	-1.9(1)	-2.2(1)	0.0310	-6.6
(R1)	1.1(1)	2.1(2)	2.5(2)	-1.5(1)	-1.3(1)	-1.5(1)	0.0309	
(R2)	-0.4(2)	0.3(2)	1.7(3)	-2.1(2)	-1.9(2)	-2.3(1)	0.0308	-6.9
(EN)	1.21(6)	1.49(6)	2.28(5)	-1.27	-1.13	-1.29		
(3) Fe-olivine								
(L1)	1.3(1)	1.9(1)	1.9(2)	-1.2(1)	-1.3(1)	-1.3(1)	0.0255	
(L2)	0.4(2)	0.8(2)	1.3(2)	-1.6(1)	-1.6(1)	-1.7(2)	0.0254	-4.2
(R1)	1.3(1)	1.8(1)	1.7(2)	-1.1(1)	-1.2(1)	-1.2(1)	0.0254	
(R2)	0.4(2)	0.7(2)	1.2(3)	-1.5(1)	-1.5(1)	-1.7(1)	0.0253	-4.1
(EN)	0.85(8)	1.54(7)	2.43(6)	-1.13	-1.21	-1.24		
(4) Co-olivine								
(L1)	1.6(1)	2.1(1)	2.4(2)	-1.4(1)	-1.4(1)	-1.6(1)	0.0277	
(L2)	1.0(2)	1.4(2)	2.0(2)	-1.7(1)	-1.7(1)	-1.9(1)	0.0276	-2.8
(R1)	1.6(2)	2.1(2)	2.3(2)	-1.5(1)	-1.4(1)	-1.6(1)	0.0276	
(R2)	1.1(2)	1.5(3)	2.0(3)	-1.7(2)	-1.6(2)	-1.8(1)	0.0276	-2.2
(EN)	1.60(11)	1.45(12)	2.21(10)	-1.24	-1.24	-1.39		
(5) Ni-olivine								
(L1)	1.7(2)	1.8(2)	2.2(2)	-1.4(1)	-1.5(1)	-1.4(1)	0.0289	
(L2)	1.3(2)	1.4(3)	2.0(3)	-1.6(2)	-1.6(2)	-1.6(1)	0.0288	-1.8
(R1)	1.7(2)	1.8(2)	2.3(3)	-1.4(2)	-1.5(2)	-1.4(2)	0.0286	
(R2)	1.6(3)	1.6(3)	2.1(3)	-1.5(2)	-1.6(2)	-1.5(3)	0.0286	-0.8
(EN)	1.78(12)	1.71(12)	2.39(11)	-1.46	-1.49	-1.46		

Table 3. Continued

Orthopyroxenes

	M1	M2	SiA	SiB	O1A	O1B	O2A	O2B	O3A	O3B	R-value	Excess charges
(1) Mg-orthopyroxene												
(L2)	0.73(14)	0.88(16)	1.39(10)	1.56(10)	-1.79(5)	-1.69(5)	-1.79(5)	-1.84(5)	-1.80(5)	-1.74(6)		-6.09
(EN)	1.84(4)	1.79(4)	2.20(4)	2.36(4)	-1.51	-1.37	-1.36	-1.43	-1.31	-1.22	0.0231	
(2) Fe-orthopyroxene												
(L2)	0.28(23)	0.47(23)	1.36(24)	1.35(25)	-1.96(16)	-2.23(15)	-2.04(20)	-2.25(17)	-1.73(15)	-2.22(16)		-8.97
(EN)	1.14(12)	1.10(13)	2.21(11)	2.16(11)	-1.04	-1.19	-1.09	-1.20	-0.92	-1.18	0.0304	
(3) Co-orthopyroxene												
(L2)	0.14(22)	0.01(22)	1.30(25)	1.13(25)	-2.23(15)	-2.21(15)	-2.18(18)	-2.25(17)	-1.64(16)	-2.13(17)		-10.06
(EN)	1.29(11)	0.61(12)	1.79(9)	2.76(9)	-1.10	-1.14	-1.12	-1.16	-0.84	-1.10	0.0365	

*The atomic charges of Mg, Mn and Fe-olivines, and Co and Ni-olivines were taken from Fujino et al. (in preparation and private comm., 1979) and Tamada et al. (in preparation), respectively.

The atomic charges (L2) and (EN) of orthopyroxenes were taken from Sasaki et al. (in preparation and private comm., 1979) and Sasaki et al. (1979), respectively.

$f(s/\kappa)$ was refined together with other parameters, which was introduced by Coppens et al. (1979) as the correction of the expansion or the contraction of the electron distribution in the crystalline state against that in the free ionic state. The atomic charges (L1) and (R1) are constrained to be neutral for the summation of them in a crystal. Those of (L2) and (R2) are not constrained and then the excess charges are produced. The atomic charges (EN) are determined by the spherical summation of the electron distribution from the center of the cation to the valley of the electron distribution. The atomic charges (EN) of O atoms were determined by the fitting procedure (R1), in which the atomic charges of cations were constrained to be those (EN). The method to determine these atomic charges was described by Sasaki et al. (1978, 1979) and the details will be published by them.

The atomic charges (L1), (R1) and (EN) of Mg atom are remarkably larger than those of the transition metal atoms in the each M1 and M2 sites of olivines, although the atomic charge (EN) of Ni atom in the M1 site is slightly larger than that of Mg atom within the errors. The atomic charges (EN) of Mg atom are also larger than those of transition metal atoms in the each M1 and M2 sites of orthopyroxenes. The atomic charges (L2) and (R2) of Mg atom are not always larger than those of transition metal atoms in the each M1 and M2 sites of olivines and orthopyroxenes, but it is not so regretable because they are free from the constraint of the neutrality of a crystal and the excess charges are produced in these

charges. The requirement for the atomic charges of Mg atom against transition metal atoms is now supported by the experimental data. This is also true in the atomic charges (EN) of NaCl type crystals of MgO and transition metal oxides (Sasaki et al., 1979) as 1.9e(Mg), 1.4e(Mn), 1.2e(Co) and 0.7e(Ni).

The atomic charges of the M2 site are always larger than those of the M1 site of the each endmember of olivines in the each atomic charges (L1), (L2), (R1) and (R2) determined by the fitting procedure even if the constraint of the neutrality is released, although they are almost equal in Ni-olivine. This results indicate us that the tendency is rigidly established in the atomic charges of olivines determined by the fitting procedure. The atomic charges (EN) of the M2 site are evidently larger than those of the M1 site in Mn and Fe-olivines. On the other hand they are slightly smaller than those of the M1 site in Mg, Co and Ni-olivines, which is not corresponds to the requirement for the atomic charges, but the differences are almost within the errors. The atomic charges (EN) of the M1 site of orthopyroxenes are always larger than those of the M2 site, although the difference in the atomic charges (EN) of Fe-orthopyroxene is almost within the errors. The differences of the atomic charges (L2) between the M1 and M2 site are too small compared with the errors in all the orthopyroxenes. The requirement for the atomic charges of the M1 and M2 site of olivine and orthopyroxene endmembers is now also supported by the experimental results and, at least, the explicit negative result cannot be observed.

The atomic charges determined by the X-ray method are now consistent with the two requirements based on the electrostatic stability. It is regretable that the atomic charges (L1), (R1) and (R2) of orthopyroxenes are lacked in the above discussion. This is only because the refinements for these charges have not been carried out.

IV-2-D Conclusion

The determined atomic charges are consistent with the expected relations derived from the concept of the electrostatic stability in olivines and orthopyroxenes, for which the X-ray charge determinations were carried out. This consistency gives the theoretical basis to the relative values of the atomic charges.

In the fitting procedure the atomic charges largely depend on the atomic scattering factors used in the refinement. The atomic charges of the M1 and M2 sites of each endmember were determined based on the same set of the atomic scattering factors, the same intensity data and the same procedures of refinement. Then the reliability of the relative values is considered to be somewhat large. The consistency between the relative values of them and the expected relations in the crystals is, therefore, supposed to be meaningful.

As a conclusion the anomaly of the olivine structure which is observed in the intra-crystalline distributions of cations and the atomic charges was explained theoretically by introducing the semi-quantitative treatment of the electrostatic stability. Therefore the term of the electrostatic stability should not be neglected in the discussions of crystal chemistry of such silicate minerals as olivine and orthopyroxene.

Chapter V Conclusion

The Born's model of the bonding energy were applied on the following mineralogical problems; the order-disorder of Al and Si ions in the alkali feldspars, the stability relations of olivine, modified spinel and spinel, and the intra-crystalline cation distributions of olivines and orthopyroxenes.

The first problem is well explained by this approach as was at first expected. The second one still remains unsolved because the difference of the electrostatic energies of olivine and modified spinel or spinel is too large. This difference cannot be compensated by the repulsive energies. The reasons must be either that the estimation of the repulsive energies is not accurate enough or the application of the Born's model based on the assumption that the crystals are ionic, is unfavourable for these crystals. The third one is explained by the amendment of the Born's model. The assumption that the crystals are ionic is replaced in this case by the concept that the constituent ions have the net atomic charges. This replacement of the assumption leads to the success to explain the intra-crystalline cation distributions of olivines and orthopyroxenes. This has the important meaning that the silicate minerals cannot be always treated as the ionic crystals and that the Born's model should be amended when it is applied on the silicate minerals. The success in alkali feldspars is considered to be due to the highly ionic elements constituting the crystals and due to the evident large contributions of the

electrostatic and repulsive energies in the same sense.

It would be interesting to take the concept of the net atomic charges into consideration of the stability relations of olivine, modified spinel and spinel, but now it is impossible because of the lack of the net atomic charges and the reliable repulsive constants. The problem still remains in the future.

The concept of the electrostatic stability has the connection with the net atomic charges. This concept seems to have some of the predictional ability about the relative values of the net atomic charges. It is, therefore, important to take the concept into consideration in the X-ray charge refinements.

The accurate structure determination of two transition metal (Co and Ni-) olivines will contribute to the further energetic studies of olivines and the asphericities of the electron density distributions around transition metal ions encourage us to study directly the electron distributions of d-electrons in the octahedral sites by the X-ray method.

References

Akimoto, S., Matsui, Y. and Y. Syono (1976) High pressure crystal chemistry of orthosilicates and the formation of the mantle transition zone. In: The Physics and Chemistry of Minerals and Rocks. (R.G.J. Strens, ed.), John Wiley & Sons, Inc. New York, London, Sydney, 327-363.

Bailey, S.W. (1969) Refinement of an intermediate microcline structure. Amer. Mineral. 54, 1540-1545.

Baur, W.H. (1972) Computer-simulated crystal structures of observed and hypothetical Mg_2SiO_4 Polymorphs of low and high density. Amer. Mineral. 57, 709-731.

Bertaut, P.F. (1952) L'energie electrostatique de reseaux ioniques. J. Phys. Radium 13, 499-505.

Brown, B.E. and S.W. Bailey (1964) The structure of maximum microcline. Acta Cryst. 17, 1391-1400.

Brown, G.E. (1970) Crystal chemistry of olivines. Ph.D. Thesis, Virginia Polytechnic Institute.

Brown, G.E., Hamilton, W.C., Prewitt C.T. and S. Sueno (1971) Neutron diffraction study of Al/Si ordering in Sanidine. Progr. Geol. Soc. Amer. Mtg. Washington, D.C. 514.

Brown, G.E. and P.M. Fenn (1979) Structure energies of the alkali feldspars. Phys. Chem. Minerals 4, 83-100.

Busing, W.R., Martin, K.O. and H.A. Levy (1964) ORFFE: A Fortran crystallographic function and error program. Report ORNL-TM-306, Oak Ridge National Laboratory, Ork Ridge Tennesee.

Chao, S.H., Hargreaves, A. and W.H. Taylor (1940) The structure of orthoclase. Mineral. Mag. 25, 498-512.

Cole, W.F., Sorum, H., and O. Kennard (1949) The crystal structures of orthoclase and sanidinized orthoclase. Acta Cryst. 2, 280-287.

Colville, A.A. and P.H. Ribbe (1968) The crystal structure of an adularia and a refinement of the structure of orthoclase. Amer. Mineral. 53, 25-37.

Coppens, P. and W.C. Hamilton (1970) Anisotropic extinction corrections in the Zachariasen approximation. Acta Cryst. A26, 71-87.

Coppens, P., Pantler, D. and J.F. Griffin (1971) Electron population analysis of accurate diffraction data. II. Application of one-center formalism to some organic and inorganic molecules. J. Amer. Chem. Soc. 93, 1051-1058.

Coppens, P., Guru Row, T.N., Leung, P., Stevens, E.D., Becker, P.J. and Y.W. Yang (1979) Net atomic charges and molecular dipole moments from spherical-atom X-ray refinements, and the relation between atomic charge and shape. Acta Cryst. A35, 63-72.

Ferguson, R.B., Traill, R.J. and W.H. Taylor (1958) The crystal structures of low-temperature and high-temperature albites. Acta Cryst. 11, 331-348.

Finger, L.W. (1970) Fe/Mg ordering of olivines. Carnegie Inst. Wash. Year Book, 69, 302-305.

Fujino, K., Sasaki, S., Takeuchi, Y. and R. Sadanaga (1976) The charge distribution analysis of silicates by the X-ray method(III) (abstr.) Cryst. Soc. Japan Abstracts with Programs, 73. (in Japanese)

Fukamachi, T. (1971) Mean X-ray scattering factors calculated from analytical Roothaan-Hartree-Fock wave functions by Clementi. Technical Report of ISSP, B12, 8-62.

Gait, R.I. and R.B. Ferguson (1970) Electrostatic charge distributions in the structure of low albite, $NaAlSi_3O_8$. Acta Cryst. B26, 68-77.

Ghose, S. and C. Wan (1974) Strong site preference of Co^{2+} in olivine, $Co_{1.10}Mg_{0.90}SiO_4$. Contrib. Mineral. Petrol. 47, 131-140.

Harlow, G.E., Brown, G.E. and W.C. Hamilton (1973) Neutron diffraction study of Amelia low albite. Trans. Amer. Geophys. Union 54, 497.

Huggins, M.L. and Y. Sakamoto (1957) Lattice energies and other properties of crystals of alkaline earth chalcogenides. J. Phys. Soc. Japan 12, 241-251.

International Tables for X-ray Crystallography Vol. I, III and IV (1969, 1968 and 1974) Birmingham: Kynoch Press.

Ito, E., Matsumoto, T. and N. Kawai (1974) High-pressure decompositions in manganese silicates and their geophysical implications. Phys. Earth Planet. Inter. 8, 241-245.

Iwata, M. and Y. Saito (1973) The crystal structure of Hexamminecobalt (III) Hexacyanocobaltate (III): An accurate determination. Acta Cryst. B29, 822-832.

Jones, R.E. and D.H. Templeton (1956) Optimum atomic shape for Bertaut series. J. Chem. Phys. 25, 1062-1063.

Kamb, B. (1968) Structural basis of the olivine-spinel stability relation. Amer. Mineral. 53, 1439-1454.

Kittel, C. (1967) Introduction to Solid State Physics. Third ed. John Wiley & Sons, Inc. New York, London, Sydney. 81-107.

Marumo, F., Isobe, M., Saito, Y., Yagi, T. and S. Akimoto (1974) Electron-density distribution in crystals of γ-Ni_2SiO_4. Acta Cryst. B30, 1904-1906.

Marumo, F., Isobe, M. and S. Akimoto (1977) Electron-density distributions in crystals of γ-Fe_2SiO_4 and γ-Co_2SiO_4. Acta Cryst. B33, 713-716.

Miyamoto, M., Takeda, H. and Y. Matsui (1979) The prediction of crystal structures under high pressures by the method of energetic minimization: Olivine and spinel (abstr.). Cryst. Soc. Japan. Abstracts with Programs, 3B-4. (in Japanese)

Moore, P.B. and J.V. Smith (1969) High pressure modification of Mg_2SiO_4: Crystal structure and crystallochemical and geophysical implications. Nature, 221, 653-655.

Moore, P.B. and J.V. Smith (1970) Crystal structure of β-Mg_2SiO_4: Crystal-chemical and geophysical implications. Phys. Earth Planet. Inter. 3, 166-177.

Morimoto, N., Akimoto, S., Koto, K. and M. Tokonami (1969) Modified spinel, Beta-Manganous orthogermanate: Stability and crystal structure. Science 165, 586-588.

Morimoto, N., Akimoto, S., Koto, K. and M. Tokonami (1970) Crystal structures of high pressure modifications of Mn_2GeO_4 and Co_2SiO_4. Phys. Earth Planet. Inter. 3, 161-165.

Morimoto, N., Tokonami, M. Watanabe, M. and K. Koto (1974) Crystal structures of three polymorphs of Co_2SiO_4. Amer. Mineral. 59, 475-485.

Ohashi, Y. and C.W. Burnham (1972) Electrostatic and repulsive energies of the M1 and M2 cation sites in pyroxenes. J. Geopys. Res. 77, 5761-5766.

Phillips, M.W. and P.H. Ribbe (1973) The structures of monoclinic potassium-rich feldspars. Amer. Mineral. 58, 263-270.

Prewitt, C.T., Sueno, S. and J.J. Papike (1976) The crystal structures of high albite and monoalbite at high temperature. Amer. Mineral. 61, 1213-1225.

Prince, E., Donney, G. and R.F. Martin (1973) Neutron diffraction refinement of an ordered orthoclase structure. Amer. Mineral. 58, 500-507.

Rajamani, V., Brown, G.E. and C.T. Prewitt (1975) Cation ordering in Ni-Mg olivine. Amer. Mineral. 60, 292-299.

Raymond, M. (1971) Madelung constants for several silicates. Carnegie Inst. Wash. Year Book, 70, 255-227.

Ribbe, P.H., Megaw, H.D., Taylor, W.H., Ferguson, R.B. and R.J. Traill (1969) The albite structures. Acta Cryst. B25, 1503-1518.

Sasaki, S., Fujino, K., Takeuchi, Y. and R. Sadanaga (1977) The charge distribution analysis of silicates by the X-ray method (III). (abstr.) Cryst. Soc. Japan. Abstracts with Programs, PB-2. (in Japanese)

Sasaki, S., Fujino, K., Takeuchi, Y. and R. Sadanaga (1978) Acta Cryst. A34, S4, S21.

Sasaki, S., Fujino, K. and Y. Takeuchi (1979) X-ray determination of electron-density distributions in oxides, MgO, MnO, CoO and atomic scattering factors of their constituent atoms. Proc. Japan Acad. 55B, 43-48.

Sasaki, S., Fujino, K., Takeuchi, Y. and S. Akimoto (1979) The atomic charges and electron density distributions of orthopyroxenes: $MgSiO_3$, $CoSiO_3$ and $FeSiO_3$. (abstr.) Cryst. Soc. Japan. Abstracts with Programs, 3A-12. (in Japanese)

Shannon, R.D. and C.T. Prewitt (1969) Effective ionic radii in oxides and fluoxides. Acta Cryst. 25, 925-946.

Smith, D.K., Majumdar, A. and F. Ordway (1965) The crystal structure of γ-dicalcium silicate. Acta Cryst. 18, 787-795.

Smith, J.R. (1975) High temperature crystal chemistry of fayalite. Amer. Mineral. 60, 1092-1097.

Smith, J.V. (1954) A review of the Al-O and Si-O distances. Acta Cryst. 7, 479-481.

Smith, J.V. (1974) Feldspar Minerals, Vol. 1. Springer-Verlag. Berlin, Heidelberg, New York.

Stevens, E.D. and P. Coppens (1975) Experimental measurements of the X-ray scale factor for charge density studies. Acta Cryst. 31, 612-619.

Stewart, R.F. (1970) Valence structure from X-ray diffraction data: An L-shell projection method. J. Chem. Phys. 53, 205-213.

Sueno, S., Cameron, M. and C.T. Prewitt (1976) Orthoferrosilite: High-temperature crystal chemistry. Amer. Mineral. 61, 38-53.

Sung, C. and R.G. Burns (1978) Crystal structural features of the olivine → spinel transition. Phys. Chem. Minerals, 2, 177-197.

Tamada, O. (1973) The spectroscopic research of site preference of Ni^{2+} ions in the Ni-olivine $(Ni_xMg_{1-x})_2SiO_4$. M. Sc. Thesis submitted to Dept. Geol. & Mineral, Kyoto Univ.

Tamada, O. (1976) The effect of electrostatic energy and ionic radius on the cation ordering in olivines and orthopyroxenes. (abstr.) Soc. Mining Geol. and Mineral. Soc. Japan. Abstracts with Programs, C20, 114. (in Japanese)

Tamada, O. and T. Ueda (1976) Electrostatic energies of K-feldspars. Tsukumo Earth Sci. 11, 1-6. (in Japanese)

Tamada, O. (1977) The X-ray refinement of Ni_2SiO_4 olivine. (abstr.) Mineral. Soc. Japan. Abstracts with Programs, B17, 65.

Tamada, O., Sawada, T. and T. Ueda (1977) The effect of electrostatic energy on the Al/Si ordering of albites. Tsukumo Earth Sci. 12, 11-17. (in Japanese)

Templeton, D.H. (1955) Rate of convergence of Madelung series by the method of Bertaut. J. Chem. Phys. 23, 1629-1630.

Tokonami, M. (1965) Atomic scattering factor for O^{2-}. Acta Cryst. 19, 486.

Tokonami, M., Morimoto, N., Akimoto, S., Syono, Y. and H. Takeda (1972) Stability relations between olivine, spinel and modified spinel. Earth Planet. Sci. Letters, 14, 65-69.

Wainwright, J.E. and J. Starkey (1968) Crystal structure of a metamorphic low albite. (abstr.) Geol. Soc. America. Abstracts with programs, 31C.

Weitz, G. (1972) Die struktur des sanidins bei verschiedenen ordnungsgraden. Z. Krist. 136, 418-426.

Whittaker, E.J.W. (1971) Madelung energies and site preferences in amphiboles. I. Amer. Mineral 56, 980-996.

Wood, B.J. (1974) Crystal field spectrum of Ni^{2+} in olivine. Amer. Mineral 59, 244-248.

Zachariasen, W.H. (1967) A general theory of X-ray diffraction in crystals. Acta Cryst. 23, 558-564.

Appendix 1. The program to calculate the electrostatic energies of crystal and the constituent ions. (The output data of low albite are shown together as an example.)

```
SPECIFIED O
C     CALCULATION OF MADELUNG ENERGY IN CRYSTAL AND ALL THE SITES                    MAL    1
C     MADELUNG ENERGIES OF ALL THE ATOMS AND THE CRYSTAL FOR ORTHORUMBIC             MAL    2
C     WRITTEN BY OSAMU TAMADA                                                        MAL    3
C     MODIFIED BY OSAMU TAMADA IN DEC.24TH,1974
ISN 00001      DIMENSION X(500),Y(500),Z(500),Q(500),M(500)                          MAL    5
ISN 00002      DIMENSION SIT(50),NAME(36),SUMS(50),SUMMS(50),MIKS(50),UI(50),       MAL    6
              1UERG(50),UEV(50),UACAL(50),PUKLAL(50)                                MAL    7
ISN 00003      READ(5,1)(NAME(I),I=1,36)                                            MAL    8
ISN 00004     1 FORMAT(18A4)                                                        MAL    9
ISN 00005      WRITE(6,20)(NAME(I),I=1,36)                                          MAL    9-1
ISN 00006     20 FORMAT(1H1,//1H ,5X,18A4,//1H ,10X,18A4)                           MAL    9-2
ISN 00007      READ(5,2)A,B,C,AL,BE,GA                                              MAL   10
ISN 00008     2 FORMAT(6F10.5)                                                      MAL   11
ISN 00009      WRITE(6,70)
ISN 00010     70 FORMAT(//1H ,10X,26H** LATTICE PARAMETERS **)
ISN 00011      WRITE(6,21)A,B,C,AL,BE,GA                                            MAL   12
ISN 00012     21 FORMAT(1H ,15X,2HA=F10.5,5X,2HB=F10.5,5X,2HC=F10.5,5X,            MAL   13
              23HAL=F10.5,5X,3HBE=F10.5,5X,3HGA=F10.5)                              MAL   14
ISN 00013      READ(5,3)R,NZ                                                        MAL   15
ISN 00014     3 FORMAT(F10.5,I10)                                                   MAL   16
ISN 00015      WRITE(6,71)
ISN 00016     71 FORMAT(/ 1H ,10X, 75H** RADIUS OF CHARGE DISTRIBUTION******NUMBER
              1 OF MOLECULES IN UNIT CELL **)
ISN 00017      WRITE(6,22)R,NZ                                                      MAL   17
ISN 00018     22 FORMAT(1H ,23X,2HR=F10.5,24X,3HNZ=I10)                             MAL   18
ISN 00019      READ(5,4)BET,G,GC                                                    MAL   19
ISN 00020     4 FORMAT(3F10.7)                                                      MAL   20
ISN 00021      WRITE(6,72)
ISN 00022     72 FORMAT(/ 1H ,10X,111H** RADIUS RANGE OF ALPHA SUMMATION******CORREC
              1CTION FACTOR OF SELF-ENERGY******CORRECTION FACTOR OF SUMMATION **)
              2)
ISN 00023      WRITE(6,23)BET,G,GC                                                  MAL   21
ISN 00024     23 FORMAT(1H ,23X,4HBET=F7.4 ,4H=PAI,2X,2HG=F10.7,2X,2HG=F10.7)
ISN 00025      READ(5,5)NP,NS                                                       MAL   22
ISN 00026     5 FORMAT(2I10)                                                        MAL   23
ISN 00027      WRITE(6,73)
ISN 00028     73 FORMAT(/ 1H ,10X,66H** NUMBER OF UNEQUIVALENT ATOMS******NUMBER OF
              1 GENERAL POSITIONS **)
ISN 00029      WRITE(6,24)NP,NS                                                     MAL   24
ISN 00030     24 FORMAT(1H ,23X,3HNP=I10,19X,3HNS=I10)                              MAL   25
ISN 00031      READ(5,6)(X(I),Y(I),Z(I),Q(I),M(I),SIT(I),I=1,NP)                    MAL   26
ISN 00032     6 FORMAT(4F10.5,I10,A4)                                               MAL   27
ISN 00033      WRITE(6,74)
ISN 00034     74 FORMAT(/ 1H ,10X,80H** ATOMS**********MULTIPLICITY***CHARGE******
              1***ATOMIC CO-ORDINATES (X,Y,Z) **)
ISN 00035      WRITE(6,75)(SIT(I),M(I),Q(I),X(I),Y(I),Z(I),I=1,NP)
ISN 00036     75 FORMAT(1H ,15X,A4,6X,I8,7X,F10.5,10X,1H(,F10.5,2X,1H,F10.5,2X,1H,
              1F10.5,3X,1H),)
ISN 00037      CALL SYMM(X,Y,Z,Q,M,NP)                                              MAL   31
ISN 00038      PAI=3.14159265                                                       MAL   32
ISN 00039      BET=BET*PAI
ISN 00040      AL=AL*PAI/180.0                                                      MAL   33
ISN 00041      BE=BE*PAI/180.0                                                      MAL   34
ISN 00042      GA=GA*PAI/180.0                                                      MAL   35
ISN 00043      S11=B*B*C*C*SIN(AL)*SIN(AL)                                          MAL   36
ISN 00044      S22=C*C*A*A*SIN(BE)*SIN(BE)                                          MAL   37
ISN 00045      S33=A*A*B*B*SIN(GA)*SIN(GA)                                          MAL   38
ISN 00046      S23=A*A*B*C*(COS(BE)*COS(GA)-COS(AL))                                MAL   39
ISN 00047      S31=A*B*B*C*(COS(GA)*COS(AL)-COS(BE))                                MAL   40
ISN 00048      S12=A*B*C*C*(COS(AL)*COS(BE)-COS(GA))                                MAL   41

FACOM OS1V/F4 FORTRAN 1V (HE)  V04L12        MAIN  DATE 79.06.21  TIME 11.32.08                                PAGE 2

ISN 00049          V=SQRT(1.0-COS(AL)**2-COS(BE)**2-COS(GA)**2                      MAL   42
                  +2.0*COS(AL)*COS(BE)*COS(GA))                                    MAL   43
ISN 00050          V=A*B*C*V                                                        MAL   44
ISN 00051          HM=BET/(2.0*PAI*R)                                               MAL   45
ISN 00052          ILM=HM*C
ISN 00053          IKM=HM*B
ISN 00054          IHM=HM*A
ISN 00055          WRITE(6,76)
ISN 00056     76 FORMAT(/ 1H ,10X,91H** VOLUME OF UNIT CELL(IN ANG***3)**********MAX.RANGE
              2AX.RANGE OF SUMMATION IN RECIPROCAL SPACE **)
ISN 00057          WRITE(6,26)V,HM                                                  MAL   47
ISN 00058     26 FORMAT(1H ,17X,2HV=F10.4,40X,3HHM=F10.7)                           MAL    3
ISN 00059          WRITE(6,77)
ISN 00060     77 FORMAT(/ 1H ,10X,46H** MAX.RANGE OF SUMMATION OF INDEX (H,K,L) **)
              1)
ISN 00061          WRITE(6,27)IHM,IKM,ILM                                           MAL   51
ISN 00062     27 FORMAT(1H ,17X,4HIHM=I10,5X,4HIKM=I10,5X,4HILM=I10)                MAL   52
ISN 00063          DO 30 IP=1,NP                                                    MAL   53
ISN 00064          SUMS(IP)=0.0                                                     MAL   54
ISN 00065     30 CONTINUE                                                           MAL   55
ISN 00066          DO 50 IH1=1,IHM+1                                                MAL   56
ISN 00067          IH=IH1-1                                                         MAL   57
ISN 00068          DO 51 IK1=1,IKM+1                                                MAL   58
ISN 00069          IK=IK1-1                                                         MAL   59
ISN 00070          DO 52 IL1=1,ILM+1                                                MAL   60
ISN 00071          IL=IL1-1                                                         MAL   61
ISN 00072          H2=FLOAT(IH)**2*S11+FLOAT(IK)**2*S22+FLOAT(IL)**2*S33            MAL   62
                  2+2.0*FLOAT(IK*IL)*S23+2.0*FLOAT(IL*IH)*S31+2.0*FLOAT(IH*IK)*S12 MAL   63
ISN 00073          H=SQRT(H2)/V                                                     MAL   64
ISN 00074          ALP=2.0*PAI*HM*R                                                 MAL   65
ISN 00075          IF(ALP)41,52,41                                                  MAL   66
ISN 00076     41 IF(BET-ALP)52,40,40                                                MAL   67
ISN 00077     40 FAI=ERR.C*(ALP*SIN(ALP)+2.0*COS(ALP)-2.0)**2/ALP**10               MAL   68
ISN 00078          AH=2.0                                                           MAL   69
ISN 00079          AK=2.0                                                           MAL   70
ISN 00080          AL=2.0                                                           MAL   71
ISN 00081          IF(IH)61,60,61                                                   MAL   72
ISN 00082     60 AH=1.0                                                             MAL   73
ISN 00083     61 IF(IK)62,63,62                                                     MAL   74
ISN 00084     63 AK=1.0                                                             MAL   75
ISN 00085     62 IF(IL)64,65,64                                                     MAL   76
ISN 00086     65 AL=1.0                                                             MAL   77
ISN 00087     64 BH=AH*AK*AL                                                        MAL   78
ISN 00088          DO 54 IP=1,NP                                                    MAL   79
ISN 00089          X1=X(IP)                                                         MAL   80
ISN 00090          Y1=Y(IP)                                                         MAL   81
ISN 00091          Z1=Z(IP)                                                         MAL   82
ISN 00092          S1=0.0                                                           MAL   83
ISN 00093          DO 55 I=1,NP*NS                                                  MAL   84
ISN 00094          GLSH=2.0*PAI*FLOAT(IH)*(A(I)-X1)                                 MAL   85
ISN 00095          GLSK=2.0*PAI*FLOAT(IK)*(Y(I)-Y1)                                 MAL   86
ISN 00096           GLSL=2.0*PAI*FLOAT(IL)*(Z(I)-Z1)                                MAL   87
ISN 00097          ACOS=COS(GLSH)*COS(GLSK)*COS(GLSL)/FLOAT(M(I))                   MAL   88
ISN 00098          S1=S1+Q(I)*ACOS                                                  MAL   89
ISN 00099     55 CONTINUE                                                           MAL   90
ISN 00100          SUMS(IP)=SUMS(IP)+BH*S1*FAI                                      MAL   91
ISN 00101     54 CONTINUE                                                           MAL   92
ISN 00102     52 CONTINUE                                                           MAL   93
ISN 00103     51 CONTINUE                                                           MAL   94
ISN 00104     50 CONTINUE                                                           MAL   95
ISN 00105          E=4.80325E-10
ISN 00106          W1=0.0
```

```
ISN 00107          DO 57 IP=1,NP                                                  MUL  104
ISN 00108          SUMMS(IP)=2.0*PAI*R*R*U(IP)*SUMS(IP)/V                         MUL  105
ISN 00109          HIKS(IP)=2.0*(G-GC)*Q(IP)*U(IP)/R                              MUL  106
ISN 00110          U1(IP)=SUMMS(IP)-HIKS(IP)                                      MUL  107
ISN 00111          W1=W1+U1(IP)*FLOAT(NS/M(IP))/2 )
ISN 00112          UERG(IP)=U1(IP)*E*E*1.0E08                                     MUL  108
ISN 00113          UEV(IP)=UERG(IP)/1.60219E-12                                   MUL  109
ISN 00114          UKCAL(IP)=UEV(IP)/4.33849E-02                                  MUL  110
ISN 00115          PUKCAL(IP)= UKCAL(IP)/Q(IP)                                    MUL110-1
ISN 00116       57 CONTINUE                                                       MUL  111
ISN 00117          WERG=W1*E*E*1.0E08/FLOAT(NZ)                                   MUL  112
ISN 00118          WEV=WERG/1.60219E-12                                           MUL112-1
ISN 00119          WKCAL=WEV/4.33849E-02                                          MUL  113
ISN 00120          WRITE(6,78)
ISN 00121       78 FORMAT(/ 1H ,10X,51H** ELECTROSTATIC ENERGIES OF CRYSTAL AND ATOMS **)
                   15  **)                                                       MUL110-1
ISN 00122          WRITE(6,37)WERG,WEV,WKCAL
ISN 00123       37 FORMAT(1H ,15X,7HCRYSTAL,3X,5HWERG=E15.8,5X,4HWEV=E15.8,6X,5HWKCAL=E15.8)
                  1=E15.8)
ISN 00124          DO 58 IP=1,NP                                                  MUL  114
ISN 00125          WRITE(6,36)SIT(IP),UERG(IP),UEV(IP),UKCAL(IP),PUKCAL(IP)       MUL  115
ISN 00126       36 FORMAT(1H ,15X,A4,6X,5HUERG=E15.8,5X,4HUEV=E15.8,6X,5HUKCAL=E15.8,MUL  116
                  6X,7HPUKCAL=E15.8)                                             MUL114-1
ISN 00127       58 CONTINUE                                                       MUL114-1
ISN 00128          STOP                                                           MUL  120
ISN 00129          END
```

FACOM OS1V/F4 FORTRAN IV (HE) V04L12 DATE 79.09.05 TIME 22.25.30 PAGE 16

SPECIFIED OPTIONS: MAP,ASTER

```
ISN 00257          SUBROUTINE SYMM(X,Y,Z,G,M,NP)                                  01    1
ISN 00258          DIMENSION X(1500),Y(1500),Z(1500),G(1500),M(1500)              01    2
ISN 00259          DO 101 J=1,NP                                                  01    3
ISN 00260          I=1*NP+J                                                       01    4
ISN 00261          X(I)=-X(J)                                                     01    5
ISN 00262          Y(I)=-Y(J)                                                     01    6
ISN 00263          Z(I)=-Z(J)                                                     01    7
ISN 00264          G(I)=G(J)                                                      01    8
ISN 00265          M(I)=M(J)                                                      01    9
ISN 00266          I=2*NP+J                                                       01   10
ISN 00267          X(I)=0.5+X(J)                                                  01   11
ISN 00268          Y(I)=0.5+Y(J)                                                  01   12
ISN 00269          Z(I)=Z(J)                                                      01   13
ISN 00270          G(I)=G(J)                                                      01   14
ISN 00271          M(I)=M(J)                                                      01   15
ISN 00272          I=3*NP+J                                                       01   16
ISN 00273          X(I)=0.5-X(J)                                                  01   17
ISN 00274          Y(I)=0.5-Y(J)                                                  01   18
ISN 00275          Z(I)=-Z(J)                                                     01   19
ISN 00276          G(I)=G(J)                                                      01   20
ISN 00277          M(I)=M(J)                                                      01   21
ISN 00278       101 CONTINUE                                                      01   22
ISN 00279          RETURN                                                         01   23
ISN 00280          END                                                            01   24
```

LOW ALBITE NAALSI3O8 MAMONA R=0.068

FROM RIBBE ET AL.(1969) ACTA,25,1503-1518

** LATTICE PARAMETERS **
A= 8.13400 B= 12.78900 C= 7.15600 AL= 94.33000 BE= 116.57001 GA= 87.64999

** RADIUS OF CHARGE DISTRIBUTION****** NUMBER OF MOLECULES IN UNIT CELL **
R= 0.80000 NZ= 4

** RADIUS RANGE OF ALPHA SUMMATION***** CORRECTION FACTOR OF SELF-ENERGY***** CORRECTION FACTOR OF SUMMATION **
BET= 3.0000*PAI G= 0.7429571 G= 0.0000000

** NUMBER OF UNEQUIVALENT ATOMS***** NUMBER OF GENERAL POSITIONS **
NP= 12 NS= 4

** ATOMS********** MULTIPLICITY*** CHARGE********** ATOMIC CO-ORDINATES (X,Y,Z) **

NA	1	1.00000	(0.26820 ,	0.95886 ,	0.14620)
T1C	1	3.00000	(0.00950 ,	0.18921 ,	0.22181)
T1M	1	4.00000	(0.00410 ,	0.82020 ,	0.22750)
T2O	1	4.00000	(0.69190 ,	0.11020 ,	0.91460)
T2M	1	4.00000	(0.68130 ,	0.88220 ,	0.26040)
OA1	1	-2.00000	(0.00050 ,	0.13060 ,	0.96840)
OA2	1	-2.00000	(0.59290 ,	0.99740 ,	0.22080)
OBC	1	-2.00000	(0.81240 ,	0.11010 ,	0.19050)
OBM	1	-2.00000	(0.82010 ,	0.85120 ,	0.25070)
OCO	1	-2.00000	(0.01320 ,	0.20350 ,	0.22690)
OCM	1	-2.00000	(0.02690 ,	0.69350 ,	0.22690)
ODO	1	-2.00000	(0.20750 ,	0.10910 ,	0.28900)
ODM	1	-2.00000	(0.18400 ,	0.68810 ,	0.42480)

** VOLUME OF UNIT CELL(IN ANG***3)********** MAX.RANGE OF SUMMATION IN RECI.*KOOAL SPACE **
V= 664.1948 HM= 1.8750000

** MAX.RANGE OF SUMMATION OF INDEX (H,K,L) **
IHM= 15 IKM= 23 ILM= 15

** ELECTROSTATIC ENERGIES OF CRYSTAL AND ATOMS **

CRYSTAL	WERG=-0.9290350?E-04	WEV=-0.5?6L9717E+03	WKCAL=-0.1350?42?E+03	
NA	UERG=-0.???39573E-10	UEV=-0.1297?2?6E+02	UKCAL=-0.???1?0?3E+02	PUKCAL=-0.???1?0?3E+02
T1O	UERG=-0.17636?3EE-04	UEV=-0.1100?7?7E+03	UKCAL=-0.?537?66E+04	PUKCAL=-0.?45?595?E+03
T1M	UERG=-0.30711544E-04	UEV=-0.1?1E?4?1E+03	UKCAL=-0.441?7?44E+04	PUKCAL=-0.11?455??E+04
T2O	UERG=-0.3042?2E4E-04	UEV=-0.1?9?66?4E+03	UKCAL=-0.427?2?5?E+04	PUKCAL=-0.1?94?E4?E+04
T2M	UERG=-0.?164?616E-04	UEV=-0.1?1?4?53E+03	UKCAL=-0.44?4?555E+04	PUKCAL=-0.11?655?4E+04
OA1	UERG=-0.?7113691E-10	UEV=-0.?437164?E+02	UKCAL=-0.1?52?5??E+04	PUKCAL= 0.?6?6193?E+03
OA2	UERG=-0.96267272E-10	UEV=-0.?00?4?05E+02	UKCAL=-0.1?84?45?E+04	PUKCAL= 0.69?46?1?E+03
OBO	UERG=-0.912?1691E-10	UEV=-0.5697?0?3E+02	UKCAL=-0.1?13?007E+04	PUKCAL= 0.?5?6?05?E+03
OBM	UERG=-0.1?2?6?4?E-04	UEV=-0.?37170?0E+02	UKCAL=-0.14?6??44E+04	PUKCAL= 0.?345???7E+03
OCO	UERG=-0.?09446?3E-10	UEV=-0.5?67?695E+02	UKCAL=-0.13?5?513E+04	PUKCAL= 0.?5417?54E+03
OCM	UERG=-0.99?628?9E-10	UEV=-0.619??093E+02	UKCAL=-0.14?5?534E+04	PUKCAL= 0.?14?166?E+03
ODO	UERG=-0.913601?3E-10	UEV=-0.57?22?64E+02	UKCAL=-0.13143?9?E+04	PUKCAL= 0.?5?16479E+03
ODM	UERG=-0.1?31?151E-04	UEV=-0.644??99?E+02	UKCAL=-0.14?43943E+04	PUKCAL= 0.?4?197?E+03

Appendix 2. The program to calculate the electrostatic energies of crystal and the constituent ions, together with the standard errors derived from those of the structural data. (The output data of high albite are shown together as an example.)

```
                C     CALCULATION OF MADELUNG ENERGY IN CRYSTAL AND ALL THE SITES        MDSG   1
                C     WRITTEN BY OSAMU TAMADA      1976 11 20                            MDSG   2
                C     MODIFIED BY OSAMU TAMADA IN DEC.24TH,1974                          MDSG   3
  ISN 00001           DIMENSION X(500),Y(500),Z(500),E(500),M(500)                       MDSG   4
  ISN 00002           DIMENSION SIT(50),NAME(36),SUMS(50),SUMHS(50),HIKS(50),UI(50),     MDSG   5
                     1UERG(50),UEV(50),UKCAL(50),PUKCAL(50)                             MDSG   6
  ISN 00003           DIMENSION AU(50),SUERG(50),SUEV(50),SUKCL(50),SPUKC(50)            MDSG   7
                     1 ,RUERG(50),SX(50),SY(50),SZ(50)                                  MDSG   8
  ISN 00004           COMMON A,NZ,BET,G,GC,NP,NS,UERG,UEV,UKCAL,PUKCAL,                  MDSG   9
                     1WERG,WEV,WKCAL                                                    MDSG  10
  ISN 00005           READ(5,1)(NAME(I),I=1,36)                                          MDSG  11
  ISN 00006         1 FORMAT(18A4)                                                       MDSG  12
  ISN 00007           WRITE(6,20)(NAME(I),I=1,36)                                        MDSG  13
  ISN 00008        20 FORMAT(1H1,///1H ,5X,18A4,//1H ,10X,18A4)                        MDSG  14
  ISN 00009           READ(5,2)A,B,C,AL,BE,GA                                          MDSG  15
  ISN 00010         2 FORMAT(6F10.5)                                                   MDSG  16
  ISN 00011           WRITE(6,70)                                                      MDSG  17
  ISN 00012        70 FORMAT(///1H ,10X,28H**  LATTICE PARAMETERS  **)                 MDSG  18
  ISN 00013           WRITE(6,21)A,B,C,AL,BE,GA                                        MDSG  19
  ISN 00014        21 FORMAT(1H ,15X,2HA=F10.5,5X,2HB=F10.5,5X,2HC=F10.5,5X,          MDSG  20
                     2HAL=F10.5,5X,2HBE=F10.5,5X,3HGA=F10.5)                          MDSG  21
  ISN 00015           READ(5,3)N,NZ                                                    MDSG  22
  ISN 00016         3 FORMAT(F10.5,I10)                                                MDSG  23
  ISN 00017           WRITE(6,71)                                                      MDSG  24
  ISN 00018        71 FORMAT(/ 1H ,10X, 75H**  RADIUS OF CHARGE DISTRIBUTION******NUMBERMDSG  25
                     1 OF MOLECULES IN UNIT CELL  **)                                 MDSG  26
  ISN 00019           WRITE(6,22)N,NZ                                                  MDSG  27
  ISN 00020        22 FORMAT(1H ,22X,2HN=I10,24X,3HNZ=I10)                             MDSG  28
  ISN 00021           READ(5,4)BET,GGC                                                 MDSG  29
  ISN 00022         4 FORMAT(2F10.7)                                                   MDSG  30
  ISN 00023           WRITE(6,72)                                                      MDSG  31
  ISN 00024        72 FORMAT(/ 1H ,10X,111H**  RADIUS RANGE OF ALPHA SUMMATION*****CORRE
                     1CTION FACTOR OF SELF-ENERGY*****CORRECTION FACTOR OF SUMMATION  **   6  32
                     2)                                                               MDSG  34
  ISN 00025           WRITE(6,23)BET,G,GC                                              MDSG  35
  ISN 00026        23 FORMAT(1H ,22X,4HBET=F7.4 ,4H=PAI,21X,2HG=F10.7,27X,2H=F10.7)    MDSG  36
  ISN 00027           READ(5,5)NP,NS                                                   MDSG  37
  ISN 00028         5 FORMAT(2I10)                                                     MDSG  38
  ISN 00029           WRITE(6,73)                                                      MDSG  39
  ISN 00030        73 FORMAT(/ 1H ,10X,66H**  NUMBER OF UNEQUIVALENT ATOMS*****NUMBER OFMDSG  40
                     1 GENERAL POSITIONS  **)                                         MDSG  41
  ISN 00031           WRITE(6,24)NP,NS                                                 MDSG  42
  ISN 00032        24 FORMAT(1H ,23X,3HNP=I10,19X,3HNS=I10)                            MDSG  43
  ISN 00033           READ(5,6)(A(I),X(I),Y(I),Z(I),E(I),M(I),SIT(I),I=1,NP)           MDSG  44
  ISN 00034         6 FORMAT(4F10.5,I10,A4)                                            MDSG  45
  ISN 00035           WRITE(6,74)                                                      MDSG  46
  ISN 00036        74 FORMAT(/ 1H ,10X,80H**  ATOMS**********MULTIPLICITY***CHARGE******MDSG  47
                     1***ATOMIC CO-ORDINATES (X,Y,Z)  **)                             MDSG  48
  ISN 00037           WRITE(6,75)(SIT(I),M(I),E(I),A(I),X(I),Y(I),Z(I),I=1,NP)         MDSG  49
  ISN 00038        75 FORMAT(1H ,15X,A4,6X,I6,7X,F10.5,10X,1H(,F10.5,2X,1H,,F10.5,2X,1H),,MDSG  50
                     1F10.5,5X,1H),)                                                  MDSG  51
  ISN 00039           CALL MAD(A,B,C,AL,BE,GA,X,Y,Z,,,M,SIT)                           MDSG  52
  ISN 00040           WRITE(6,76)                                                      MDSG  53
  ISN 00041        76 FORMAT(/ 1H ,10X,51H**  ELECTROSTATIC ENERGIES OF CRYSTAL AND ATOMMDSG  54
                     1S  **)                                                          MDSG  55
  ISN 00042           WRITE(6,27)WERG,WEV,WKCAL                                        MDSG  56
  ISN 00043        27 FORMAT(1H ,15X,7HCRYSTAL,2X,5HWERG=E15.5,5X,4HWEV=E15.5,6X,6HWKCALMDSG  57
                     1=E15.8)                                                         MDSG  58
  ISN 00044           DO 28 IP=1,NP                                                    MDSG  59
  ISN 00045           WRITE(6,26)SIT(IP),UERG(IP),UEV(IP),UKCAL(IP),PUKCAL(IP)         MDSG  60

FACOM OSIV/F4 FORTRAN IV (HE)  V04L12        MAIN  DATE 79.09.03  TIME 23.26.44                    PAGE    2

  ISN 00046        26 FORMAT(1H ,15X,A4,4X,5HUERG=E15.8,5X,4HUEV=E15.8,6X,6HUKCAL=E15.8,MDSG  61
                     64X,7HPUKCAL=E15.8)                                              MDSG  62
  ISN 00047           RUERG(IP)=UERG(IP)                                               MDSG  63
  ISN 00048        28 CONTINUE                                                         MDSG  64
  ISN 00049           READ(5,120) SA,SB,SC,SAL,SBE,SGA                                 MDSG  65
  ISN 00050       120 FORMAT(6F10.5)                                                   MDSG  66
  ISN 00051           WRITE(6,122)                                                     MDSG  67
  ISN 00052       122 FORMAT(//1H ,10X,"**  SIGMA OF LATTICE PARAMETER   **",)        MDSG  68
  ISN 00053           WRITE(6,124) SA,SB,SC,SAL,SBE,SGA                                MDSG  69
  ISN 00054       124 FORMAT(1H ,15X,2HSA=F10.5,5X,2HSB=F10.5,5X,2HSC=F10.5,5X,4HSAL=F10MDSG  70
                     1.5,5X,4HSBE=F10.5,5X,4HSGA=F10.5)                               MDSG  71
  ISN 00055           WRITE(6,125)                                                     MDSG  72
  ISN 00056       125 FORMAT(//1H ,10X,"**   ATOMS  **  SIGMA OF (X,Y,Z)  **",)       MDSG  73
  ISN 00057           DO 121 IS=1,NP                                                   MDSG  74
  ISN 00058           READ(5,122) SX(IS),SY(IS),SZ(IS)                                 MDSG  75
  ISN 00059       122 FORMAT(3F10.5)                                                   MDSG  76
  ISN 00060           WRITE(6,126) SIT(IS),SX(IS),SY(IS),SZ(IS)                        MDSG  77
  ISN 00061       126 FORMAT(1H ,15X,A4,10X,1H(,3F20.5,1H) )                           MDSG  78
  ISN 00062       121 CONTINUE                                                         MDSG  79
  ISN 00063           RWERG=WERG                                                       MDSG  80
  ISN 00064           RW=0.0                                                           MDSG  81
  ISN 00065           DO 81 IS=1,NP                                                    MDSG  82
  ISN 00066           RU(IS)=0.0                                                       MDSG  83
  ISN 00067        81 CONTINUE                                                         MDSG  84
  ISN 00068           A=A+SA                                                           MDSG  85
  ISN 00069           IF(SA)82,84,82                                                   MDSG  86
  ISN 00070        82 CALL MAD(A,B,C,AL,BE,GA,X,Y,Z,W,M,SIT)                           MDSG  87
  ISN 00071           RW=RW+(WERG-RWERG)**2                                            MDSG  88
  ISN 00072           DO 83 IS=1,NP                                                    MDSG  89
  ISN 00073           RU(IS)=RU(IS)+(UERG(IS)-RUERG(IS))**2                            MDSG  90
  ISN 00074        83 CONTINUE                                                         MDSG  91
  ISN 00075        84 A=A-SA                                                           MDSG  92
  ISN 00076           B=B+SB                                                           MDSG  93
  ISN 00077           IF(SB)85,87,85                                                   MDSG  94
  ISN 00078        85 CALL MAD(A,B,C,AL,BE,GA,X,Y,Z,W,M,SIT)                           MDSG  95
  ISN 00079           RW=RW+(WERG-RWERG)**2                                            MDSG  96
  ISN 00080           DO 86 IS=1,NP                                                    MDSG  97
  ISN 00081           RU(IS)=RU(IS)+(UERG(IS)-RUERG(IS))**2                            MDSG  98
  ISN 00082        86 CONTINUE                                                         MDSG  99
  ISN 00083        87 B=B-SB                                                           MDSG 100
  ISN 00084           C=C+SC                                                           MDSG 101
  ISN 00085           IF(SC)88,90,88                                                   MDSG 102
  ISN 00086        88 CALL MAD(A,B,C,AL,BE,GA,X,Y,Z,W,M,SIT)                           MDSG 103
  ISN 00087           RW=RW+(WERG-RWERG)**2                                            MDSG 104
  ISN 00088           DO 89 IS=1,NP                                                    MDSG 105
  ISN 00089           RU(IS)=RU(IS)+(UERG(IS)-RUERG(IS))**2                            MDSG 106
  ISN 00090        89 CONTINUE                                                         MDSG 107
  ISN 00091        90 C=C-SC                                                           MDSG 108
  ISN 00092           AL=AL+SAL                                                        MDSG 109
  ISN 00093           IF(SAL)91,93,91                                                  MDSG 110
  ISN 00094        91 CALL MAD(A,B,C,AL,BE,GA,X,Y,Z,W,M,SIT)                           MDSG 111
  ISN 00095           RW=RW+(WERG-RWERG)**2                                            MDSG 112
  ISN 00096           DO 92 IS=1,NP                                                    MDSG 113
  ISN 00097           RU(IS)=RU(IS)+(UERG(IS)-RUERG(IS))**2                            MDSG 114
  ISN 00098        92 CONTINUE                                                         MDSG 115
  ISN 00099        93 AL=AL-SAL                                                        MDSG 116
  ISN 00100           BE=BE+SBE                                                        MDSG 117
  ISN 00101           IF(SBE)94,96,94                                                  MDSG 118
  ISN 00102        94 CALL MAD(A,B,C,AL,BE,GA,X,Y,Z,W,M,SIT)                           MDSG 119
  ISN 00103           RW=RW+(WERG-RWERG)**2                                            MDSG 120
  ISN 00104           DO 95 IS=1,NP                                                    MDSG 121
  ISN 00105           RU(IS)=RU(IS)+(UERG(IS)-RUERG(IS))**2                            MDSG 122
```

```
ISN 00106        99 CONTINUE                                                    MDSG 123
ISN 00107        96 BE=BE-SBE                                                   MDSG 124
                    GA=GA+SGA                                                   MDSG 125
ISN 00108           IF(SGA)97,99,97                                             MDSG 126
ISN 00109        97 CALL MAD(A,B,C,AL,BE,GA,X,Y,Z,G,M,SIT)                      MDSG 127
ISN 00110           RW=RW*(WERG-RWERG)**2                                       MDSG 128
ISN 00111           DO 98 IS=1,NP                                               MDSG 129
ISN 00112           RU(IS)=RU(IS)+(UERG(IS)-RUERG(IS))**2                       MDSG 130
ISN 00113        98 CONTINUE                                                    MDSG 131
ISN 00114        99 GA=GA-SGA                                                   MDSG 132
ISN 00115           DO 100 IS=1,NP                                              MDSG 133
ISN 00116           X(IS)=X(IS)+SX(IS)                                          MDSG 134
ISN 00117           IF(SX(IS))101,103,101                                       MDSG 135
ISN 00118       101 CALL MAD(A,B,C,AL,BE,GA,X,Y,Z,G,M,SIT)                      MDSG 136
ISN 00119           RW=RW*(WERG-RWERG)**2                                       MDSG 137
ISN 00120           DO 102 I =1,NP                                              MDSG 138
ISN 00121           RU(I )=RU(I )+(UERG(I )-RUERG(I ))**2                       MDSG 139
ISN 00122       102 CONTINUE                                                    MDSG 140
ISN 00123       103 X(IS)=X(IS)-SX(IS)                                          MDSG 141
ISN 00124           Y(IS)=Y(IS)+SY(IS)                                          MDSG 142
ISN 00125           IF(SY(IS))104,106,104                                       MDSG 143
ISN 00126       104 CALL MAD(A,B,C,AL,BE,GA,X,Y,Z,G,M,SIT)                      MDSG 144
ISN 00127           RW=RW*(WERG-RWERG)**2                                       MDSG 145
ISN 00128           DO 105 I =1,NP                                              MDSG 146
ISN 00129           RU(I )=RU(I )+(UERG(I )-RUERG(I ))**2                       MDSG 147
ISN 00130       105 CONTINUE                                                    MDSG 148
ISN 00131       106 Y(IS)=Y(IS)-SY(IS)                                          MDSG 149
ISN 00132           Z(IS)=Z(IS)+SZ(IS)                                          MDSG 150
ISN 00133           IF(SZ(IS))107,113,107                                       MDSG 151
ISN 00134       107 CALL MAD(A,B,C,AL,BE,GA,X,Y,Z,G,M,SIT)                      MDSG 152
ISN 00135           RW=RW*(WERG-RWERG)**2                                       MDSG 153
ISN 00136           DO 108 I =1,NP                                              MDSG 154
ISN 00137           RU(I )=RU(I )+(UERG(I )-RUERG(I ))**2                       MDSG 155
ISN 00138       108 CONTINUE                                                    MDSG 156
ISN 00139       113 CONTINUE                                                    MDSG 157
ISN 00140       100 CONTINUE                                                    MDSG 158
ISN 00141           SWERG=SQRT(RW)                                              MDSG 159
ISN 00142           SWEV=SWERG/1.60219E-12                                      MDSG 160
ISN 00143           SWKCL=SWEV/4.336E45E-02                                     MDSG 161
ISN 00144           WRITE(6,109)                                                MDSG 162
ISN 00145       109 FORMAT(/ ,1H ,10X,"SIGMA OF E.S.ENERGY OF CRYSTAL AND ATOMS IS  **MDSG 163
                   1 " ,)                                                       MDSG 164
ISN 00146           WRITE(6,110) SWERG,SWEV,SWKCL                               MDSG 165
ISN 00147       110 FORMAT(1H ,15X,7HCRYSTAL,3X,6HSWERG=E15.8,4X,5HSWEV=E15.8   MDSG 166
                   1 ,3X,7HSWKCAL=E15.8)                                        MDSG 167
ISN 00148           DO 111 IS=1,NP                                              MDSG 168
ISN 00149           SUERG(IS)=SQRT(RU(IS))                                      MDSG 169
ISN 00150           SUEV(IS)=SUERG(IS)/1.602E19E-12                             MDSG 170
ISN 00151           SUKCL(IS)=SUEV(IS)/4.336E49E-02                             MDSG 171
ISN 00152           SPUKC(IS)=SUKCL(IS)/W(IS)                                   MDSG 172
ISN 00153           WRITE(6,112)SIT(IS),SUERG(IS),SUEV(IS),SUKCL(IS),SPUKC(IS)  MDSG 173
ISN 00154       112 FORMAT(1P ,15X,A4,2X,6HSUERG=E15.8,4X,5HSUEV=E15.8,5X,6HSUKCL=E15.MDSG 174
                   18,4X,6HSPUKC=E15.8)                                         MDSG 175
ISN 00155       111 CONTINUE                                                    MDSG 176
ISN 00156           STOP                                                        MDSG 177
ISN 00157           END                                                         MDSG 178
```

```
ISN 00158           SUBROUTINE MAD(A,B,C,AL,BE,GA,X,Y,Z,G,M,SIT)                MDSG 179
ISN 00159           DIMENSION X(500),Y(500),Z(500),W(500),M(500),SIT(50)        MDSG 180
                   1 ,SUMS(50),SUMMS(50),MIKS(50),UI(50),UERG(50),UEV(50),UKCAL(50)  MDSG 181
                   2 ,PUKCAL(50)                                                MDSG 182
ISN 00160           COMMON X,NZ,BET,G,GG,NP,NS,UERG,UEV,UKCAL,PUKCAL ,          MDSG 183
                   1WERG,WEV,WKCAL                                              MDSG 184
ISN 00161           CALL SYMM(A,Y,Z,G,M,NP)                                     MDSG 185
ISN 00162           PAI=3.14159265                                              MDSG 186
ISN 00163           BET=BE*PAI                                                  MDSG 187
ISN 00164           DL=AL*PAI/180.0                                             MDSG 188
ISN 00165           DE=BE*PAI/180.0                                             MDSG 189
ISN 00166           DA=GA*PAI/180.0                                             MDSG 190
ISN 00167           S11=B*B*C*C*SIN(DL)*SIN(DL)                                 MDSG 191
ISN 00168           S22=C*C*A*A*SIN(DE)*SIN(DE)                                 MDSG 192
ISN 00169           S33=A*A*B*B*SIN(DA)*SIN(DA)                                 MDSG 193
ISN 00170           S23=A*A*B*C*(COS(DE)*COS(DA)-COS(DL))                       MDSG 194
ISN 00171           S31=A*B*B*C*(COS(DA)*COS(DL)-COS(DE))                       MDSG 195
ISN 00172           S12=A*B*C*C*(COS(DL)*COS(DE)-COS(DA))                       MDSG 196
ISN 00173           V=SQRT(1.0-COS(DL)**2-COS(DE)**2-COS(DA)**2
                   4+2.0*COS(DL)*COS(DE)*COS(DA))
ISN 00174           V=A*B*C*V                                                   MDSG 199
ISN 00175           HM=DET/(2.0*PAI*V)                                          MDSG 200
ISN 00176           LM=HM*C                                                     MDSG 201
ISN 00177           KM=HM*B                                                     MDSG 202
ISN 00178           HM=HM*A                                                     MDSG 203
ISN 00179           DO 50 IP=1,NP                                               MDSG 204
ISN 00180           SUMS(IP)=0.0                                                MDSG 205
ISN 00181        50 CONTINUE                                                    MDSG 206
ISN 00182           DO 50 IH1=1,IHM                                             MDSG 207
ISN 00183           IH=IH1                                                      MDSG 208
ISN 00184           DO 51 IK1=1,2*IKM+1                                         MDSG 209
ISN 00185           IK=-IKM-1+IK1                                               MDSG 210
ISN 00186           DO 52 IL1=1,2*LM+1                                          MDSG 211
ISN 00187           IL=-LM-1+IL1                                                MDSG 212
ISN 00188           H2=FLOAT(IH)**2*S11+FLOAT(IK)**2*S22+FLOAT(IL)**2*S33       MDSG 213
                   2+2.0*FLOAT(IK*IL)*S23+2.0*FLOAT(IL*IH)*S31+2.0*FLOAT(IH*IK)*S12  MDSG 214
ISN 00189           H=SQRT(H2)/V                                                MDSG 215
ISN 00190           ALP=2.0*PAI*H*R                                             MDSG 216
ISN 00191           IF(ALP)41,52,41                                             MDSG 217
ISN 00192        41 IF(BET-ALP)52,40,40                                         MDSG 218
ISN 00193        40 PAI=200.0*(ALP*SIN(ALP)+2.0*COS(ALP)-2.0)**2/ALP**10        MDSG 219
ISN 00194           DO 54 IP=1,NP                                               MDSG 220
ISN 00195           XI=X(IP)                                                    MDSG 221
ISN 00196           YI=Y(IP)                                                    MDSG 222
ISN 00197           ZI=Z(IP)                                                    MDSG 223
ISN 00198           SI=0.0                                                      MDSG 224
ISN 00199           DO 55 I=1,NP*NS                                             MDSG 225
ISN 00200           ALS=FLOAT(IH)*(X(I)-XI)+FLOAT(IK)*(Y(I)-YI)+FLOAT(IL)*(Z(I)-ZI)  MDSG 226
ISN 00201           ALS=2.0*PAI*ALS                                             MDSG 227
ISN 00202           ACOS=COS(ALS)/FLOAT(M(I))                                   MDSG 228
ISN 00203           SI=SI+W(I)*ACOS                                             MDSG 229
ISN 00204        55 CONTINUE                                                    MDSG 230
ISN 00205           SUMS(IP)=SUMS(IP)+SI*PAI                                    MDSG 231
ISN 00206        54 CONTINUE                                                    MDSG 232
ISN 00207        52 CONTINUE                                                    MDSG 233
ISN 00208        51 CONTINUE                                                    MDSG 234
ISN 00209        50 CONTINUE                                                    MDSG 235
ISN 00210           DO 59 IP=1,NP                                               MDSG 236
ISN 00211           SUMS(IP)=2.0*SUMS(IP)                                       MDSG 237
ISN 00212        59 CONTINUE                                                    MDSG 238
```

```
ISN 00214          IM=0                                                          MDSG 239
ISN 00215          DO 81 IK1=1,2*IKM+1                                           MDSG 240
ISN 00216          IK=-IKM-1+IK1                                                 MDSG 241
ISN 00217          DO 82 IL1=1,2*ILM+1                                           MDSG 242
ISN 00218          IL=-ILM-1+IL1                                                 MDSG 243
ISN 00219          HC=FLOAT(IM)**2*S11+FLOAT(IK)**2*S22+FLOAT(IL)**2*S33         MDSG 244
                  5+2.0*FLOAT(IK*IL)*S23+2.0*FLOAT(IL*IM)*S31+2.0*FLOAT(IM*IK)*S12  MDSG 245
ISN 00220          H=SQRT(HC)/V                                                  MDSG 246
ISN 00221          ALP=2.0*PAI*H*R                                               MDSG 247
ISN 00222          IF(ALP)91,82,91                                               MDSG 248
ISN 00223       91 IF(DET-ALP)92,90,90                                           MDSG 249
ISN 00224       90 FAI=2*3.0*(ALP*SIN(ALP)+2.0*COS(ALP)-2.0)**2/ALP**6           MDSG 250
ISN 00225          DO 84 IP=1,NP                                                 MDSG 251
ISN 00226          AI=X(IP)                                                      MDSG 252
ISN 00227          YI=Y(IP)                                                      MDSG 253
ISN 00228          ZI=Z(IP)                                                      MDSG 254
ISN 00229          SI=0.0                                                        MDSG 255
ISN 00230          DO 85 I=1,NP*NS                                               MDSG 256
ISN 00231          GLS=FLOAT(IM)*(X(I)-AI)+FLOAT(IK)*(Y(I)-YI)+FLOAT(IL)*(Z(I)-ZI)  MDSG 257
ISN 00232          GLS=2.0*PAI*GLS                                               MDSG 258
ISN 00233          ACOS=COS(GLS)/FLOAT(M(I))                                     MDSG 259
ISN 00234          SI=SI+W(I)*ACOS                                               MDSG 260
ISN 00235       85 CONTINUE                                                      MDSG 261
ISN 00236          SUMS(IP)=SUMS(IP)+SI*FAI                                      MDSG 262
ISN 00237       84 CONTINUE                                                      MDSG 263
ISN 00238       83 CONTINUE                                                      MDSG 264
ISN 00239       81 CONTINUE                                                      MDSG 265
ISN 00240          E=4.0*3.5E-10                                                 MDSG 266
ISN 00241          W1=0.0                                                        MDSG 267
ISN 00242          DO 87 IP=1,NP                                                 MDSG 268
ISN 00243          SUMHS(IP)=2.0*PAI*R*R*G(IP)*SUMS(IP)/V                        MDSG 269
ISN 00244          HIKS(IP)=2.0*(G-GO)*G(IP)*G(IP)/R                             MDSG 270
ISN 00245          UI(IP)=SUMHS(IP)-HIKS(IP)                                     MDSG 271
ISN 00246          W1=W1+UI(IP)*FLOAT(NS/M(IP))/2 )                              MDSG 272
ISN 00247          UERG(IP)=UI(IP)*E*E*1.0E06                                    MDSG 273
ISN 00248          UEV(IP)=UERG(IP)/1.60219E-12                                  MDSG 274
ISN 00249          UKCAL(IP)=UEV(IP)/4.338E49E-02                                MDSG 275
ISN 00250          PUKCAL(IP)= UKCAL(IP)/G(IP)                                   MDSG 276
ISN 00251       87 CONTINUE                                                      MDSG 277
ISN 00252          WERG=W1*E*E*1.0E06/FLOAT(NZ)                                  MDSG 278
ISN 00253          WEV=WERG/1.60219E-12                                          MDSG 279
ISN 00254          WKCAL=WEV/4.338E49E-02                                        MDSG 280
ISN 00255          RETURN                                                        MDSG 281
ISN 00256          END                                                           MDSG 282
```

HIGH ALBITE NAALSI3O8 700C 5KB HYDRO 1060C 40DAYS URO.5AB98.3AN1.2

24C 1843REF R1 =.8% R1/4 4.1% FROM PREWITTAT AL.(1976) AM.MIN.P1213

** LATTICE PARAMETERS **
A= 8.15350 B= 12.86940 C= 7.10700 AL= 93.52100 BE= 116.45799 GA= 90.25700

** RADIUS OF CHARGE DISTRIBUTION***** NUMBER OF MOLECULES IN UNIT CELL **
R= 0.80000 NZ= 4

** RADIUS RANGE OF ALPHA SUMMATION***** CORRECTION FACTOR OF SELF-ENERGY***** CORRECTION FACTOR OF SUMMATION **
BET= 1.5000*PAI G= 0.7428571 Q= 0.0036371

** NUMBER OF UNEQUIVALENT ATOMS***** NUMBER OF GENERAL POSITIONS **
NP= 13 NS= 4

** ATOMS********** MULTIPLICITY*** CHARGE********** ATOMIC CO-ORDINATES (X,Y,Z) **

NA	1	1.00000	(0.27370	, 0.00730	, 0.13290	)
T1O	1	3.75000	(0.00900	, 0.16500	, 0.21480	)
T1M	1	3.75000	(0.00480	, 0.81450	, 0.22900	)
T2O	1	3.75000	(0.69020	, 0.10790	, 0.32020	)
T2M	1	3.75000	(0.68490	, 0.87760	, 0.35350	)
OA1	1	-2.00000	(0.00550	, 0.13510	, 0.98450	)
OA2	1	-2.00000	(0.59160	, 0.99070	, 0.27630	)
OBO	1	-2.00000	(0.82120	, 0.10840	, 0.19900	)
OBM	1	-2.00000	(0.81840	, 0.84700	, 0.24550	)
OCO	1	-2.00000	(0.01620	, 0.29020	, 0.27700	)
OCM	1	-2.00000	(0.02130	, 0.66730	, 0.21800	)
ODO	1	-2.00000	(0.19590	, 0.11230	, 0.38760	)
ODM	1	-2.00000	(0.18850	, 0.86750	, 0.42660	)

** ELECTROSTATIC ENERGIES OF CRYSTAL AND ATOMS **

CRYSTAL	WERG=-0.93136698E-09	WEV=-0.58130859E+03	WKCAL=-0.13398867E+05	
NA	UERG=-0.21557867E-10	UEV=-0.13455252E+02	UKCAL=-0.31013672E+03	PUKCAL=-0.31013672E+03
T1O	UERG=-0.26774316E-09	UEV=-0.16711076E+03	UKCAL=-0.38518186E+04	PUKCAL=-0.10271516E+04
T1M	UERG=-0.27318214E-09	UEV=-0.17050546E+03	UKCAL=-0.39300649E+04	PUKCAL=-0.10480171E+04
T2O	UERG=-0.27262992E-09	UEV=-0.17016081E+03	UKCAL=-0.39221206E+04	PUKCAL=-0.10458987E+04
T2M	UERG=-0.27065949E-09	UEV=-0.16893098E+03	UKCAL=-0.38937737E+04	PUKCAL=-0.10383396E+04
OA1	UERG=-0.92109445E-10	UEV=-0.57489716E+02	UKCAL=-0.13251089E+04	PUKCAL= 0.66255444E+03
OA2	UERG=-0.90403227E-10	UEV=-0.56424789E+02	UKCAL=-0.13005627E+04	PUKCAL= 0.65028125E+03
OBO	UERG=-0.95539521E-10	UEV=-0.59630585E+02	UKCAL=-0.13744548E+04	PUKCAL= 0.68722729E+03
OBM	UERG=-0.97044900E-10	UEV=-0.60570160E+02	UKCAL=-0.13961116E+04	PUKCAL= 0.69805566E+03
OCO	UERG=-0.95514874E-10	UEV=-0.59615204E+02	UKCAL=-0.13741003E+04	PUKCAL= 0.68705005E+03
OCM	UERG=-0.93661079E-10	UEV=-0.58458160E+02	UKCAL=-0.13474309E+04	PUKCAL= 0.67371533E+03
ODO	UERG=-0.96197619E-10	UEV=-0.60041336E+02	UKCAL=-0.13839224E+04	PUKCAL= 0.69196118E+03
ODM	UERG=-0.96491440E-10	UEV=-0.60224716E+02	UKCAL=-0.13881492E+04	PUKCAL= 0.69407446E+03

** SIGMA OF LATTICE PARAMETER **
SA= 0.00040 SB= 0.00050 SC= 0.00040 SAL= 0.00400 SBE= 0.00300 SGA= 0.00300

** ATOMS ** SIGMA OF (X,Y,Z) **

NA	(0.00030	0.00030	0.00050)
T1O	(0.00010	0.00010	0.00010)
T1M	(0.00010	0.00010	0.00010)
T2O	(0.00010	0.00010	0.00010)
T2M	(0.00010	0.00010	0.00010)
OA1	(0.00040	0.00020	0.00040)
OA2	(0.00030	0.00020	0.00040)
OBO	(0.00040	0.00020	0.00040)
OBM	(0.00040	0.00020	0.00040)
OCO	(0.00030	0.00020	0.00040)
OCM	(0.00030	0.00020	0.00040)
ODO	(0.00030	0.00020	0.00040)
ODM	(0.00030	0.00020	0.00040)

SIGMA OF E.S.ENERGY OF CRYSTAL AND ATOMS IS **

CRYSTAL	SWERG= 0.47577524E-12	SWEV= 0.29695306E+00	SWKCAL= 0.68446178E+01	
NA	SUERG= 0.77005514E-13	SUEV= 0.48062667E-01	SUKCL= 0.11078196E+01	SPUKC= 0.11078196E+01
T1O	SUERG= 0.60975140E-12	SUEV= 0.38057375E+00	SUKCL= 0.87720318E+01	SPUKC= 0.23392076E+01
T1M	SUERG= 0.97684534E-12	SUEV= 0.60969388E+00	SUKCL= 0.14053136E+02	SPUKC= 0.37475023E+01
T2O	SUERG= 0.61283400E-12	SUEV= 0.38249774E+00	SUKCL= 0.88165786E+01	SPUKC= 0.23510342E+01
T2M	SUERG= 0.83304625E-12	SUEV= 0.51994228E+00	SUKCL= 0.11984406E+02	SPUKC= 0.31958408E+01
OA1	SUERG= 0.34921496E-12	SUEV= 0.21796101E+00	SUKCL= 0.50238905E+01	SPUKC=-0.25119448E+01
OA2	SUERG= 0.16577137E-12	SUEV= 0.10346550E+00	SUKCL= 0.23848267E+01	SPUKC=-0.11924133E+01
OBO	SUERG= 0.20100132E-12	SUEV= 0.12545413E+00	SUKCL= 0.28916540E+01	SPUKC=-0.14458265E+01
OBM	SUERG= 0.24212067E-12	SUEV= 0.15111858E+00	SUKCL= 0.34832067E+01	SPUKC=-0.17416029E+01
OCO	SUERG= 0.22051680E-12	SUEV= 0.13763463E+00	SUKCL= 0.31724081E+01	SPUKC=-0.15862036E+01
OCM	SUERG= 0.19973481E-12	SUEV= 0.12466359E+00	SUKCL= 0.28734322E+01	SPUKC=-0.14367161E+01
ODO	SUERG= 0.24058441E-12	SUEV= 0.15015972E+00	SUKCL= 0.34611059E+01	SPUKC=-0.17305527E+01
ODM	SUERG= 0.32246292E-12	SUEV= 0.20126384E+00	SUKCL= 0.46390295E+01	SPUKC=-0.23195143E+01

Appendix 3. The final observed and calculated structure factors of Co_2SiO_4 olivine.

H	K	L	FOBS	FCALC	AC	BC	DF	SIGN*DF	SIGF	AI	BT	Y	IQ	F(INPUT)	THETA	PHI	CHI	EPSILON
2	0	0	104.15	105.03	104.74	7.79	-0.881	-0.881	0.47	102,23	0.00	0.6372	1	93.84	0.00	0,00	0,00	0,00
4	0	0	131.49	131.02	130.83	7.05	0.463	0.463	0.45	128.71	0.00	0.6994	1	126.33	0.00	0,00	0,00	0,00
6	0	0	39.66	39.08	38.60	6.14	0.582	0.582	0.38	36,87	0.00	0.9709	1	46.23	0.00	0,00	0,00	0,00
8	0	0	37.39	37.08	36.70	5.24	0.314	0.314	0.38	35.24	0.00	0.9764	1	45.36	0.00	0,00	0,00	0,00
10	0	0	33.69	32.56	32.25	4.42	1.133	1.133	0.38	30,92	0.00	0.9822	1	42.84	0.00	0,00	0,00	0,00
12	0	0	22.35	21.23	20.91	3.62	1.125	1.125	0.38	19,72	0.00	0.9926	1	30.06	0.00	0,00	0,00	0,00
1	1	0	14.57	13.72	13.57	2.00	0.856	0.856	0.37	12,98	0.00	0.9970	1	19.14	0.00	0,00	0,00	0,00
11	1	0	11.14	10.08	10.03	1.06	1.061	1.061	0.37	9,78	0.00	0.9983	1	14.29	0.00	0,00	0,00	0,00
10	1	0	19,38	18.81	18.64	2.49	0.577	0.577	0.38	17,80	0.00	0.9938	1	24.25	0.00	0,00	0,00	0,00
9	1	0	43,71	43.18	43.09	2.89	0.525	0.525	0.38	42,06	0.00	0.9677	1	51.75	0.00	0,00	0,00	0,00
7	1	0	24,74	24.91	24.89	1.09	-0.170	-0.170	0.38	24,52	0.00	0.9879	1	29.10	0.00	0,00	0,00	0,00
6	1	0	39,44	38.66	38.53	3.09	0.786	0.786	0.38	37,49	0.00	0.9666	1	45.16	0.00	0,00	0,00	0,00
5	1	0	13.61	13.65	13.62	0.92	-0.034	-0.034	0.38	13,23	0.00	0.9944	1	15.60	0.00	0,00	0,00	0,00
4	1	0	64,54	63.94	63.86	3.09	0.604	0.604	0.40	62,95	0.00	0.8633	1	88.22	0.00	0,00	0,00	0,00
3	1	0	40.55	39.82	39.82	0.54	0.726	0.726	0.39	39,57	0.00	0.9112	1	43.70	0.00	0,00	0,00	0,00
2	1	0	39,26	38.45	38.33	3.02	0.812	0.812	0.40	37,55	0.00	0.8558	1	40.81	0.00	0,00	0,00	0,00
1	1	0	31.48	30.68	30.68	0.31	0.800	0.800	0.40	30,51	0.00	0.8848	1	33.26	0.00	0,00	0,00	0,00
0	2	0	26,77	25.78	-25.78	-0.18	0.995	-0.995	0.39	-25,64	0.00	0.9400	1	29.20	0.00	0,00	0,00	0,00
1	2	0	8,52	8.72	8.71	0.30	-0.204	-0.204	0.37	8,57	0.00	0.9955	1	9.60	0.00	0,00	0,00	0,00
2	2	0	30,93	30.34	-30.34	-0.44	0.590	-0.590	0.38	-30,03	0.00	0.9649	1	34.60	0.00	0,00	0,00	0,00
3	2	0	4,50	4.87	4.86	0.31	-0.366	-0.366	0.37	4,78	0.00	0.9993	1	5.18	0.00	0,00	0,00	0,00
4	2	0	18,71	18.35	-18.34	-0.48	0.365	-0.365	0.38	-18,06	0.00	0.9923	1	21.73	0.00	0,00	0,00	0,00
5	2	0	7,47	5.32	-5.31	-0.36	2.151	-2.151	0.37	-5,20	0.00	0.9995	1	9.00	0.00	0,00	0,00	0,00
7	2	0	4.22	2.02	1.95	0.52	2.203	2.203	0.37	1,84	0.00	0.9999	1	5.19	0.00	0,00	0,00	0,00
8	2	0	6.24	6.60	6.60	-0.22	-0.368	-0.368	0.37	6,56	0.00	0.9992	1	7.83	0.00	0,00	0,00	0,00
9	2	0	11.09	6.33	6.28	0.80	4.760	4.760	0.37	6,00	0.00	0.9993	1	14.98	0.00	0,00	0,00	0,00
12	2	0	11.79	11.53	-11.48	-1.08	0.269	-0.269	0.37	-11,05	0.00	0.9978	1	15.94	0.00	0,00	0,00	0,00
12	3	0	18.4	18.12	17.85	3.09	0.280	0.280	0.38	16,90	0.00	0.9948	1	24.18	0.00	0,00	0,00	0,00
11	3	0	11.48	12.72	-12.66	-1.22	-1.241	1.241	0.37	-12,15	0.00	0.9972	1	14.74	0.00	0,00	0,00	0,00
10	3	0	31.89	31.62	31.48	3.73	0.261	0.261	0.38	30,28	0.00	0.9827	1	39.75	0.00	0,00	0,00	0,00
9	3	0	13.90	13.81	-13.76	-1.12	0.091	-0.091	0.37	-13,35	0.00	0.9966	1	17.08	0.00	0,00	0,00	0,00
8	3	0	31.87	30.78	30.46	4.37	1.098	1.098	0.38	29,16	0.00	0.9833	1	38.13	0.00	0,00	0,00	0,00
7	3	0	65,67	64.67	64.48	4.97	1.004	1.004	0.39	62,98	0.00	0.9167	1	73.42	0.00	0,00	0,00	0,00
6	3	0	16,36	16.12	16.12	-0.42	0.239	0.239	0.38	16,07	0.00	0.9927	1	18.78	0.00	0,00	0,00	0,00
5	3	0	86,03	85.03	84.86	5.44	0.991	0.991	0.42	83,18	0.00	0.8037	1	87.94	0.00	0,00	0,00	0,00
2	3	0	17.60	17.79	17.79	-0.15	-0.190	-0.190	0.38	17,68	0.00	0.9835	1	19.75	0.00	0,00	0,00	0,00
1	3	0	146,74	143.30	143.19	5.71	3.434	3.434	0.54	141,39	0.00	0.4875	1	115.46	0.00	0,00	0,00	0,00
0	4	0	90,45	88.41	88.16	6.63	2.037	2.037	0.45	86,27	0.00	0.6864	1	84.52	0.00	0,00	0,00	0,00
1	4	0	63,44	62.91	62.91	0.05	0.533	0.533	0.41	62,95	0.00	0.8177	1	64.79	0.00	0,00	0,00	0,00
2	4	0	138,36	137.30	137.14	6.56	1.055	1.055	0.48	135,22	0.00	0.6000	1	121.59	0.00	0,00	0,00	0,00
3	4	0	49.60	48.20	-48.20	0.19	1.400	-1.400	0.39	-48,13	0.00	0.9271	1	54.57	0.00	0,00	0,00	0,00
4	4	0	80,97	79.41	79.16	6.30	1.553	1.553	0.40	77,19	0.00	0.8629	1	86.82	0.00	0,00	0,00	0,00
6	4	0	73,87	72.98	72.75	5.78	0.894	0.894	0.39	70,86	0.00	0.9110	1	83.78	0.00	0,00	0,00	0,00
8	4	0	43,65	43.96	43.68	4.97	-0.312	-0.312	0.38	42,05	0.00	0.9673	1	52.95	0.00	0,00	0,00	0,00
9	4	0	8,08	9.56	9.52	0.85	-1.479	-1.479	0.37	9,18	0.00	0.9984	1	10.17	0.00	0,00	0,00	0,00
10	4	0	29,99	29.30	29.02	4.01	0.687	0.687	0.38	27,77	0.00	0.9857	1	38.35	0.00	0,00	0,00	0,00
11	4	0	12.73	11.78	11.75	0.83	0.954	0.954	0.37	11,41	0.00	0.9978	1	16.79	0.00	0,00	0,00	0,00
12	4	0	18.17	18.11	17.85	3.07	0.063	0.063	0.38	16,96	0.00	0.9945	1	24.56	0.00	0,00	0,00	0,00
12	5	0	6.99	7.01	6.97	1.71	-0.017	-0.017	0.37	6,77	0.00	0.9992	1	9.49	0.00	0,00	0,00	0,00
11	5	0	12.44	12.70	12.66	1.09	-0.267	-0.267	0.37	12,29	0.00	0.9974	1	16.43	0.00	0,00	0,00	0,00
8	5	0	15.96	15.96	15.95	0.77	-0.004	-0.004	0.37	15,72	0.00	0.9955	1	19.69	0.00	0,00	0,00	0,00
6	5	0	5.65	5.92	-5.88	0.71	-0.268	0.268	0.37	-6,11	0.00	0.9993	1	6.73	0.00	0,00	0,00	0,00
5	5	0	9.42	9.11	-9.06	0.87	0.318	-0.318	0.37	-9,22	0.00	0.9982	1	11.05	0.00	0,00	0,00	0,00
4	5	0	27.52	27.08	27.08	0.56	0.442	0.442	0.38	26,87	0.00	0.9816	1	31.56	0.00	0,00	0,00	0,00
3	5	0	30.33	29.86	29.84	1.05	0.472	0.472	0.38	29,48	0.00	0.9723	1	34.28	0.00	0,00	0,00	0,00
2	5	0	7.27	6.52	-6.51	0.31	0.759	-0.759	0.37	-6,63	0.00	0.9982	1	8.27	0.00	0,00	0,00	0,00
1	5	0	46.11	45.10	45.09	1.21	1.003	1.003	0.39	44,54	0.00	0.9094	1	49.80	0.00	0,00	0,00	0,00
0	6	0	13,86	12.95	12.87	1.41	0.906	0.906	0.38	12,62	0.00	0.9924	1	15.67	0.00	0,00	0,00	0,00
1	6	0	15.42	14.71	14.71	-0.12	0.711	0.711	0.38	14,71	0.00	0.9908	1	17.45	0.00	0,00	0,00	0,00
2	6	0	3.55	4.13	3.84	1.50	-0.578	-0.578	0.37	3,49	0.00	0.9994	1	4.05	0.00	0,00	0,00	0,00
4	6	0	28.85	27.43	27.37	1.69	1.423	1.423	0.38	26,82	0.00	0.9822	1	33.22	0.00	0,00	0,00	0,00
6	6	0	29.08	29.17	29.12	1.79	-0.091	-0.091	0.38	28,42	0.00	0.9845	1	34.47	0.00	0,00	0,00	0,00
7	6	0	7.49	7.14	-7.09	-0.90	0.345	-0.345	0.37	-6,81	0.00	0.9991	1	9.10	0.00	0,00	0,00	0,00
8	6	0	18.34	17.60	17.51	1.69	0.739	0.739	0.38	16,87	0.00	0.9945	1	22.68	0.00	0,00	0,00	0,00
9	6	0	11.74	11.69	-11.64	-1.12	0.055	-0.055	0.37	-11,28	0.00	0.9976	1	14.85	0.00	0,00	0,00	0,00
10	6	0	13.65	14.27	14.20	1.44	-0.624	-0.624	0.37	13,73	0.00	0.9966	1	17.64	0.00	0,00	0,00	0,00
11	6	0	6.44	6.16	-6.08	-0.99	0.284	-0.294	0.37	-5,72	0.00	0.9994	1	8.54	0.00	0,00	0,00	0,00
11	7	0	27.26	27.17	26.92	3.65	0.090	0.090	0.38	25,78	0.00	0.9885	1	36.06	0.00	0,00	0,00	0,00
9	7	0	27.11	26.67	26.30	4.44	0.437	0.437	0.38	24,98	0.00	0.9877	1	34.23	0.00	0,00	0,00	0,00
7	7	0	43.97	43.61	43.29	5.26	0.368	0.368	0.38	41,76	0.00	0.9678	1	52.79	0.00	0,00	0,00	0,00
6	7	0	8.70	8.03	-8.02	-0.47	0.662	-0.662	0.37	-7,81	0.00	0.9988	1	10.42	0.00	0,00	0,00	0,00
5	7	0	54.56	54.32	53.98	6.06	0.248	0.248	0.38	52,17	0.00	0.9458	1	62.73	0.00	0,00	0,00	0,00
4	7	0	23.94	22.75	-22.75	-0.50	1.190	-1.190	0.38	-22,44	0.00	0.9884	1	27.78	0.00	0,00	0,00	0,00
3	7	0	99.96	99.32	99.09	6.74	0.636	0.636	0.42	97,00	0.00	0.8072	1	103.68	0.00	0,00	0,00	0,00
2	7	0	20.54	19.75	-19.75	-0.34	0.783	-0.783	0.38	-19,52	0.00	0.9877	1	23.40	0.00	0,00	0,00	0,00
1	7	0	131.02	129.79	129.59	7.14	1.229	1.229	0.46	127,31	0.00	0.6685	1	122.25	0.00	0,00	0,00	0,00
0	8	0	54,23	53.02	52.83	4.47	1.207	1.207	0.39	51,45	0.00	0.9181	1	59.50	0.00	0,00	0,00	0,00
1	8	0	10.02	9.46	-9.45	0.31	0.568	-0.568	0.37	-9,63	0.00	0.9972	1	11.48	0.00	0,00	0,00	0,00
2	8	0	79.83	78.26	78.14	4.38	1.568	1.568	0.40	76,78	0.00	0.8605	1	85.29	0.00	0,00	0,00	0,00
3	8	0	47.03	46.31	46.30	4.82	0.719	0.719	0.38	45,87	0.00	0.9506	1	53.19	0.00	0,00	0,00	0,00
4	8	0	40.20	39.16	38.94	4.13	1.037	1.037	0.38	37,68	0.00	0.9684	1	46.39	0.00	0,00	0,00	0,00
5	8	0	12.20	12.38	12.33	1.05	-0.181	-0.181	0.37	11,88	0.00	0.9970	1	14.46	0.00	0,00	0,00	0,00
6	8	0	36.36	36.36	36.17	3.74	-0.004	-0.004	0.38	35,03	0.00	0.9768	1	43.28	0.00	0,00	0,00	0,00
7	8	0	13.52	13.23	13.19	1.03	0.296	0.296	0.37	12,87	0.00	0.9969	1	16.55	0.00	0,00	0,00	0,00
8	8	0	25,20	25.08	24.86	3.27	0.124	0.124	0.38	23,86	0.00	0.9890	1	31.32	0.00	0,00	0,00	0,00
10	8	0	17.21	16.83	16.60	2.76	0.378	0.378	0.37	15,76	0.00	0.9954	1	22.39	0.00	0,00	0,00	0,00
11	9	0	4.51	3.75	-3.71	0.52	0.762	-0.762	0.37	-3,86	0.00	0.9998	1	6.05	0.00	0,00	0,00	0,00
10	9	0	4.14	3.31	3.30	0.25	0.831	0.831	0.37	3,12	0.00	0.9998	1	5.42	0.00	0,00	0,00	0,00
9	9	0	15.32	16.19	16.19	2.51	-0.872	-0.872	0.37	15,98	0.00	0.9955	1	19.58	0.00	0,00	0,00	0,00
8	9	0	6.88	6.50	6.49	0.18	0.382	0.382	0.37	6,38	0.00	0.9993	1	8.63	0.00	0,00	0,00	0,00
7	9	0	6.24	4.70	-4.68	.42	1.548	-1.548	0.37	-4,90	0.00	0.9996	1	7.69	0.00	0,00	0,00	0,00
6	9	0	6.80	6.17	-6.17	0.01	0.629	-0.629	0.37	-6,12	0.00	0.9993	1	8.23	0.00	0,00	0,00	0,00
5	9	0	22.63	22.37	22.37	1.22	0.254	0.254	0.38	22,24	0.00	0.9907	1	26.86	0.00	0,00	0,00	0,00
4	9	0	12.35	11.51	-11.51	-0.13	0.845	-0.845	0.37	-11,33	0.00	0.9973	1	14.54	0.00	0,00	0,00	0,00
3	9	0	17.19	16.50	-16.50	-0.04	0.696	-0.696	0.38	-16,46	0.00	0.9938	1	20.00	0.00	0,00	0,00	0,00
2	9	0	15.77	15.85	-15.85	-0.13	-0.087	0.087	0.38	-15,70	0.00	0.9936	1	18.19	0.00	0,00	0,00	0,00
1	9	0	10.08	8.99	-8.99	-0.23	1.089	-1.089	0.37	-8,82	0.00	0.9977	1	11.61	0.00	0,00	0,00	0,00
0	10	0	60.88	59.71	59.57	3.96	1.175	1.175	0.39	58,18	0.00	0.9194	1	67.58	0.00	0,00	0,00	0,00
1	10	0	8.25	8.31	8.30	-0.15	-0.055	-0.055	0.37	8,33	0.00	0.9983	1	9.56	0.00	0,00	0,00	0,00
2	10	0	67.64	66.58	66.47	3.80	1.059	1.059	0.39	65,20	0.00	0.9101	1	75.19	0.00	0,00	0,00	0,00
3	10	0	5.59	4.77	-4.75	-0.46	0.820	-0.820	0.37	-4,66	0.00	0.9995	1	6.56	0.00	0,00	0,00	0,00
4	10	0	27.38	27.55	27.34	3.41	-0.166	-0.166	0.38	26,33	0.00	0.9855	1	32.22	0.00	0,00	0,00	0,00
6	10	0	16.95	16.62	16.36	2.96	0.327	0.327	0.37	15,59	0.00	0.9951	1	20.58	0.00	0,00	0,00	0,00
7	10	0	8.15	7.43	-7.36	-1.00	0.726	-0.726	0.37	-7,05	0.00	0.9990	1	10.09	0.00	0,00	0,00	0,00
8	10	0	16.00	16.30	16.09	2.61	-0.302	-0.302	0.37	15,42	0.00	0.9953	1	20.14	0.00	0,00	0,00	0,00
9	10	0	11.26	11.25	-11.20	-1.11	0.002	-0.002	0.37	-10,82	0.00	0.9978	1	14.47	0.00	0,00	0,00	0,00
10	10	0	11.11	10.89	10.63	2.34	0.218	0.218	0.37	9,94	0.00	0.9981	1	14.60	0.00	0,00	0,00	0,00
11	10	0	6.84	5.64	-5.54	-1.07	1.196	-1.196	0.37	-5,17	0.00	0.9995	1	9.21	0.00	0,00	0,00	0,00
11	11	0	17.57	17.48	17.16	3.36	0.086	0.086	0.38	16,15	0.00	0.9949	1	23.74	0.00	0,00	0,00	0,00
9	11	0	37.68	36.91	36.65	4.36	0.774	0.774	0.38	35,23	0.00	0.9778	1	48.20	0.00	0,00	0,00	0,00
8	11	0	5.28	5.54	5.54	1.26	-0.265	-0.265	0.37	5,47	0.00	0.9995	1	6.69	0.00	0,00	0,00	0,00
7	11	0	44.72	44.79	44.48	5.28	-0.071	-0.071	0.38	42,71	0.00	0.9661	1	54.75	0.00	0,00	0,00	0,00
5	11	0	64.51	64.55	64.28	5.94	-0.041	-0.041	0.39	62,35	0.00	0.9323	1	75.16	0.00	0,00	0,00	0,00
4	11	0	10.53	11.14	11.14	0.25	-0.611	-0.611	0.37	11,02	0.00	0.9977	1	12.54	0.00	0,00	0,00	0,00
3	11	0	60.98	60.32	59.99	6.29	0.656	0.656	0.39	58,10	0.00	0.9340	1	69.62	0.00	0,00	0,00	0,00
1	11	0	62.75	62.32	61.99	6.41	0.425	0.425	0.39	60,18	0.00	0.9221	1	70.37	0.00	0,00	0,00	0,00
0	12	0	46.28	45.50	45.46	2.00	0.780	0.780	0.38	44,73	0.00	0.9588	1	53.24	0.00	0,00	0,00	0,00
2	12	0	15.83	15.51	15.39	1.92	0.313	0.313	0.37	14,73	0.00	0.9952	1	18.65	0.00	0,00	0,00	0,00
3	12	0	9.30	9.36	-9.35	0.31	-0.059	0.059	0.37	-9,32	0.00	0.9983	1	11.05	0.00	0,00	0,00	0,00
4	12	0	23.99	22.22	22.15	1.73	1.776	1.776	0.38	21,64	0.00	0.9911	1	28.66	0.00	0,00	0,00	0,00
7	12	0	5.35	5.18	5.10	1.91	0.163	0.163	0.37	4,82	0.00	0.9995	1	6.70	0.00	0,00	0,00	0,00
8	12	0	9.91	9.08	8.96	1.45	0.831	0.831	0.37	8,60	0.00	0.9986	1	12.63	0.00	0,00	0,00	0,00
9	12	0	12.04	12.03	11.98	1.09	0.014	0.014	0.37	11,56	0.00	0.9976	1	15.65	0.00	0,00	0,00	0,00
10	12	0	8.67	8.18	8.06	1.39	0.493	0.493	0.37	7,65	0.00	0.9989	1	11.53	0.00	0,00	0,00	0,00
11	12	0	8.18	8.14	8.07	1.06	0.040	0.040	0.37	7,65	0.00	0.9988	1	11.13	0.00	0,00	0,00	0,00
8	13	0	16.92	16.52	-16.50	-1.61	0.404	-0.404	0.37	-16,25	0.00	0.9953	1	21.67	0.00	0,00	0,00	0,00
7	13	0	6.11	7.01	6.99	0.59	-0.907	-0.907	0.37	6,79	0.00	0.9991	1	7.70	0.00	0,00	0,00	0,00
6	13	0	11.96	11.54	11.53	-0.38	0.424	0.424	0.37	11,58	0.00	0.9976	1	14.83	0.00	0,00	0,00	0,00
5	13	0	6.27	5.11	5.09	0.42	1.168	1.168	0.37	4,97	0.00	0.9995	1	7.51	0.00	0,00	0,00	0,00
2	13	0	17.22	17.15	17.15	-1.00	0.068	0.068	0.38	17,02	0.00	0.9944	1	20.43	0.00	0,00	0,00	0,00
1	13	0	3.83	1.39	1.35	1.34	2.437	2.437	0.37	1,27	0.00	1.0000	1	4.54	0.00	0,00	0,00	0,00